SAPIENZA
UNIVERSITÀ DI ROMA

Facoltà di Scienze Matematiche Fisiche e Naturali

DOTTORATO DI RICERCA

IN GENETICA E BIOLOGIA MOLECOLARE

XXXI Ciclo

(A.A. 2017/2018)

Elucidating Omomyc specific action in cancer: a sensitive controller of oncogenic Myc

Dottorando
Fiorella Scagnoli

Docente guida
Dr. Sergio Nasi

Coordinatore
Prof. Fulvio Cruciani

INDEX

4.2 Burkitt's lymphoma (BL)

AIM OF THE RESEARCH

5. Results

5.1 Omomyc suppresses tumorigenic features of glioblastoma stem-like cells and Burkitt's lymphoma cells

5.2 Impact of Omomyc expression on Myc genome occupancy

5.3 Impact of Omomyc on GSCs transcriptome

5.4 Omomyc minimally – or not at all - influences the global RNAPII binding at promoters and affects transcription only in a subset of target genes

5.5 Myc strengthens the regulatory nodes of glioblastoma gene expression networks

5.6 Omomyc decreases the expression of a gene set specifically bound by Myc

5.7 Myc promotes the symmetrical di-methylation of Arginine 1810 (R1810) residue of RNAPII

5.8 Myc-dependent R1810 symmetrical di-methylation requires PRMT5 catalytic activity

GLOSSARY

FO	Flag-Omomyc
DOX	Doxycycline
GSC	Glioblastoma Cancer Stem Cell
GFP	Green Fluorescent Protein
TRE	Tetracycline Responsive Element
SOX2	SRY-box 2
CCND1	Cyclin D1
PTEN	Phosphatase And Tensin Homolog
NCL	Nucleolin
ODC	Ornithine decarboxylase
HDAC	Histone deacetylase
DUSP10	Dual-specificity phosphatase
OLIG2	Oligodendrocyte transcription factor 2
KDM1A	Lysine Demethylase 1A
RCOR2	REST Corepressor 2
TF	Transcription Factor
ChIP-seq	Chromatin Immunoprecipitation sequencing
qChIP	quantitative Chromatin Immunoprecipitation
E-boxes	Enhancer boxes
PI	Propidium Iodide
FITC	Fluorescein isothiocyanate
TSS	Transcriptional Start Site
TTS	Transcriptional Termination Site
FPKM	Fragments Per Kilobase of gene Million mapped reads
RPKM	Reads Per Kilobase of gene per Million mapped reads
GSEA	Gene Set Enrichment Analysis
MsigDB	Molecular signature database
GO	Gene Ontology
CTD	Carbossi-Terminal Domain

PRMT5	Protein Arginine Methyl Transferase 5
GBM	Glioblastoma
FC	Fold Change

SUMMARY

The involvement of Myc in a wide range of molecular functions makes it, probably, the most studied transcription factor for 30 years. Myc deregulation is common in at least 70% of human tumors and gives rise to a wide variety of oncogenic phenotypes, including breast, lung, cervical, ovarian and brain cancer. Therefore, our primary interest was to interfere with Myc function in Glioblastoma Stem Cells (GSCs) and Burkitt's lymphoma cells, using a small peptide, named Omomyc. It is a Myc-bHLH mutant with outstanding capabilities to inhibit several types of human cancers. Omomyc displayed a significant impact on tumoral behavior in both model systems. This occurs because Omomyc replaces Myc at promoters and disrupts Myc protein network (Savino et al., 2011), affecting the expression of all those key genes - Myc target and not - directly involved in tumorigenesis. Furthermore, we found that Myc and Omomyc interact with the Protein Arginine Methyltransferase 5 (PRMT5) (Mongiardi et al. 2015), which catalyses the symmetrical di-methylation of RNA polymerase II (RNAPII) at R1810, allowing proper termination and splicing of transcripts (Zhao et al., 2016). Myc regulates many aspects of transcription by RNAPII, as activation, pause release and elongation, but its role in termination is unknown. We found that Myc overexpression strongly increases symmetrical RNAPII arginine di-methylation (R1810me2s), while the concomitant expression of Omomyc counteracts this capacity. In addition, Omomyc expression modulates the RNAPII amount at Termination Transcription sites (TTSs) *versus* Transcription Start Sites (TSSs) in several genes. Altogether, these findings suggest that Myc modulates transcription termination through R1810me2s-RNAPII. Therefore, Myc overexpression may deregulate this process by influencing RNAP II arginine di-methylation levels, contributing to tumorigenesis. In this regard, Omomyc may fine-tune the expression of a variety of genes altered by Myc in cancer, affecting the PRMT5/Myc/RNAPII-R1810me2s axis.

Introduction

1. Myc

1.1 Structure of c-Myc. *myc* is a family of three related gene products (c-Myc, n-Myc, and l-Myc; *in this thesis, Myc will refer to c-Myc*). The *myc* gene was first identified as the transforming agent within chicken retroviruses (Sheiness et al., 1978). In the human genome, *c-myc* localizes to human chromosome 8q24, it contains three exons which encode a translation product of 439 amino acids with a molecular weight of 64-kDa. The sequence of the Myc protein consists of two independent, functional and highly conserved polypeptide regions: a N-terminal transactivating domain and a C-terminal DNA binding segment. The transcriptional activation domain (TAD) contains two conserved regions known as Myc boxes (MBI and MBII). MBI box is involved in transcriptional activation in some context. In particular, MBI is the first contact point with P-TEFb, a cyclin CDK-complex that phosphorylates RNA polymerase II (RNAPII), stimulating transcriptional elongation (Rahl et al., 2010). MBII is essential for Myc ability to promote cellular transformation, to drive tumorigenesis, to activate and repress transcription of the majority of Myc targets; it also regulates Myc protein turnover. Further, Myc architecture has a middle region rich in proline, glutamic acid, serine and threonine residues (PEST), followed by two other conserved boxes (MBIII and MBIV), and a nuclear localization sequence. Myc MBIII box is involved in transcriptional repression by recruitment of histone deacetylase 3 (HDAC3), while MBIV seems to be required for the pro-apoptotic Myc function. Finally, a 100-amino-acid carboxyterminal region contains the basic helix-loop-helix-leucine zipper (bHLH-LZ) domain which mediates the heterodimerization with a small bHLH-LZ protein named Max (Fig. 1). This interaction is absolutely necessary to form a stable Myc-Max heterodimer able to contact directly specific DNA sequences called “Enhancer boxes” (E-boxes) to stimulate

transcription. Indeed, full-length Myc alone is unable to bind DNA (Grandori et al., 2000). Besides Myc-Max also Max-Max homodimers bind E-boxes (Dang et al., 1999; Nair et al., 2006; Tansey 2014). Although many functions of Myc appears to be dependent on its interaction with Max, there are considerable evidences that Myc retains some activity even without Max (Hopewell et al., 1995). Among the many identified Myc-interacting proteins, only a few exclusively bind to Myc alone. The transcription factor YY1, which usually inhibits Myc-Max activity, can also interact with Myc. Myc alone interferes with p21-PCNA interaction during DNA replication, while p21 inhibits Myc-Max transcriptional activation. Moreover, Myc was reported to associate with replication proteins and to localize to the origins of replication–whereas Max was found at this level only at the sub-stoichiometric amount (Dominguez-Sola et al., 2007; Gallant and Steiger 2009). Finally, a cleaved, cytoplasmic, form of Myc, named Myc-nick, is able to trigger tumor migration and metastasis independently of its transcriptional function (Conacci-Sorrell et al., 2010, 2014).

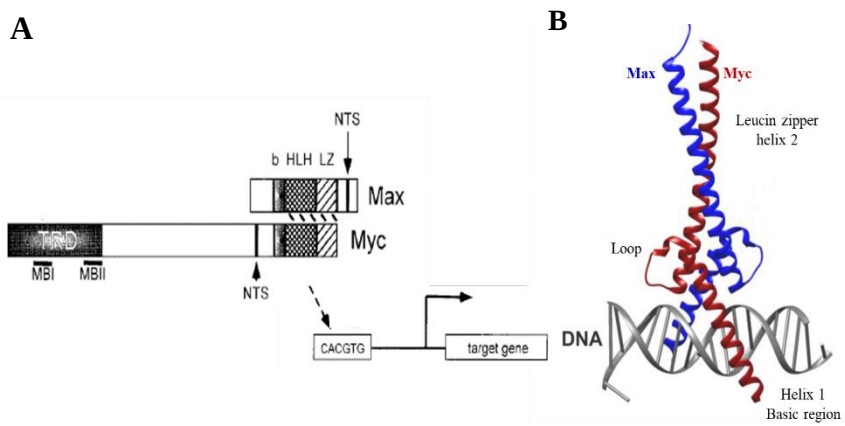

Fig. 1 - Myc-Max heterodimer. **A.** The diagram depicts Myc and Max protein structure with their major domains (modified by Dang et al., 1999). **B.** Crystal structure of Myc/Max bHLH regions bound to the E-box. (Tansey 2014).

1.2 The Myc/Max/Mad network: a matter of balance in the cellular milieu. The heterodimerization of Myc with Max plays a fundamental role in proliferation, transformation, and apoptosis processes. Max has a short half-life but it is stable and constitutively expressed also in the absence of Myc, suggesting that Max activity is largely dependent on the abundance of Max-associated transcription factors. Max homodimers may block Myc biological activity, probably through competition for the E-box-binding sites. Other bHLH-LZ Max interactors are Mad1-4 (Mad1, Mxi1, Mad3, and Mad4), Mnt and Mga (Fig. 2). These proteins are characterized by some Myc properties: a) weak homodimerization and DNA-binding capacities; b) efficient heterodimerization with Max and consequent binding to the E-boxes; c) interference with Myc-Max activity. Specifically, Mad1, Mxi1 and related members constitute a family of transcriptional repressors at the same Myc-Max binding sites. A competition between Myc-Max and Mad-Max heterodimers determines cell decisions between proliferation/transformation and differentiation/quiescence (Eisenmann 1997). Indeed, increased expression of Mad proteins is associated with cellular differentiation and growth arrest. This occurs because Mad1-4 proteins share a repression motif that interacts with Sin3a and Sin3b corepressors, which in turn recruit HDACs and other chromatin modifying proteins to the complex. In summary, the opposite functions of Myc and Mad may be explained at three levels: competition for available Max to form heterodimers; competition between heterodimers and E-box-binding sites; transcriptional activation and repression of bound genes (Cultraro et al., 1997; Farhana et al., 2015). Interestingly, Mnt is a unique antagonist of Myc among Max protein partners. Indeed, it is constitutively expressed, and its expression overlaps with the expression of Myc (Billin et al., 1999; Grandori et al., 2000; Link et al., 2012; Yang & Hurlin, 2017). Recent studies show that Myc and Mnt compete for binding to limiting amounts of Max and, in turn, Max availability is further modulated by the turnover of Mxd protein family, whch display a short half-life, by ubiquitin-

mediated proteasomal degradation. Therefore, the complexity of the Myc-Max-Mad network implies a stoichiometric control of all its components. Moreover, Myc can also act as a transcriptional repressor at distinct subsets of genes impairing p300 recruitment by the transcriptional activator Miz-1 (Nair et al., 2006; Grandori et al., 2000). There are also differences in the subnuclear localization and binding affinities of Myc-Max and Mxd-Max complexes, indicating that the modulation of the levels of individual family members may have a distinct effect on network activity. Myc, for instance, is able also to upregulate the expression of MondoA and ChREBP, nutrient-sensing transcription factors, which control different facets of cellular metabolism, and their accumulation in the nucleus depends on changes in the metabolic flux. In turn, these two factors influence Myc-driven metabolic reprogramming during tumor progression (Lin et al., 2009; Kaadige et al., 2010). Furthermore, increased amount of MondoA and ChREBP sequestrates Mlx (Max dimerization protein X), increasing the competition between Myc and co-expressed Mxd proteins for Max. Therefore, an imbalance in the network may arise alterations typical of cancer cells.

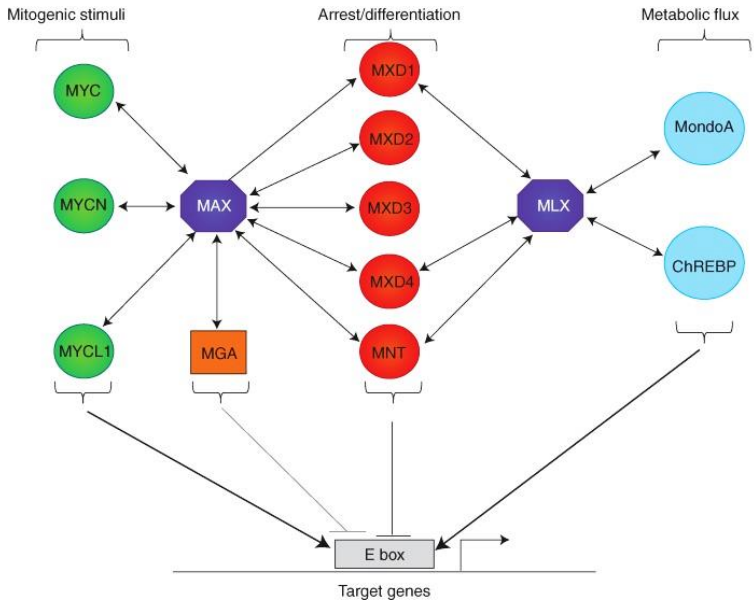

Fig. 2 – The Myc/Max/Mad network. Schematic diagram of individual interactions among Myc network components (double-headed arrows), (Conacci-Sorell et al., 2014).

1.3 Biological activities of Myc. In normal, non-dividing cells, Myc levels are low, while in dividing cells Myc expression is induced in a highly controlled manner and is maintained at a relatively constant, intermediate level during the cell cycle. This scenario changes when Myc expression overcomes two orders of magnitude in cancer cells. The control of Myc expression and activity starts at transcription. Myc is an *intermediate early gene*, rapidly induced in response to a wide range of growth factor, cytokines and mitogens, such as Wnt, Notch, Stat, receptor tyrosine kinases (RTKs), as well as hormone receptor pathways (Spencer and Groudine 1991; Morrow et al., 1992; Meyer et al., 2008; Eilers and Eisenman 2008). Regulation of Myc transcription is exerted at both the initiation and RNA polymerase (RNAP) II pause release level upon proper mitogenic stimulation (Grandori et al., 2000). eIF4E binds the Myc message early during the transcription process, avoiding free Myc mRNA escape from the nucleus, without appropriate restraints. Once in the cytoplasm, translation of the Myc mRNA is finely regulated and temporally limited by its short half-life. The Myc protein is even subjected to several post-translational modifications including phosphorylation, acetylation, glycosylation, and ubiquitylation. The rapid Ub-mediated proteolysis of Myc is crucial for keeping Myc levels low (Vervoorts et al., 2003, 2006; Chou et al., 1995). Myc is required for maintaining pluripotency and self-renewal of embryonic, neural stem cells and progenitors (Knoepfler et al., 2002) and at the same time is also required for the exit from the stem cell niche, balancing differentiation and growth of progenitor cells (Wilson et al., 2004). Indeed, the suppression of *myc* expression is an essential component to trigger—differentiation (Johansen et al., 2001) (Fig. 3). Interestingly, Myc and other transcription factors, such as Klf4, Oct4 and Sox2, are able to convert differentiated mouse and human fibroblasts into pluripotent stem cells (iPS) by affecting

the epigenetic state of the target cell (Takahashi et al., 2007; Laurenti et al., 2009; Singh and Dalton 2009). Another important Myc function is the ability to induce apoptosis. Specifically, normal cells seem to be sensitive to unchecked Myc expression and activate programmed cell death in this condition. This phenomenon depends on Myc expression levels and extracellular stimuli. In normal conditions, the presence of high concentration of growth factors, in response to sustained Myc levels, pushes the cells towards proliferation; in limited growth factors conditions, cells respond undergoing apoptosis. Conversely, transformed cells frequently resist the apoptotic effects induced by deregulated Myc expression, responding only to its pro-proliferative signals (Zindy et al., 1998; Juin et al., 1999; Soucie et al., 2000; Eischen et al., 2001; Larsson and Henriksson 2010; McMahon 2014). To note, the ability of Myc to induce apoptosis in normal cells is consistent with the model in which Myc derepresses at least one level of apoptotic control, making cells more susceptible to death in only some contexts (Fig. 3). It is not clear whether Myc constitutively regulates all downstream effector pathways or whether each pathway becomes fully activated only upon the occurrence of a second stimulus. For example, both high levels of Myc expression and growth inhibitory signals are required to trigger cell death (Sears et al. 1999). For this reasons, Myc-dependent apoptosis has been referred to as a *Myc latent or intrinsic tumor suppressor activity*. Further, Myc is able to induce cellular senescence, a mechanism which impairs tumor development at the pre-malignant stage, under certain conditions. In general low levels of Myc were shown to induce or inhibit senescence (Zhuang et al., 2008). This apparent contradiction suggests that the role of Myc in promoting senescence is strictly dependent from overlapping pathways, cell context and, more specifically, protective factors deficiency (Vita and Henriksson 2006; Campaner et al., 2010) (Fig. 3).

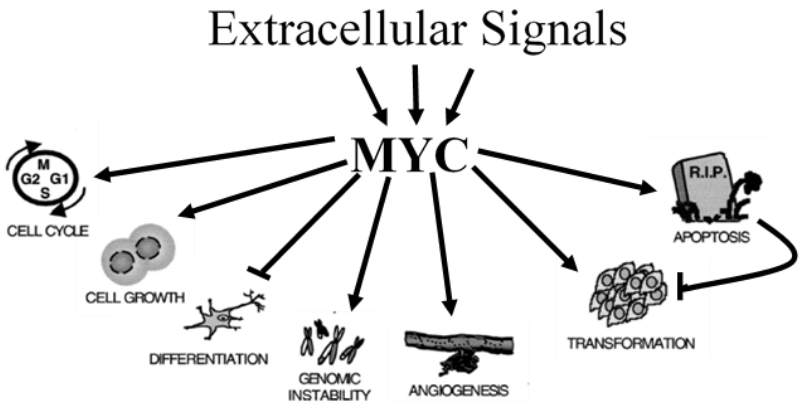

Fig. 3 – Myc biological activity. Depending on changes of the extracellular microenvironment Myc may affect several biological functions (Figure from Oster et al., 2001).

1.4 Myc and cancer. Deregulation of the *myc* protoncogene is a catastrophic event which makes cells vulnerable to further oncogenic hits. In general, the principal hallmarks of cancer, acquired during the process of tumorigenesis, are self-sufficiency, growth signals, insensitivity to antigrowth signals, escape from apoptosis, sustained angiogenesis and tissue invasion with consequent metastasization. Myc may promote several of these capabilities simultaneously. Although *myc* gene alterations have initially been reported in a myeloid leukemia cell line (Dalla Favera et al., 1982b), they have also been found in colon carcinomas (Alitalo et al., 1983), in neuroblastoma, a childhood solid tumor with *mycn* gene amplification (N-Myc) (Khol et al., 1983), in small cell lung carcinomas (l-Myc; Neu et al., 1985). After these initial findings, several studies had confirmed that genetic alterations of *myc* gene family member probably underlie the etiology of all cancers. Therefore, understanding how and when cells lose the control of Myc is crucial to predict tumor outcome and to design successful therapies. The principal alterations, such as viral insertional events, chromosomal

translocations and gene amplification do not disrupt its protein sequence. Indeed, Myc deregulation in cancer does not depend on mutations in the coding sequence. High levels of Myc are due to the cell inability to modulate its expression in response to normal cellular and extracellular signals. Notably, aberrant Myc expression can be promoted by defects in signal-transduction pathways, which are frequently mutated in cancer, that activate or repress *myc* gene family expression, such as Wnt-β-catenin, Sonic hedgehog-Gli, and Notch (Vita and Henriksson 2006; Song et al., 2015; Morris and Huang 2016). Myc activation occurs also at the post-transcriptional level by increasing both Myc mRNA (Vita and Henriksson 2006) and protein stability. In particular, it has been shown that the stability of the Myc mRNA is promoted by the overexpression of the eIF4E translation factor that exports Myc mRNA from the nucleus to the cytoplasm (Oster et al., 2002; Schmidt, 2004; Matsumoto et al., 2015) while the Myc protein is stabilized by loss of critical regulators, such as the SCF^{Fbw7} ubiquitin ligase (Yada et al., 2004; Popov et al., 2010). In this regard, it has been demonstrated that mutations of T58 or around this residue impair Myc ubiquitination and proteasome degradation in Burkitt's lymphoma (Hoang et al., 1995; Chang et al., 2000; Cowling et al., 2014). Alternative mechanisms for the regulation of Myc stability involve the MBI and MBII conserved sequences, characterized by lysine residues which may be potentially ubiquitinated, while Myc PEST sequence has been shown to be necessary for its rapid turnover (Salghetti et al., 1999; Sears et al., 2000; Gregory and Hann 2000). When these Myc domains are mutated, the increased Myc stability contribute to tumorigenesis. Paradoxically, deregulation of Myc also triggers intrinsic tumor suppressor mechanisms including apoptosis, cellular senescence, and DNA damage responses. These anti-cancer mechanisms can be latent in tumor cells and can be activated or reactivated by molecular intervention (Lowe et al., 2004).

2. Myc transcriptional activity

The precise role of Myc in transcriptional regulation is still strongly debated. The predominant function of Myc-Max heterodimer is gene activation. This is consistent with Myc's ability to recruit multiple coactivator complexes (Adhikary and Eilers 2005; Cole and Nikiforov 2006; Rahl et al., 2010, Poole and van Riggelen 2017). However, when the Myc-Max complex interacts with a zinc finger protein named Miz-1, Myc has been associated also with transcriptional repression (Wiese et al., 2013). Notably, as distinct types of cancer have different Myc expression levels (Fig. 4), the differential increase in Myc production may explain, at least in part, why different tumors acquire a specific Myc-dependent transcriptional profile (Tansey 2014). Specifically, when Myc is at physiological levels, it weakly binds to low-affinity promoters, while high-affinity promoters may be already saturated. Therefore, Myc binds better to some promoters than others altering the activity of the corresponding gene (Zheng and Levens 2016; Lorenzin et al., 2016; Allevato et al., 2017).

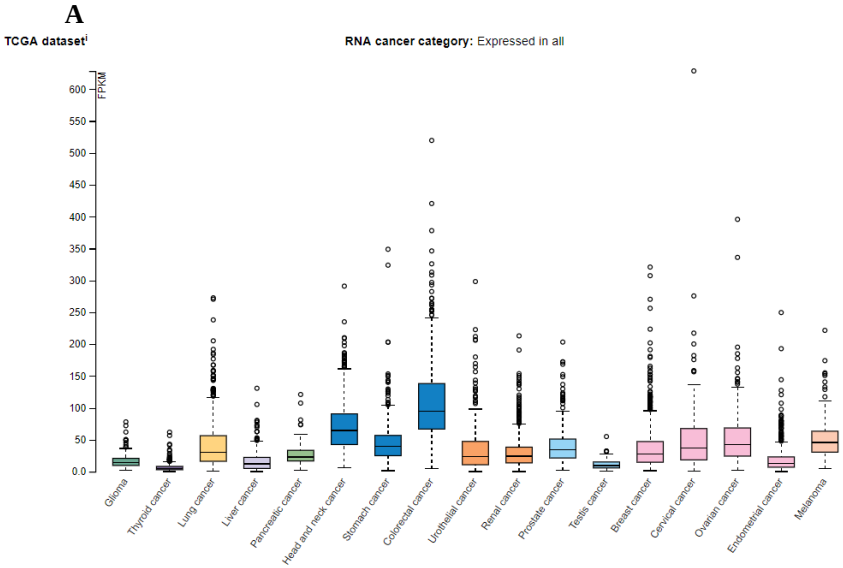

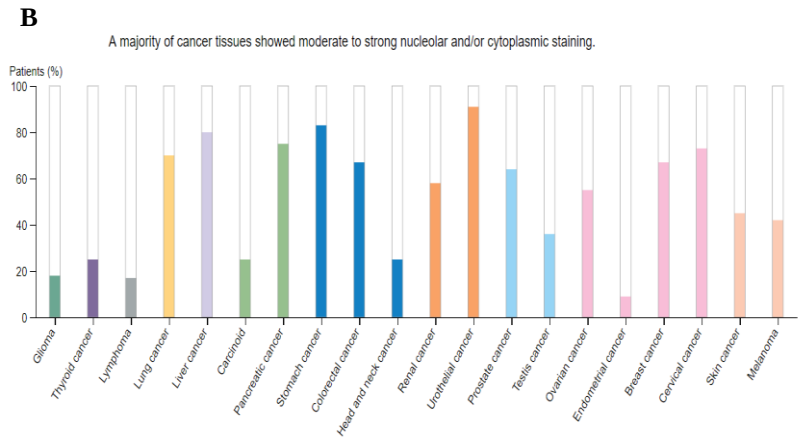

Fig. 4 - The human protein atlas of Myc. **A**. RNA-seq data from The Cancer Genome Atlas (TCGA). **B**. The graph depicts Myc protein expression overview in different types of cancer. Protein expression level is shown for each cancer by color-coded bars. The y-axis indicates the percentage of patients. Cancer types are color-coded according to the organ of origin (https://www.proteinatlas.org/ENSG00000136997-MYC/pathology#top).

Neverthless, the frequency of the E-boxes throughout the genome and the ability of Myc to bind also to sequences lacking these consensus regions makes difficult to predict specific sets of Myc-regulated genes. Indeed, genome-wide approaches have revealed that Myc has a preference for certain chromatin states, which may not contain E-boxes. Generally, Myc binds to E-boxes located proximal to CpG islands, in chromatin regions carrying active histone marks, such as histone H3 methylation at lysine residues 4 and 79 or H3 acetylation at lysine residue 27. Therefore, Myc transcriptional response may depend on the epigenetic state and on the type and history of each cell within a specific tumor (Eilers and Eisenman 2008; Zeller et al., 2006; Lin et al., 2012; Walz et al., 2014). Most of Myc-induced genes are transcribed by RNAPII. Some studies show that Myc additionally stimulates transcription of genes by RNAPIII (Gomez-Roman et al., 2003; Arabi et al., 2005; Grandori et al., 2005). Myc facilitates transcriptional elongation by stimulating the recruitment of P-

TEFb and Mediator complex and increases the levels of transcripts per cell. The Mediator complex is an essential co-activator of RNAPII involved in chromatin "looping", which brings distant chromosomal regions closer to each other. Specifically, MBI and MBII Myc box also mediate the association of Myc with Bromodomain Containing Protein 4 (BRD4) that in turn promotes P-TEFb recruitment (Rahl et al., 2010; Rahl et., 2014; Poole and van Riggelen 2017). It has to be considered that other factors prepare the chromatin to be easily recognized by Myc-Max (the so-called chromatin "open state") and the interactions among chromatin-modifying proteins and the basal transcriptional machinery determine the localization of Myc-Max dimers at active loci. This is allowed by a sequence of a specific hierarchy of binding events. WDR5, BPTF, and TIP60, for example, are some of these *helper* factors that guide Myc to the promoters of active genes (Thomas et al., 2015; Kress et al., 2015). Hence, the increase of Myc molecules amount, in tumors, may cause not only the saturation of high- and low-affinity binding promoters but also an abnormal increase of Myc co-factors recruitment in protein complexes. This may contribute to altered transcription processes with consequent aberrant gene expression typical in cancer.

2.1 Global versus selective: two conflicting models? Two models have been proposed for Myc function: Myc is a *universal amplifier*, which binds virtually to all active promoters in the genome, stimulating gene transcription, whereas the other model suggests Myc as a gene-specific regulator (*specifier*).
Several studies support the idea that Myc is an *amplifier* because of its presence on promoters with an open chromatin structure, as well as on thousands of enhancers and intergenic sites in multiple cell types, globally enhancing transcription (Lin et al., 2012; Nie et al., 2012). As a consequence, Myc overexpression modulates the expression of genes involved in a broad range of biological functions, such as cell growth, ribosome biogenesis, protein synthesis, and metabolism (Eilers and Eisenman, 2008). In tumor cells, overexpressed Myc accumulates in the promoter regions of

active genes, causing transcriptional amplification in particular of proliferation-associated genes (Lin et al., 2012). Thus, while in normal cells Myc is induced by mitogenic growth factors (Dang et al., 2012; Eilers and Eisenman 2008; Meyer and Penn 2008), in tumor cells, its high expression uncouples growth-factor stimulation and cellular proliferation. Furthermore, elevated expression of Myc allows global changes in chromatin architecture (Guccione et al., 2006; Knoepler et al., 2006; Van Riggelen et al., 2010), influencing transcription. Thus, Myc amplifies the output of existing gene expression programs by directly binding all actively transcribed genes at the E-box-containing core promoter sequences. Notably, the magnitude of Myc-driven transcriptional amplification depends on the levels of Myc within the cell. In tumor cells expressing low Myc, the transcription factor is bound almost exclusively to E-boxes of most actively transcribed genes. Conversely, elevated Myc binds also to the enhancers of these active genes and at low-affinity E-box-like sequences, the so-called non-canonical E-boxes. In particular, differences in Myc occupancy determine the degree of expression of each active gene: high-affinity promoters are Myc-saturated in proliferating cells and a further growth in Myc levels only increase its occupancy at low-affinity promoters (Walz et al., 2014; Wolf et al., 2015) (Fig. 5).It has to be considered that the dose-dependent binding of Myc to chromatin may change even within a single cell population. This means that all Myc-bound sites in one cell may not necessarly correlate with those in another one (Tansey 2014). In summary, Myc is a *universal amplifier* because increased levels of Myc result in increased Myc binding to active genes. This behavior of Myc is consistent with the evidence that open chromatin at active promoters is important for Myc binding (Guccione et al., 2006) and that enhancer loops, in the proximity of core promoters at active genes, may facilitate binding of Myc to close enhancer elements, once Myc binding sites in core promoters are saturated.

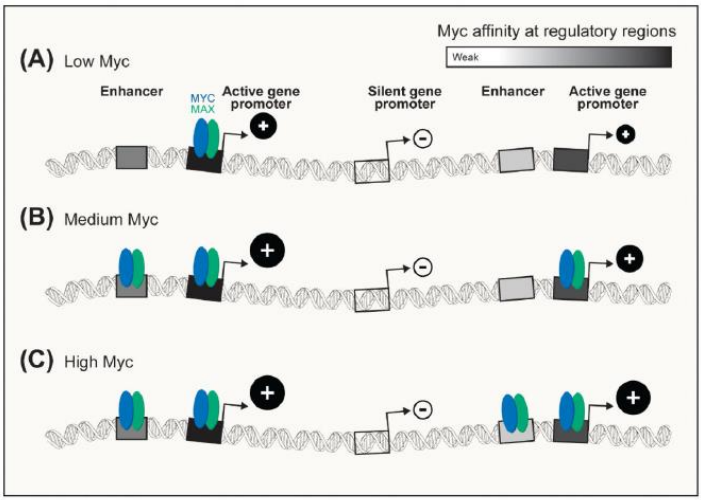

Fig. 5 – **Myc affinity at genome**. The picture shows progressively increasing genomic Myc binding at (**A**) low, (**B**) medium and (**C**) high Myc concentrations (Wolf et al., 2015).

To summarize, at high concentrations, Myc is not sequence-independent, but it is simply less selective.
This view of Myc transcriptional activity as an *amplifier* does not discriminate between direct and indirect Myc effects on gene expression. Myc activity modifies cell behavior in response to extracellular stimuli (either in normal or in pathological contexts), changing cell size, energy metabolism, translation, and nucleotide biosynthesis. These processes have a potential feedback on global RNA synthesis, processing, and turnover and are controlled by different Myc-regulated genes. Consistent with this evidence, RNA amplification is observed in different physiological transition states, such as quiescent *versus* activated, but also normal *versus* tumor or tumors with variable Myc levels (Fig. 6). Therefore, Myc may regulate specific gene sets that increase the expression of other indirect Myc target genes, through a sort of *domino* effect, rather than inducing a general amplification, and RNA amplification is independent from chromatin invasion (Perna et al., 2012; Sabò et al., 2014).

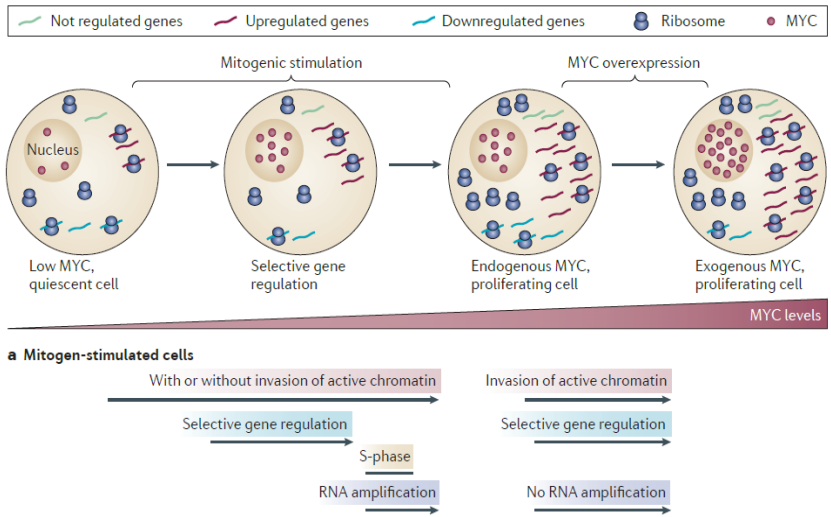

Fig. 6 – **Schematic representation of Myc effects at different expression levels. Left**: low Myc is required for selective regulation of a set of Myc-dependent genes preceding S-phase entry and RNA amplification. **Right**: super-activation of Myc and chromatin invasion, but without further RNA amplification (Kress et al., 2015).

In this view, global changes in RNA and mRNA levels occur indirectly as a consequence of Myc-driven cell growth (Sabò and Amati, 2014). This is in an apparent contradiction with the general amplification model, considering also that the *specifier model* proposes that most of Myc binding to chromatin is non-productive in terms of transcriptional regulation (Kress et al., 2015). New insights about Myc ability to widely affect gene expression come from the observation that the increasing amount of Myc, from normal to tumor-specific levels, do not affect Myc binding at promoters where the transcription factor is already strongly bound in normal cells. Indeed, Myc increases only at weakly bound promoters. In this view, the transition state from a normal to a tumor cell is due to abnormal Myc levels which locate at previously empty binding sites or with a lower Myc amount. Therefore, Myc regulates distinct sets of genes in normal and

tumor cells according to its concentration: it is a *specifier* in some biological settings; in others it enhances the expression of all genes as a *general amplifier*. This novel hypothesis overcomes the apparent contradiction between the *specifier* and the *amplifier models* (Lorenzin et al., 2016): a dose-dependent correlation exists between Myc concentration and gene response. Hence, Myc may contribute to oncogenic transformation via two different mechanisms: low levels of constitutive Myc enhance the expression of genes controlled by high-affinity promoters, such as genes involved in ribosome function. The further increase in Myc levels will enhance occupancy of promoters that are barely occupied in normal and proliferating cells, triggering tumorigenesis (Fig. 7).

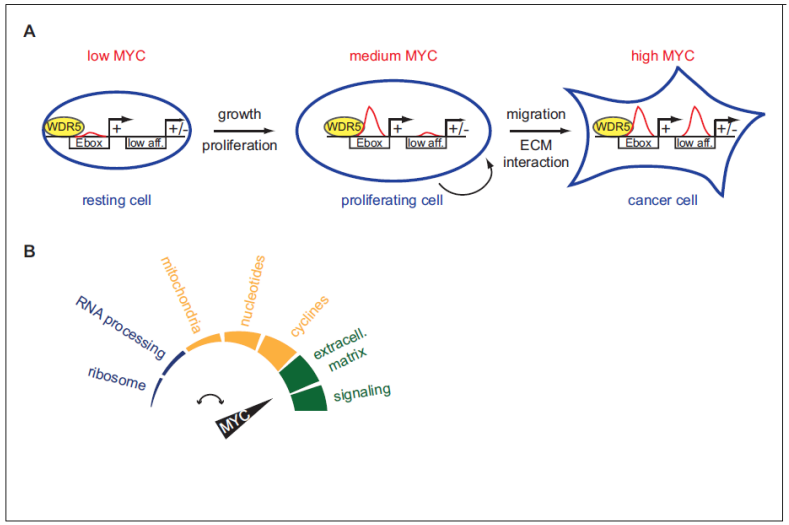

Fig. 7 – **Schematic model of Myc DNA-binding ability**. (**A**) high-affinity binding sites, e.g. E-boxes, are already highly occupied at physiological Myc levels (medium Myc), in dividing cells. At oncogenic concentration (high Myc) also low-affinity (low aff.) binding sites may become occupied by Myc and the up-regulation of these low-affinity genes is suggestive for transformation. (**B**) Different Myc levels regulate distinct biological processes (Lorenzin et al., 2016).

A very recent study provides important insight into Myc capacity to affect the gene expression as a *specifier*. Only few hundred of genes show decreased messenger RNA output upon Myc loss, while the large majority of the transcriptome remains unaffected (Muhar et al., 2018) (Fig. 8). This Myc-dependent signature is composed by a group of genes involved in protein and nucleic acid biosynthetic pathways, confirming that Myc mainly contributes to the activation of specific transcriptional patterns which, in turn, promote the increase in RNA biosynthesis, generally associated with cell activation and transformation (Kress et al., 2015).

Based on these observations, the Myc expression levels are crucial to proper cellular function. Indeed, in normal cells Myc levels are finely regulated and Myc induces the expression of a specific set of genes (Sabò et al., 2014). In summary, during the transition from a quiescent to a proliferating state, Myc molecules (Fig. 6 and 7) increase, enhancing the expression of direct secondary target genes, that in turn promote the transcription of downstream genes (a domino effect). In tumors, at supraphysiological levels, Myc retains this ability but also overamplifies the transcription of genes which Myc normally does not or weakly binds (Lorenzin et al., 2016). This Myc behavior is called *secondary RNA amplification* (Fig. 8, late effects – indirect) in contrast to the genome-wide, direct transcriptional amplification model. In this view, the amplifier and the specifier model may be reconciled.

3. Omomyc

About twenty-five years later the discovery of myc gene, Sergio Nasi and Laura Soucek engineered a small peptide of 90 amino acids, named Omomyc, able to interfere with Myc function (Soucek et al. 1998). Omomyc action is different when compared to drugs or RNA interference, designed to fully inhibit Myc activity. In several genetic mouse models of cancer, Omomyc exerts extraordinary therapeutic capacity, with mild and well-tolerated side effects. Therefore, Omomyc is not only a tool to inhibit Myc activity to understand its molecular functions but represents also a hopeful and a successful agent for cancer therapy.

3.1 Structure of Omomyc and its interactors. Omomyc is a 90 amino acids Myc-bHLH mutant, with a molecular weight of 11 KD. It was designed by the accurate analysis of the crystallographic structure of DNA-bound Max homodimers (Ferrè-D'Amarè et al., 1993), to identify those amino acids crucial for heterodimerization with Myc. Four are the amino acids located in the Myc leucine zipper involved in dimerization: two glutamate residues (E57, E64) and two arginines (R70, R71); the corresponding positions in Max are occupied by two asparagines (N57 and N71), one isoleucine (I64) and one glutamine (Q70). In Omomyc, Myc E57 is substituted by a threonine (T), while the other three amino acids are the same as in Max (Fig.10). Omomyc also lacks Myc transactivation domain, it efficiently homodimerizes, can still heterodimerize with Myc, Max and Miz-1 (Soucek et al. 1998; Savino et al., 2011; Jung et al., 2017). Omomyc forms a complex with Max with high efficiency, like Myc/Max dimers, while DNA binding affinity of Myc-Omomyc heterodimer is low (Soucek et al., 1998).

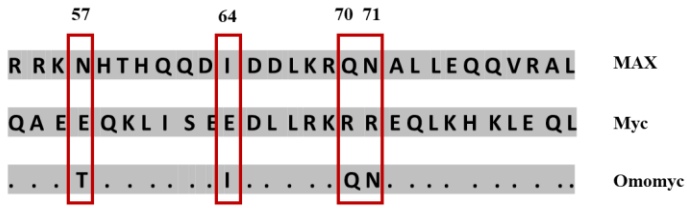

Fig. 10 – bHLH sequence comparison of Max, Myc and Omomyc. Amino-acidic bHLH sequence are shown. Red rectangles highlight the four mutated amino-acids.

In the presence of Omomyc, Myc-dependent gene transcription undergoes general repression. This occurs because Omomyc selectively targets Myc protein interactions, as confirmed by its binding with Miz-1, a known Myc co-repressor (Wiess et al., 2013). Specifically, Omomyc interferes with Myc binding to E-boxes and prevents the transactivation of target genes, retaining Myc transrepression properties in association with Miz-1. In parallel, broad epigenetic changes occur, such as decreased acetylation and increased methylation at lysine 9 of histone H3 (Savino et al., 2011). Further, both Myc and Omomyc functionally associate with the Methylosome 50-Protein Arginine Methyltransferase 5 (PRMT5-MEP50) complex, inducing H4R3 symmetric di-methylation (H4R3me2s), supporting Omomyc function as a transcriptional repressor of Myc target genes (Mongiardi et al., 2015). Consistently, Omomyc induces histone deacetylation while Myc promotes acetylation (Savino et al., 2011, Ullius et al., 2014; Mongiardi et al., 2015). These findings further suggest that Omomyc may be considered a sort of transcriptional repressor. A recent and accurate crystallographic analysis (Fig.11) confirms that Omomyc forms more stable homodimers compared to Myc-Max heterodimers because of ionic and hydrophobic interactions. Indeed, Omomyc dimers with Myc or Max appear to contain repulsive interactions or to lack stabilizing interactions that decrease their stability, suggesting

that Omomyc preferentially forms homodimers (Savino et al., 2011; Jung et al., 2017). Omomyc homodimers bind DNA with higher affinity compared to Myc-Max complexes, showing also a competition for E-boxes binding (Jung et al., 2017).

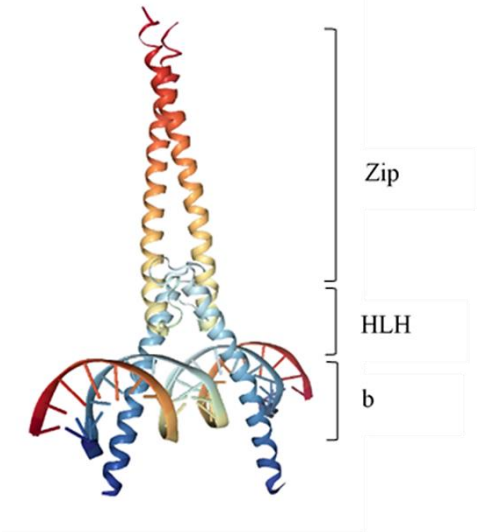

Fig.11 – Structure and DNA binding of Omomyc. Crystal structure of the Omomyc homodimer bound to a consensus E-box. The CACGTC sequence is highlighted in blue (Jung et al., 2017). Omomyc forms a homodimer with an overall structure that is very similar to those other b/HLH/Zip structure, in particular to that of Myc-Max.

3.2 Overview of Omomyc action in cancer. The outstanding capacity of Omomyc to inhibit Myc oncogenic action is supported by several *in vitro* and *in vivo* studies. Omomyc can potentiate Myc-induced apoptosis and, inhibiting Myc DNA-binding to the E-boxes, antagonizes Myc-induced papillomatosis (Soucek et al., 2002). While Myc-induced apoptosis requires ARF and p53, Omomyc-dependent apoptosis does not require ARF, although p53 remains necessary. Its proapoptotic action is most likely related to Myc transrepression function and it is intriguingly limited only to cells harboring activated Myc (Soucek et al., 2004;

2010). Surprisingly, Omomyc prevents the development of lung tumors and trigger their rapid regression, with well-tolerated and reversible systemic side effects, upon restoration of Myc function (Soucek et al., 2008, 2013). Moreover, Omomyc suppresses cell growth by inducing apoptosis or cell cycle arrest in G1, targeting Myc in several types of Myc-addicted lung tumor cells (Fiorentino et al., 2016). The ability of Omomyc to be a potent tumor-suppressor, is further demonstrated by studies on glioma *in vitro* and *in vivo*. Here, the small peptide suppresses glioma formation, inhibits glioma cell proliferation and survival, and triggers regression of established disease in mice (Annibali et al., 2014). Additionally, Omomyc induces differentiation in specific stimuli conditions (Grayson et al., 2014). The little toxicity in Omomyc expressing normal tissues may be due to the capacity of Omomyc in discriminating between physiological and oncogenic functions of Myc (Fig. 12). Indeed, Omomyc causes a significant decrease in Myc promoter occupancy preferentially at binding sites invaded by oncogenic Myc levels, attenuating both Myc-dependent activation and repression of the gene expression (Jung et al. 2017).

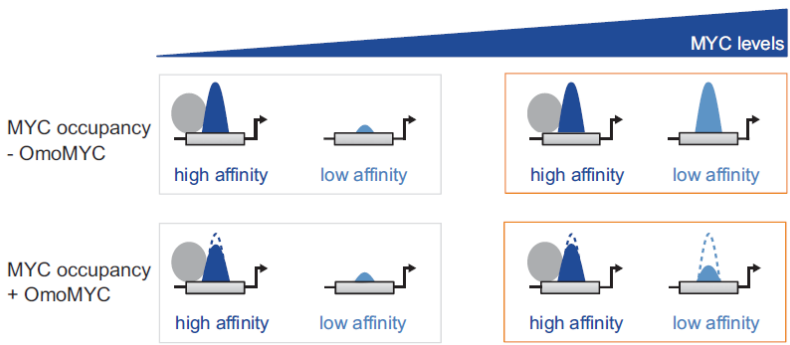

Fig. 12 – Omomyc occupancy increases at low affinity promoters that are invaded by oncogenic Myc levels (Jung et al. 2017).

4. Experimental models

4.1 Glioblastoma multiforme (GBM). Glioblastoma multiforme is one of the most malignant tumors of the brain, that remains largely incurable and with a poor prognosis. Patients usually have a median survival of 14 to 18 months from the diagnosis. With a global incidence of 10 per 100,000 people, it can occur at any age, but the peak is between 55 to 60 years (Jansen et al., 2010; Hanif et al., 2017). Glioblastoma stem cells (GSCs) are responsible for GBM development, progression, maintenance and tumor recurrence. They are multipotent, resistant to therapies and they are located in specific *niches,* characterized by different stromal cells such as mesenchymal and immune cells, with abnormal extracellular matrix components and an atypical vascular network. Furthermore, they are characterized by developmental and repair programs, typical of normal stem and progenitor cells, to support the expansion of the tumor (Lee et al., 2006; Bao et al., 2006; Cloughesy et al., 2014; Lathia et al., 2015) (Fig. 13). Glioma stem cells express high Myc levels (Wang et al., 2008), which are required to sustain GSCs phenotypic features such as growth, proliferation, self-renewal and survival. Indeed, it correlates with the grade of malignancy (Herms et al., 1999).

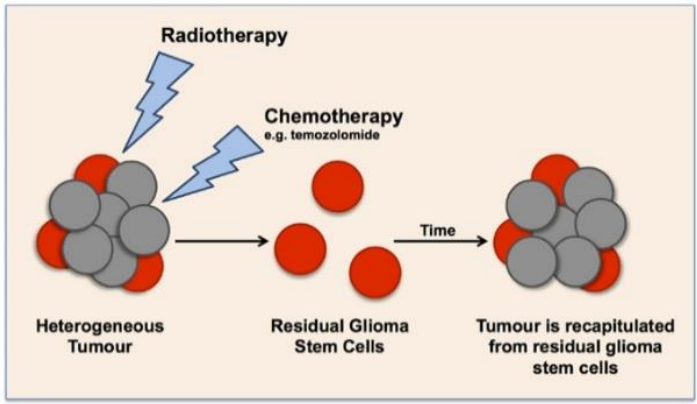

Fig. 13 - Schematic representation of the cancer stem cell in glioma. Current therapies target highly proliferating cells, leaving a small population of quiescent cells that are thought to be responsible for tumor recurrence (Seymour et al., 2015).

4.2 Burkitt's lymphoma (BL). Burkitt's lymphoma is the fastest growing human tumor and is a highly aggressive B-cells, non-Hodgkin lymphoma. Infection by the Epstein Barr Virus (EBV) precedes tumorigenesis. The incidence is frequent in childhood and increases in immuno-depressed patients such as in HIV infection (Molyneux et al., 2012). Burkitt's lymphoma is characterized by a significant deregulation of *myc* gene. Here, *myc* is involved in reciprocal Burkitt translocations [t (8;14), t (8;22), and t (2;8)] (Fig. 14). In t (8;14) human Burkitt cell lines, *myc* is directly translocated into the heavy chain locus of immunoglobulin (IGH) (Dalla Favera et al., 1982; Taub et al., 1982; Molyneux et al., 2012) and it is under the control of the IGH promoter, a phenomenon crucial for tumorigenesis. However, Burkitt's lymphoma cases without *myc* gene rearrangement but with high Myc expression levels and DNA methyltransferases (DNMT family member) deregulation have been identified (De Falco et al., 2015). Furthermore, in a certain number of Burkitt's lymphoma cell lines, Myc protein is also significantly stabilized, suggesting that aberrant Myc proteolysis

may play a crucial role in the pathogenesis of Burkitt's lymphoma (Mark et al., 2000).

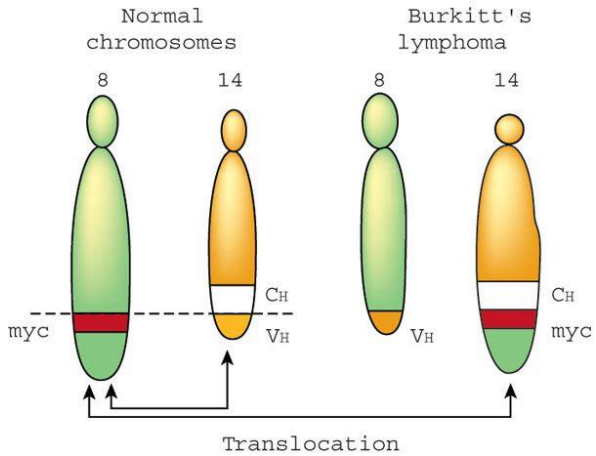

Fig. 14 – Burkitt's lymphoma mutation. The figure depicts a typical reciprocal chromosome translocation t (8;14), involving *myc* gene in BL.

AIM OF THE RESEARCH

Deregulation of Myc, common in several human cancer, makes the Myc protein an attractive therapeutic target. Omomyc is a mutant of Myc at the bHLH domain that affects Myc function at the level of protein interactions and DNA binding and strongly reduces Myc tumorigenic properties *in vitro* (Soucek et al., 1998; Savino et al., 2011). Omomyc displayed therapeutic efficacy in a variety of mouse transgenic models, such as Myc-induced papillomatosis, lung carcinoma, pancreatic islet tumor, glioma and others, with very well tolerated side effects *in vivo* (Soucek et al., 2002; Annibali et al., 2014). Thus, it is important to elucidate how Omomyc works at the cellular and mechanistic level in tumor cells besides its use as a tool to dissect the Myc molecular function in cancer. Glioblastoma multiforme (GBM) and Burkitt's lymphoma (BL) are two very aggressive tumors in which Myc contribute to maintain oncogenic programs (De Bacco et al., 2014; Dalla Favera et al., 1982; Cesarman et al., 1987). The aim of this research was to interfere with Myc action using Omomyc in Brain Tumor 168 (BT168) and Ramos cells, derived respectively from human GBM and BL specimens. Specifically, our first interest was to evaluate the impact of Omomyc expression at the transcriptional level to identify the genes most significantly and differentially modulated by Myc inhibition in BT168 cells. This may lead to a better understanding of the gene networks critical for the GBM phenotype and pivotal to the anti-tumorigenic properties of Omomyc. In the second part of the project, considering that Myc regulates many aspects of transcription, from initiation to elongation and that Myc and PRMT5 functionally interact (Rahl et al., 2010; Mongiardi et al., 2014), we investigated a potential role of Myc in the PRMT5-dependent symmetrical di-methylation of R1810 residue at the carbossi-terminal domain (CTD) of RNA polymerase II

(RNAPII), required for termination process and splicing of the transcripts (Zhao et al., 2016).

5. Results

5.1 Omomyc suppresses tumorigenic features of glioblastoma stem-like cells and Burkitt's lymphoma cells. Omomyc is a potent tumor suppressor able to induce apoptosis and inhibit oncogenesis (Soucek et al., 2002 and 2008; Annibali et al., 2014). To better investigate the impact of Myc inhibition we employed the doxycycline-inducible pSLIK-Flag-Omomyc (FO) lentivirus (Fig. 1 A). We stably transduced the lentivirus in BT168 GSCs (De Bacco et al. 2012) and BL cells Ramos (Dalla Favera et al., 1982). Omomyc was detectable at 4–12 h post-doxycycline (DOX) treatment, reaching maximal levels at 36h-48 h (Fig. 1 B).

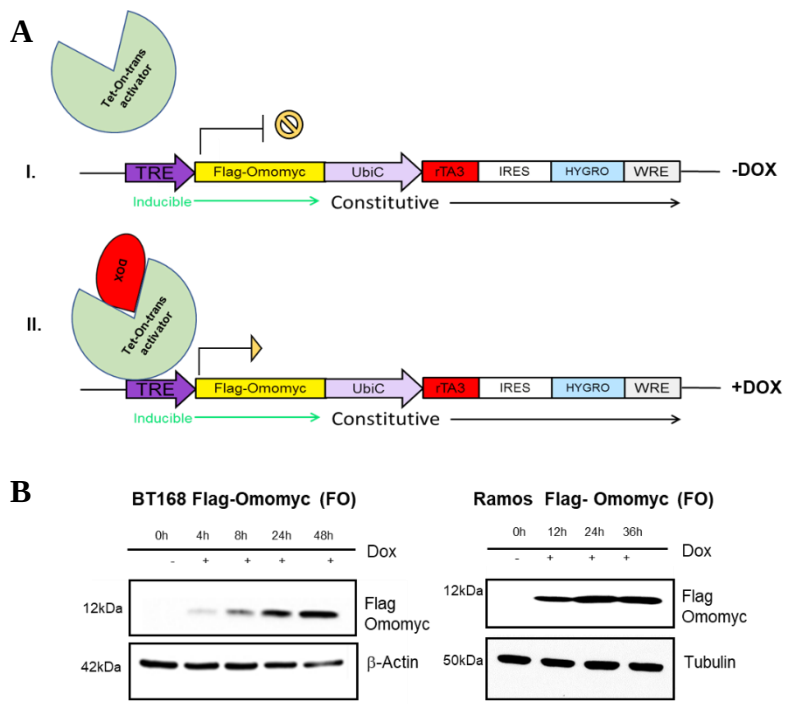

Fig. 1 - (**A**) Scheme of the inducible lentiviral expression vector pSLIK-Flag-Omomyc. **I**. In the absence of DOX, transactivator protein is not bound to the TRE (Tetracycline Responsive Element) promoter and Flag-Omomyc is not

expressed. **II.** DOX treatment induces conformational changes of transactivator protein which binds to TRE and promotes the Flag-Omomyc expression. (**B**) Representative immunoblots of Flag-Omomyc and β-Actin or Tubulin loading controls upon DOX treatment in BT168FO cells for 0–48h and Ramos FO cells for 0-36h.

DOX treatment caused a reduction of proliferation in BT168FO cells but not in control cells expressing a DOX-inducible green fluorescent protein (BT168GFP) (Fig. 2 A). Further, Omomyc expression induced a strong decrease of GSCs self-renewal capacity and neurosphere size (Fig. 2 B). In support to this observation, Omomyc decreased also the expression of genes involved in neural stem cell self-renewal and proliferation, such as SOX2, NOTCH1, CCND1 (cyclin D1), MYC and NESTIN (Gangemi et al., 2009; Piccin et al., 2013; Matsuda et al., 2015), while PTEN, a tumor suppressor, able to enhance differentiation and inhibit cell renewal (Zheng et al., 2008), increased (Fig. 2 C). Also, the migratory ability of GSCs, which accounts for their capacity to infiltrate the tumor (Chen et al., 2014), was strongly restrained by Omomyc (Fig. 2 D).

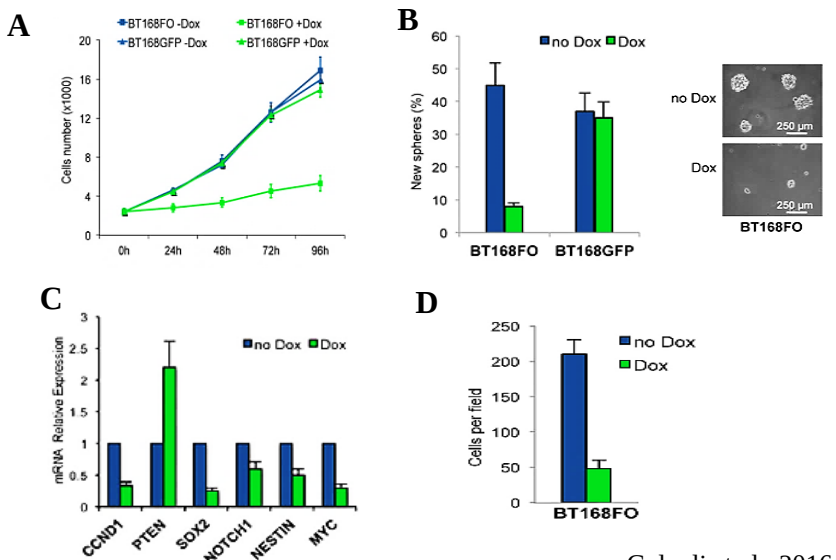

Galardi et al., 2016

Fig. 2 - Omomyc inhibits GSC cell proliferation, self-renewal, and migration. (**A)** Proliferation curves of BT168FO and BT168GFP cells upon DOX treatment for 0–96h (n=3; mean ± SD). Viable cells were counted using a hemocytometer. (**B**) Self-renewal assay upon DOX treatment. **Left**. Histograms show the percentage of BT168FO cells capable of re-forming neurospheres 7 days after dissociation and treatment (n=3; mean ± SD). **Right.** Representative image of neurospheres. (**C**) Evaluation, by qRT–PCR, of GSC markers' mRNA, CCND1, MYC, SOX2, NOTCH1, NESTIN and differentiation markers PTEN in BT168FO cells after 48h of DOX treatment, compared to uninduced cells (n=3; mean ± SD). (**D**) Transwell migration assay of BT168FO cells after 3 days with or without DOX treatment (n = 3; mean ± SD). Ten fields per assay were counted.

In RamosFO cells, Omomyc expression strongly reduced G1 phase progression (Fig. 3 A), increased the apoptotic rate (Fig. 3 B) (Soucek et al., 2002; Fiorentino et al., 2016), and upregulated the expression of the cell cycle inhibitor p21 (Fig. 3 C). This suggests that the cell cycle inhibition and apoptosis induction by Omomyc in Ramos cells may be related to an increase in p21 protein expression (Abbas et al., 2009).

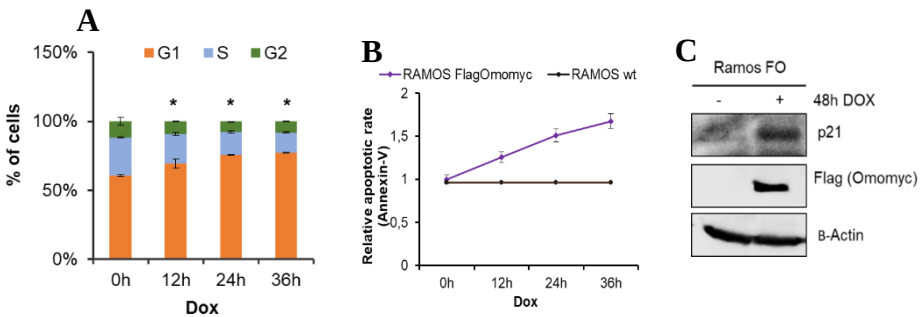

Fig. 3 - Omomyc inhibits cell cycle progression and increases apoptosis rate in RamosFO cells. (**A**) Cell cycle analysis following 12-36h DOX treatment. Cells were analyzed for cell cycle distribution by PI staining and flow cytometry. Histograms show the percentage of cells distributed respectively in G1, S and G2 phases (n=3, mean ± SD. Statistical analysis was performed by one-way ANOVA, p-value ≤ 0,05). (**B**) Apoptotic cell death analysis after 12-36h DOX treatment. Apoptosis was determined using the

Annexin V-FITC/PI double marked method by flow cytometry (n=2, mean ±SD). (**C**) Representative immunoblot showing p21 and β-actin loading control upon 48h DOX treatment of Ramos FO.

5.2 Impact of Omomyc expression on Myc genome occupancy. Myc binds to E-boxes of thousands of genomic loci with Max (Conacci-Sorrell et al., 2014), Omomyc inhibits Myc/Max heterodimers formation (Soucek et al., 1998). To assess the impact of Omomyc expression on Myc DNA binding, we performed chromatin immunoprecipitations with antibodies against Myc and Flag, followed by DNA sequencing (ChIP-seqs) in BT168FO cells treated or not with DOX for 24h. In untreated cells, we detected over 12,000 Myc peaks: 36% were localized at promoters, corresponding to 21% of all RefSeq promoters defined as -1,000 to + 100 bp regions surrounding the transcription start site (TSS), 37% were intragenic and 27% intergenic (Galardi et al., 2016). Omomyc expression led to a strong and genome-wide attenuation of Myc signals at promoters (Fig. 4). This was paralleled by the appearance of Omomyc signals in the same regions, as shown by the heat maps (Fig. 4 – left) and signal profiles of gene clusters (Fig. 4 – right). Further, in BT168FO cells, Omomyc distribution at the genomic loci of each gene clusters of Fig. 4 seems to overlap with Myc occupancy in uninduced cells. Indeed, Omomyc binds sequence motifs also bound by Myc in the minus DOX condition, as indicated by the motif enrichment analysis (Table 1, Galardi et al., 2016).

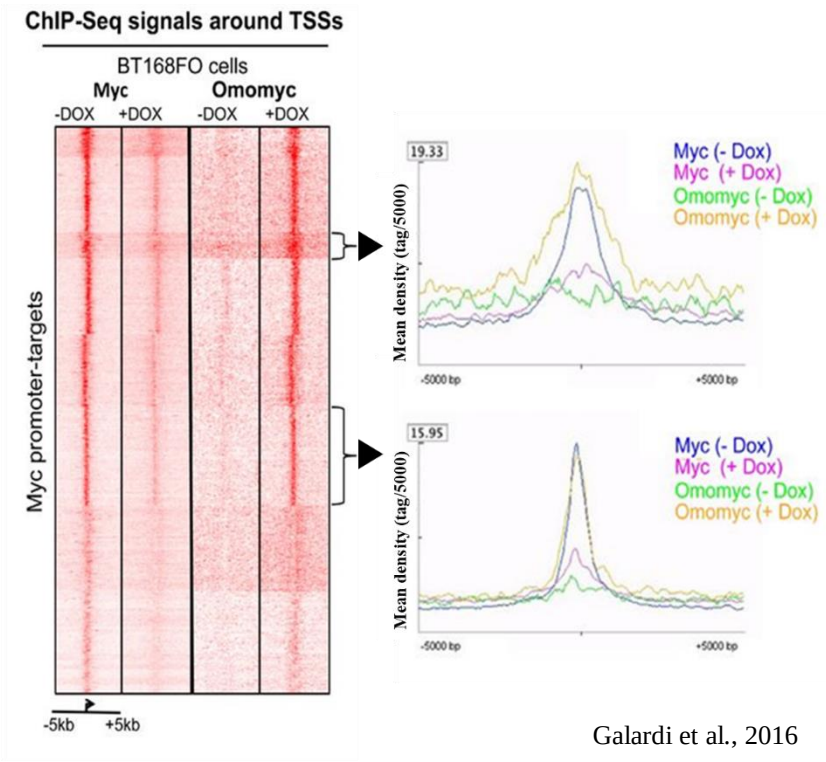

Galardi et al., 2016

Fig. 4 – Genome wide attenuation of Myc binding around TSSs upon Omomyc expression. Left**.** Seq-miner heatmaps of Myc and Omomyc occupancy at TSS of all Myc promoter-target genes in BT168FO, in the presence or absence DOX for 24h. TSSs regions are ranked by decreasing Myc occupancy in untreated cells. Colour scaled intensities are in units of tags per 50bp. The plots on the right depict Myc and Omomyc binding at cluster genes indicated by arrows, in cells, in the presence or absence DOX.

Table 1

Table 1. Motif enrichment analysis of Myc- and Omomyc-bound DNA sequences.

BT168FO no Dox			BT168FO +Dox			BT168FO +Dox		
Myc-bound motif	ID	G_P VALUE	Myc-bound motif	ID	G_P VALUE	Omomyc-bound motif	ID	G_P VALUE
Myc	MA0147.1	0	TBP	MA0108.1	7.16E-80	ZEB1	MA0103.1	4.82E-189
Mycn	MA0104.2	0	MEF2A	MA0052.1	1.56E-78	ZNF263	MA0528.1	2.34E-91
MYC::MAX	MA0059.1	0	MEF2C	MA0497.1	3.21E-78	PLAG1	MA0163.1	1.64E-70
USF1	MA0093.1	0	FOXL1	MA0033.1	1.54E-73	Klf4	MA0039.1	7.53E-43
Arnt	MA0004.1	0	Foxd3	MA0041.1	1.62E-67	Mycn	MA0104.1	2.03E-41
HIF1A::ARNT	MA0259.1	0	ARID3A	MA0151.1	6.43E-65	MZF1_5-13	MA0057.1	8.20E-35
Arnt::Ahr	MA0006.1	0	Lhx3	MA0135.1	1.17E-56	YY1	MA0095.1	8.62E-35
NRF1	MA0506.1	0	Prrx2	MA0075.1	6.80E-54	NR2C2	MA0504.1	3.39E-34
ZBTB33	MA0527.1	0	FOXP1	MA0481.1	1.67E-44	E2F6	MA0471.1	2.89E-31
EGR2	MA0472.1	0	CDX2	MA0465.1	8.95E-43	SP1	MA0079.2	1.05E-29
TFAP2A	MA0003.1	0	Pax4	MA0068.1	4.07E-42	Spz1	MA0111.1	1.79E-29
E2F3	MA0469.1	0	Nkx2-5	MA0063.1	8.36E-40	Arnt	MA0004.1	1.63E-28
E2F1	MA0024.2	0	Mecom	MA0029.1	9.81E-40	Myc	MA0147.2	4.79E-27
PLAG1	MA0163.1	0	ZEB1	MA0103.1	2.53E-39	EWSR1-FLI1	MA0149.1	6.62E-27
E2F4	MA0470.1	0	POU2F2	MA0507.1	6.76E-39	Zfx	MA0146.2	7.16E-24
NFKB1	MA0105.2	0	FOXI1	MA0042.1	1.39E-38	USF1	MA0093.1	7.27E-24
Zfx	MA0146.2	0	IRF1	MA0050.2	1.24E-36	PPARG::RXRA	MA0065.2	5.81E-22
E2F6	MA0471.1	0	HNF1A	MA0046.1	1.16E-34	MAX	MA0058.2	6.88E-22
EGR1	MA0162.2	0	Pdx1	MA0132.1	1.80E-34	MZF1_1-4	MA0056.1	1.21E-19
SP1	MA0079.3	0	SRY	MA0084.1	1.44E-31	SP2	MA0516.1	1.27E-18
Klf4	MA0039.2	0	Pou5f1::Sox2	MA0142.1	2.52E-26	PAX5	MA0014.2	1.86E-18
SP2	MA0516.1	0	Foxq1	MA0040.1	9.67E-26	E2F3	MA0469.1	2.08E-16
KLF5	MA0599.1	0	Sox2	MA0143.2	1.45E-25	Bhlhe40	MA0464.1	1.50E-15

Motif enrichment calculated by PscanChIP [64] from Myc and Omomyc ChIP-seq data in BT168FO cells, treated or not with doxycycline for 24 h. Motif IDs are from Jaspar database (http://jaspar.binf.ku.dk/).

Patterns of Myc and Omomyc ChIP-seq signals on three known Myc target genes - NCL (nucleolin), ODC (Ornithine decarboxylase) and MIR17HG (miR-17-92 microRNA cluster host gene) were thoroughly analyzed. Omomyc was enriched at target promoter regions upon the decrease of Myc signals, except for MIR17HG (Fig. 5 A).

We observed that Omomyc caused a significant increase in Max protein expression in parallel with a decrease of Myc protein expression in both DOX induced BT168FO and Ramos FO cells (Fig. 5 B). Therefore, we asked whether Omomyc replaces Myc on the genome in partnership with Max. For this purpose, we performed qChIP assays with Max antibody. Surprisingly, we found that Max binding was strongly impaired in the presence of Omomyc suggesting that Omomyc does not bind to DNA in a complex with Max (Fig. 5 C). Omomyc likely binds chromatin as homodimers, which is the most abundant form within cells (Savino et al., 2011; Jung et al., 2017).

A

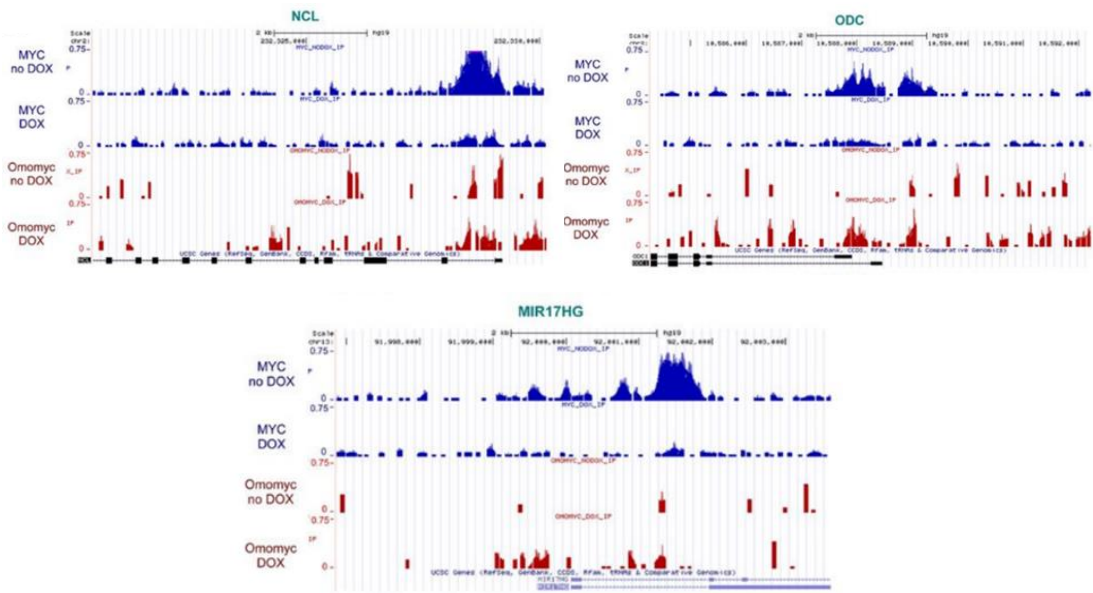

Galardi et al., 2016

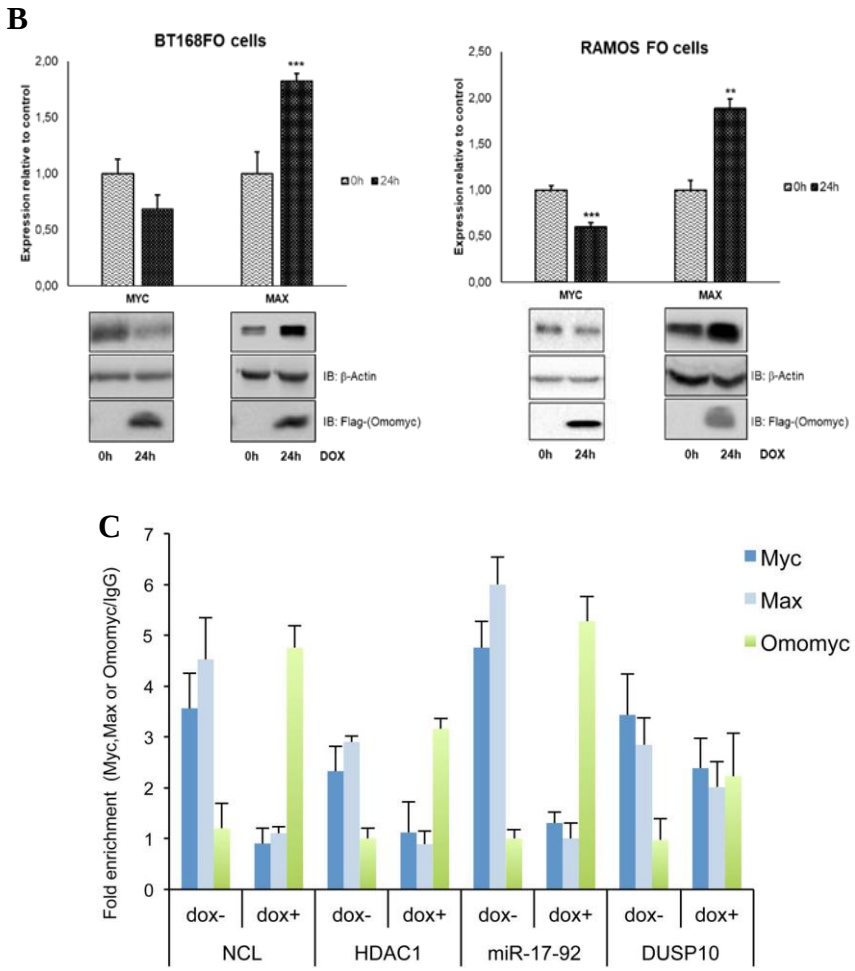

Fig. 5 - Omomyc attenuates Myc and Max binding at DNA. (**A**) Myc (blue) and Flag-Omomyc (red) ChIP-seq signals at Myc target genes in treated and untreated BT168FO cells: NCL, MIR17HG and ODC. (**B**) Representative immunoblots of BT168FO and Ramos FO cells induced for 24h and relative quantification of Myc and Max proteins expression, p-value** 0,01; p-value*** 0,0009 (mean ± SEM. Statistical analysis was performed by paired t-test). (**C**) qChIP assays from BT168FO cells, in the presence or absence DOX, and immunoprecipitated by Flag, Myc and Max antibodies (Galardi et al., 2016).

To investigate the global impact of Omomyc on the transcriptome and to analyze its relationship with Myc binding, we performed RNA-seq and compared the results with ChIP-seq. We defined the significantly modulated transcripts through CuffDiff2, as well as by applying a fold change cut-off ($log_2FC \geq 0.25$ or ≤ -0.25) and a *P*-value threshold. We also assessed significantly modulated Myc targets by Gene Set Enrichment Analysis (GSEA, www.broadinstitute.org/gsea/). The outcomes of these approaches were coherent (Galardi et al., 2016).

The analysis showed that 94% of Myc promoter-targets were transcribed (FPKM>0; FPKM: Fragments Per Kilobase of gene Million mapped reads). Myc promoter occupancy, defined in methods, grew together with transcript levels, confirming the correlation between increased transcription and increased Myc binding (Lin et al., 2012; Wolf et al., 2015). Myc promoter occupancy in the presence of Omomyc was reduced by 40-50% (Fig. 6 A, B) and the expression of Myc target genes was no longer Myc-dependent. Further, we found that Myc occupancy of downregulated genes ($log_2FC \leq -0.25$) was increased by 18% compared to upregulated genes ($log_2FC \geq 0.25$) in uninduced cells (Fig. 6 C). Although Myc occupancy was halved in both groups of genes in the presence of Omomyc, the difference in Myc occupancy between downregulated and upregulated genes was maintained, but in opposite manner: upregulated genes showed 10% increase of Myc occupancy compared to downregulated genes (Fig. 6 C).

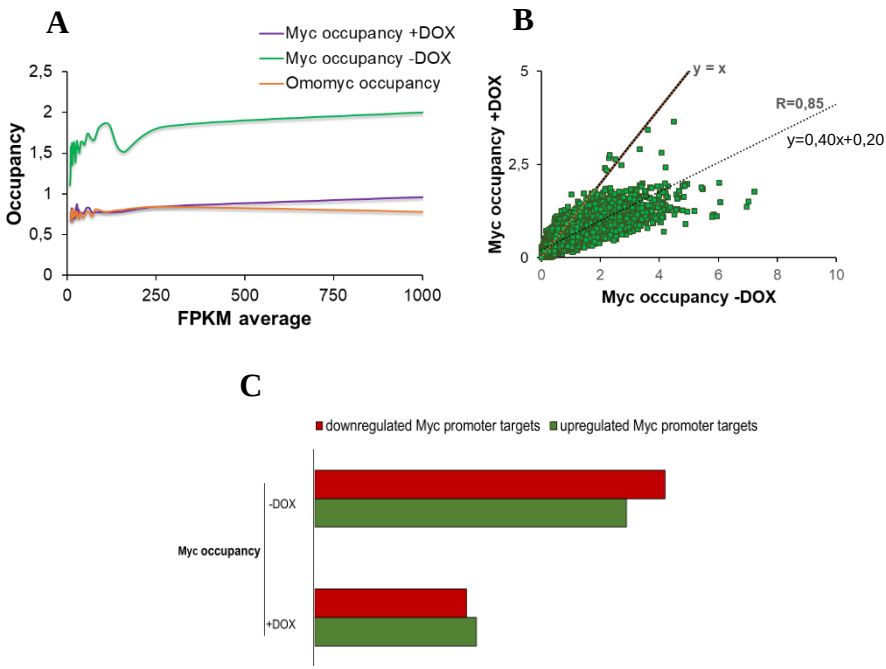

Fig. 6 - Myc and Omomyc occupancy on the genome. (**A**) Myc and Omomyc promoter occupancy correlate with transcript levels. Binned scatter plot displays Myc and Omomyc ChIP-seq reads at promoters (-1,000, +100 regions with respect to TSS) *versus* transcript levels (FPKM from RNA-seq data) in BT168FO cells untreated or upon 24h of DOX. (**B**) Scatter plot depicting the correlation between Myc occupancy in untreated *versus* treated BT168FO cells. (**C**) Bar graph shows the average of Myc occupancy, in the absence or presence of DOX, of Myc promoter-targets both downregulated and upregulated by Omomyc in BT168FO cells (cut off absolute value $\log_2$ FC 0,25).

5.3 Impact of Omomyc on GSCs transcriptome. Albeit we found that in untreated cells 94% of Myc promoter-targets were transcribed (Galardi et al., 2016), Omomyc expression does not modulate the gene expression of the majority of Myc targets, that we classified as unchanged (Fig. 7 A). Nevertheless, by comparing the average value of the expression level of Omomyc downregulated and upregulated Myc target genes in untreated *vs* treated BT168FO cells, we observed that, in the absence of Omomyc, downregulated genes were more highly expressed than the upregulated. This difference was maintained upon Omomyc expression (Fig. 7 A, B). Moreover, the degree of Omomyc influence on gene expression is described by a strong linear correlation between the expression level of genes at 0h *versus* 24h of Omomyc induction (Fig. 7 C). Indeed, we observed that as the expression of genes increases, the probability that these genes will be repressed by Omomyc increases (Fig. 7 D); conversely, Myc target genes expressed at a lower level in the absence of Omomyc are both 20% upregulated or downregulated (Fig. 7 E). Extending the analysis to all the genes, we found that Omomyc affected also the expression of those not directly bound by Myc, albeit most of the them were unchanged (Fig. 8 A). Nevertheless, also, in this case, the most highly expressed genes were preferentially downregulated by Omomyc (Fig. 8 B).

All Myc promoter-targets

A

	Myc promoter-targets (average FPKM)		n°genes	
Downregulated	87,60	68,37	12%	159
Unchanged	76,55	73,36	74%	1008
Upregulated	17,57	22,46	15%	204
	-DOX	+DOX		

B

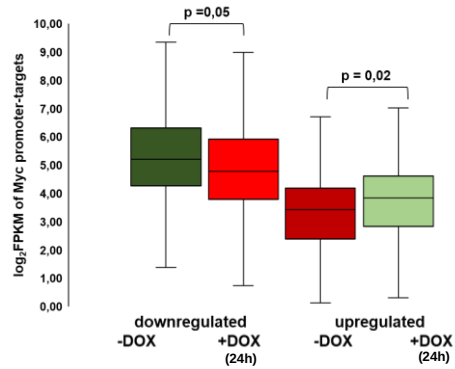

All Myc promoter-targets

C

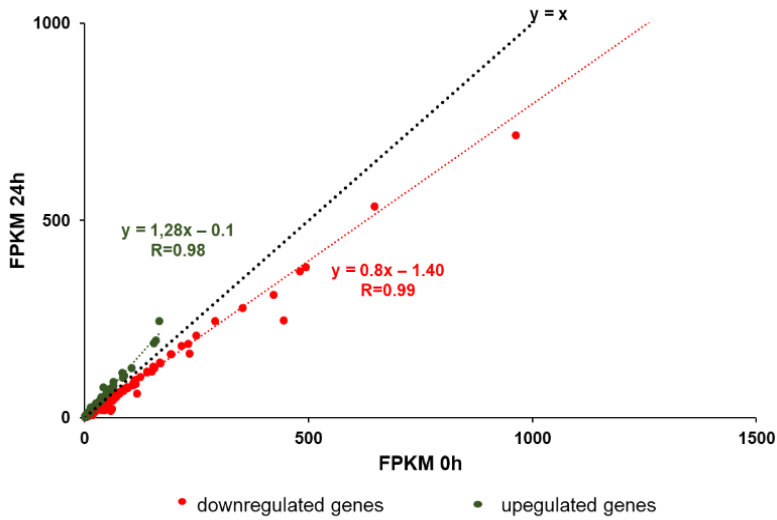

D **Myc promoter-targets (FPKM≥100 in -DOX)**

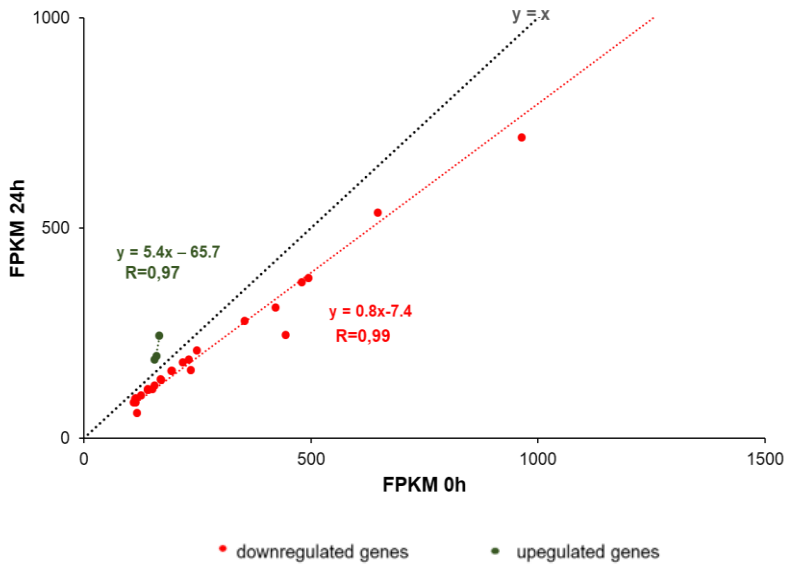

E **Myc promoter-targets (1≤FPKM≤100 in -DOX)**

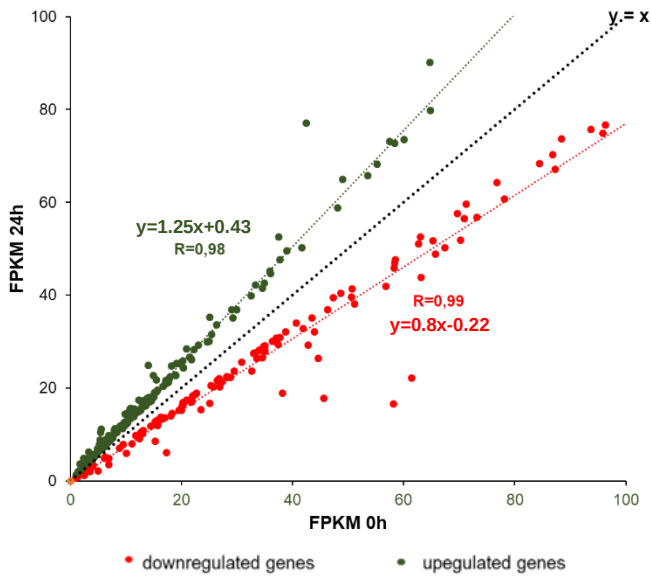

Fig. 7- Omomyc effect on the expression of Myc promoter-targets. (**A**) The table shows the average of FPKM of Myc targets (FPKM≥1) subdivided in downregulated, upregulated and unchanged genes upon 24h of Omomyc induction in BT168FO cells. (**B**) Box plot depicts the FPKM average values of downregulated or upregulated Myc targets in the presence or absence of Omomyc. n=3. The horizontal lines indicate median, whiskers extend to 1.5x interquartile range, while outliers are not shown. P-values (p) were calculated using two-sided, paired Wilcoxon signed-rank test. (**C**) Transcript level distribution (cut off absolute value $\log_2$ FC 0,25) of all Myc targets significantly downregulated (red dots) or up regulated (green dots) in cells treated with Dox for 24h *versus* untreated cells. Transcript levels, expressed as FPKM, represent the mean of three independent experiments. (**D-E**) Transcript level distribution of highly expressed Myc targets (FPKM≥100) or moderately expressed (1≤FPKM≤100).

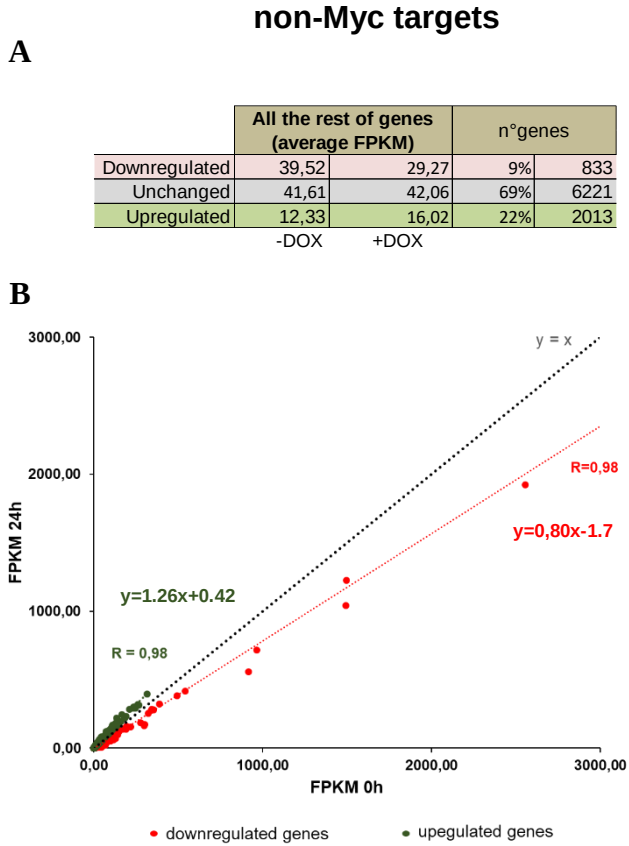

Fig. 8 – Impact of Myc inhibition on non-Myc targets. (**A**) The table shows the mean FPKM of non-Myc targets (FPKM>1) subdivided in downregulated, upregulated and unchanged genes upon 24h of Omomyc expression in BT168FO. (**B**) Dispersion graph shows the strong correlation (R=0,98 and R=0,99) between transcript level distribution of genes (cut off absolute value log_2 FC 0,25) significantly downregulated (red dots) or upregulated (green dots) in cells treated with DOX for 24h *versus* untreated cells (0h). Transcript levels, expressed as FPKM, represent the mean of three independent experiments.

To clarify the function of Omomyc modulated genes, we investigated the overlap of genes regulated by Omomyc at 4, 8, 16, 24 and 48 h in BT168FO cells with the hallmark gene sets of the Molecular Signature Database (MsigDB). For Myc targets, we found highly significant overlaps with gene sets related to epithelial-mesenchymal transition, TNFA signaling via NF-κB, hypoxia, angiogenesis, inflammatory response, p53 signaling, glycolysis, WNT beta-catenin signaling, mitotic spindle, UV response, E2F targets at 4h – 8h of Omomyc induction. At 16h - 48h, instead, we observed a significant modulation of MTORC1 signaling, DNA repair, KRAS signaling, NOTCH signaling, G2M checkpoint, oxidative phosphorylation (Fig. 9 A). Hence, we observed an early and delayed specific action of Omomyc in modulating pathways in which Myc may have a role (Fig. 9 A). The same analysis was performed on non-Myc targets and showed a significant modulation of pathways overlapping those associated to Myc targets, such as hypoxia, oxidative phosphorylation, G2M checkpoint, DNA repair, UV response (Fig. 9 B). The appearance of different pathways in MsigDB analysis at early and longer times of Omomyc induction was coherent with the growing number of genes – both Myc and non-targets - modulated by Omomyc throughout the time course (Fig. 9 C). This suggests that Omomyc may affect the expression of specific gene sets, that, in turn, cause a sort of *domino* effect, resetting the transcription of key gene networks for GSC phenotype.

A

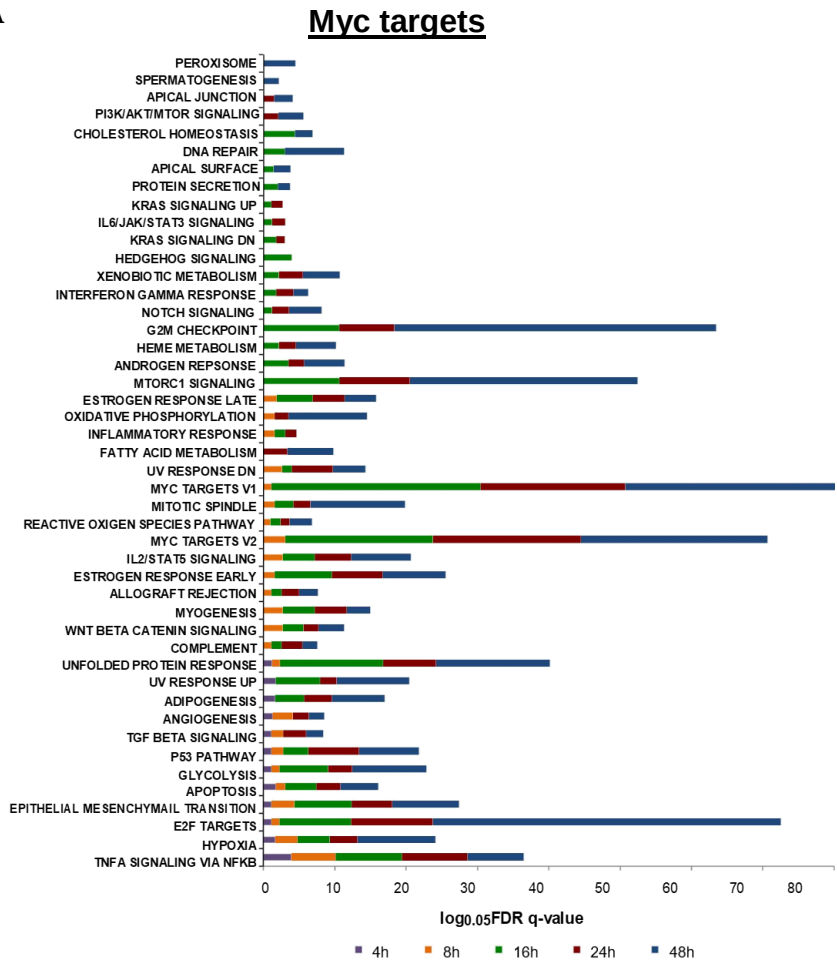

Galardi et al., 2016

B

Non-Myc targets

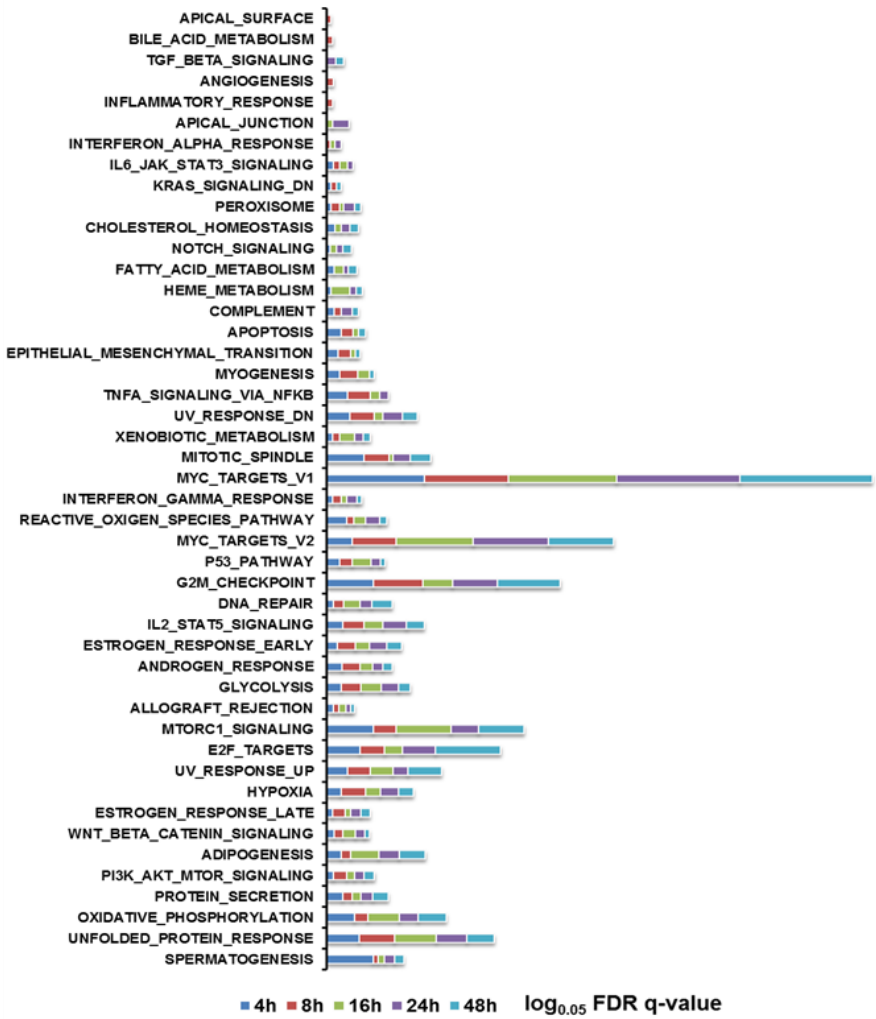

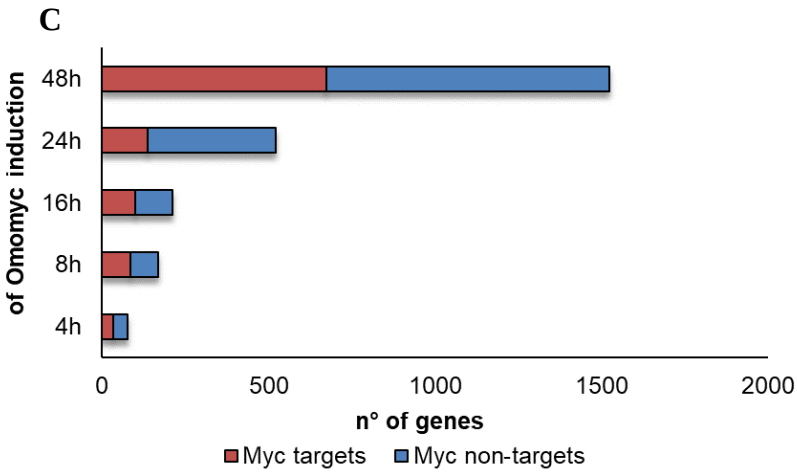

Fig. 9 - Gene Set Enrichment Analysis (GSEA) - MSigDB of all genes significantly modulated by Omomyc in BT168FO cells. (**A**) Enrichment of MsigDB hallmark gene sets among genes with a Myc peak, at promoter, intragenic, and intergenic regions in BT168FO cells and whose mRNAs are modulated by Omomyc (estimated by CuffDiff2 and GSEA; q-value ≤0,05). (**B**) Enrichment of MsigDB hallmark gene sets among all non-Myc target genes significantly modulated by Omomyc (estimated by CuffDiff2 and GSEA; q-value ≤ 0,05). FDR q-values were computed through GSEA (FDR q-values ≤ 0,05). Bar colours indicate the different time points of DOX treatment (0-48h), while their height represents the $\log_{0,05}$ of the FDR q-value of each gene set. (**C**) Each bar shows the increasing number of genes significantly (q-value ≤0,05) modulated by Omomyc along the time course 0-48h of DOX treatment.

These data show that Omomyc inhibits Myc activity at DNA-binding level and affects the expression of Myc-dependent gene regulatory networks.

5.4 Omomyc minimally – or not at all - influences the global RNAPII binding at promoters and affects transcription in a subset of target genes only. Myc is found at promoters of all active genes, triggering transcriptional amplification by pausing release, with consequent increase of transcripts level (Rahl et al.,

2010; Lin et al 2012; Nie et al., 2012). We asked whether Myc replacement by Omomyc would influence RNA polymerase II (RNAPII) loading at promoters and transcriptional elongation. To this aim, we performed ChIP-seq experiments in BT168FO cells using a RNAPII antibody in the presence or absence of Omomyc and compared the results with RNA-seq. We did not observe relevant global changes of RNAPII loading around TSSs (Fig. 10 A). Further, we analyzed RNAPII traveling ratio (TR), an index for evaluating the pause release (Rhal et al. 2010), from the RNAPII ChIP-seq experiments in minus *versus* plus Dox. We found that Omomyc minimally changes the TR, suggesting that it does not significantly impact on pause release (Fig. 10 B). These data suggest that Omomyc only marginally affects RNAPII loading at promoters and pause release.

However, we asked whether loss of Myc binding, Omomyc presence at Myc genomic loci and RNAPII distribution were correlated to a specific set of genes. To this aim, we analyzed OLIG2 and miR-17-92, together with NCL, HDAC1 and DUSP10. They all were expressed at good levels (FPKM> 4) in BT168FO cells and showed a decrease of Myc binding at their respective promoters (blue; Fig. 10 C) upon Omomyc induction. Indeed, NCL, miR-17-92 and OLIG2 clearly displayed decreased transcript levels (Fig. 10 D). Omomyc binding (green; Fig. 10 C) was associated with minimal changes of RNAPII signals at TSSs, except for OLIG2. No correlation was observed between decreased Myc binding and transcript levels of HDAC1 and DUSP10, whose mRNA levels were barely affected by Omomyc (Fig. 10 C and D). To note, a reduction of RNAPII signals at transcription termination sites (TTSs) was found for OLIG2 and miR-17-92 (Fig. 10 C). NCL and miR-17-92 are well-known Myc upregulated targets in different cell contexts; on the contrary, Myc-dependent regulation of OLIG2, one of the master controllers of neural stem cell behavior, was unknown.

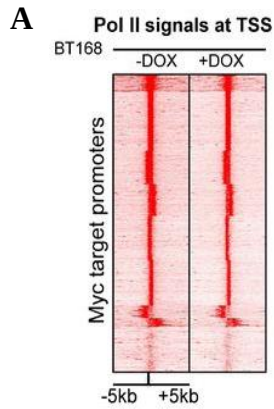

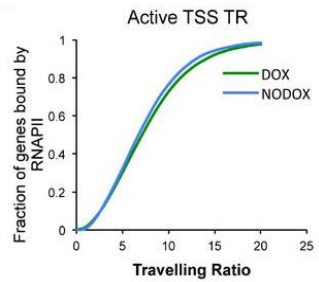

	DOX	NO DOX
TR > 2	10405	10473
%	93,85	94,5
TR <= 2	682	614
%	6,15	5,53

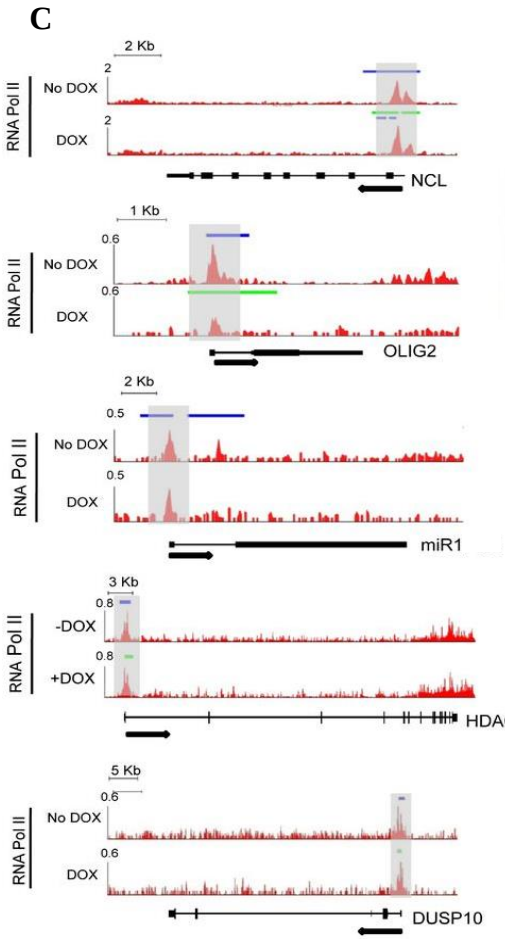

D

DOX	Gene expression level * - 0h	+ 24h	+ 48h
NCL	586.43	428.64	386.54
miR-17-92	4.03	1.23	0.60
OLIG2	57.47	13.00	10.41
HDAC1	124.53	159.03	132.40
DUSP10	7.48	6.74	7.62

*FPKM

Galardi et al., 2016

Fig. 10 – Correlation between RNAPII, Myc and Omomyc occupancy. (**A**) Heatmap of RNAPII signals around TSSs of Myc promoter-target genes in BT168FO cells, in the presence or absence of DOX for 24h. The data are ranked by decreasing Myc occupancy in uninduced BT168FO cells. Each row shows the ± 5 kb region centred on TSSs. Colour scaled intensities are in tags/50 bp. (**B**) Traveling ratio of RNAPII from ChIP-seqs in the presence or absence of Omomyc. (**C**) RNAPII tracking by ChIP-seq at NCL, OLIG2, miR-17-92, HDAC1 and DUSP10 genes in BT168FO cells (-/+DOX). The y-axis displays RNAPII binding signals as tags/500 bp per million reads, whereas x-axis shows genomic positions. Arrowheads indicate the direction of transcription. In blue Myc peaks and in green Omomyc peaks, grey boxes are TSS regions. (**D**) Gene expression levels of genes shown in B (n=3).

5.5 Myc strengthens the regulatory nodes of glioblastoma gene expression networks. The direct regulatory functions of Myc remain debated. Two models have been proposed to explain its function: one proposes that Myc acts as a *universal amplifier* of all active genes (Lin et al., 2012; Nie et al., 2012), while the other model defines Myc as a *specifier*, that is a gene-specific regulator (Walz et al., 2014; Sabò et al., 2014). Altogether, our previous observations do not clarify whether Omomyc affects GSCs transcriptome directly or indirectly and how the changes of the expression of many genes may have a tumor suppression-specific effect. A possible explanation may be that Omomyc affects the control points of gene expression networks that sustain cancer stem cell behavior.

To test this hypothesis, we investigated the expression level of a set of genes selected for being related to such control points, according to literature data. We considered some universal Myc targets, by which Myc exerts its tumorigenic properties, transcription factors and other effectors involved in tumorigenesis and tumor suppression in several tumors, including GBM, and cell-specific factors that maintain GSCs phenotype (Suvà et al., 2014). We analyzed Myc targets CCND1, CDK6 and NCL and the miR-17-92 cluster, which have a role in cell proliferation, cell growth control and glioblastomagenesis (Daniel et al., 2014; Bellail et al., 2014; Goldsmith et al., 2014). Moreover, miR-17-92 inhibits, in turn, the expression of chromatin regulatory genes

like Sin3b (cellular senescence regulator), Hbp1 (neurogenesis regulator) and Btg1 (neuronal precursor regulator), maintaining a neoplastic state (Li et al., 2014). They were all strongly downregulated by Omomyc (Fig. 11 A). Furthermore, Omomyc expression repressed FOS, JUN and ID4 transcripts, encoding transcription factors that have a role in GBM onset and progression. On the contrary, Omomyc upregulated the tumor-suppressive phosphatases PTEN and PPP2R5A (protein phosphatase A regulatory subunit), a regulator of mitotic progression, and the long non-coding RNA (lncRNA) MIAT/GOMAFU, involved in neurogenic commitment and differentiation (Aprea et al., 2013). We also examined the dual specificity protein kinase phosphatases (DUSPs) which control MAP kinase signaling. Omomyc can affect components of this family genes in either direction. Notably, Omomyc strongly affected the expression of DUSP 4, 5, 6 (Fig. 11 A) which have been implicated in glioblastomagenesis (Prabhakar et al., 2014).
GSCs phenotype *in vitro* and *in vivo* is maintained by a set of 19 TFs. A core subset of four of these TFs are enough for maintaining of GSC phenotypes. The four core TFs target a set of 325 genes (Suvà et al., 2014). By GSEA, we found that the set of 19 GSC-specific TFs was significantly associated with repression in response to Omomyc (Fig. 11 A). Omomyc downregulated the expression of three of the four core TFs, specifically POU3F2, OLIG2, and SOX2. Also, KDM1A (LSD1) lysine-specific histone demethylase/RCOR2 complex, which is a key effector of OLIG2 in GSCs, is repressed by Omomyc (Suvà et al., 2014; Yang et al., 2011). All these genes are Myc targets and their respective target genes were repressed by Omomyc (Fig. 11 A). Interestingly, Myc-dependent signatures, typical of other cell types, were significantly modulated by Omomyc in GSCs (from MSigDB Database v6.2). By GSEA-MSigDB software, we found that several Myc-upregulated gene signatures were downregulated by Omomyc in GSCs, while the opposite happened for Myc-downregulated gene signatures (Fig. 11 B and C). In conclusion, Myc inhibition by Omomyc not only strongly

influenced the transcript levels of key TFs responsible of GSC identity, of their targets and chromatin modifiers but also affected genes commonly modulated by Myc in other cellular contexts.

A

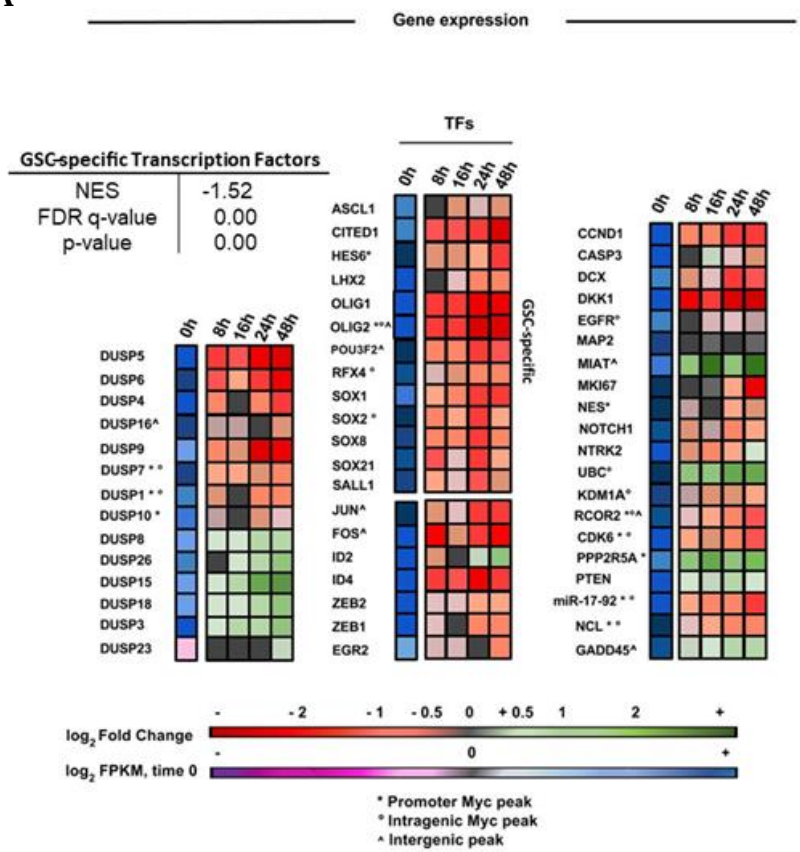

B

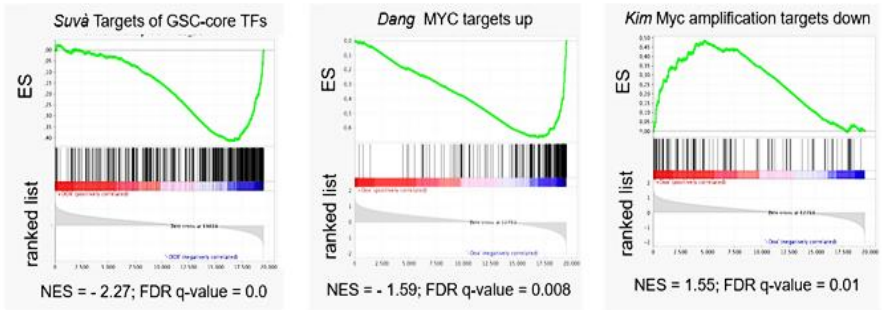

C

Repressed in response to Omomyc

gene set	NES	FDR q-value
Suvà Targets of GSC core-TFs	- 2.27	0.000
Benporath Myc targets with E-BOX	- 1.47	0.002
Dang regulated by Myc up	- 1.71	0.006
Kim Myc amplification targets up	- 1.48	0.070
Schlosser Myc targets up	- 1.63	0.000
Schuhmacher Myc targets up	- 1.67	0.002

Activated in response to Omomyc

gene set	NES	FDR q-value
Kim Myc amplification targets down	1.55	0.01
Kim N-Myc amplification targets down	1.60	0.00
Cowling N-Myc targets	1.35	0.10
Dang Myc targets down	1.26	0.14

Galardi et al., 2016

Fig. 11 - Omomyc resets regulation nodes of GSCs. (**A**) RNA-seq expression values of selected genes in BT168FO GSCs along a 48h time course of Omomyc induction (n=3). The block on the left represents DUSP family genes. The middle block contains transcription factors (TFs): the upper thirteen (from ASCL1 to SALL1) are GSC-specific and the remaining ones are oncogenes. The genes of the right block are well-known Myc targets, involved in proliferation, neurodifferentiation and gliomagenesis. The first column of each block represents the average expression (log_2 FPKM) in untreated cells (0h) in the colour scale illustrated by the lower bar: violet indicates low and blue high expression. The other columns depict relative expression versus untreated cells (average log_2FC) at different times (8 - 48h) of DOX treatment, according to the scale shown by the upper bar: red indicates low and green high expression. The table in the upper left indicates the GSEA (Gene Set Enrichment Analysis) score of 19 GSC-specific transcription factors (NES, normalized enrichment score; FDR q-value, False Discovered Rate). (**B**) Enrichment plots obtained by GSEA of RNA-seq data from BT168FO. **Left.** The set of genes targeted by the GSCs core TFs downregulated by Omomyc (Suvà et al., 2014). **Middle**. A dataset of genes upregulated by Myc in cancer cells (Zeller et al., 2003) and downregulated by Omomyc in BT168FO cells. **Right**. Genes downregulated

in small cell lung cancers carrying Myc amplification (Kim et al., 2010) and upregulated by Omomyc. (**C**) The tables show enrichment analysis of some Myc-regulated gene sets, taken from MSigDB database (Ben-Porath et al., 2008; Schlosser et al., 2005; Schuhmacher al., 2001; Cowling et al., 2008), and of the gene set targeted by the GSC core TFs (Suvà et al., 2014), *versus* genes repressed (left table) or induced (right table) by Omomyc.

5.6 Omomyc decreases the expression of a gene set specifically bound by Myc. As stated before, the *universal amplifier* model does not distinguish direct from indirect transcriptional Myc responses. Very recently, a signature of 100 most strongly downregulated genes, validated as a Myc core gene set and conserved in several cancer cell lines, was identified (Muhar et al., 2018). These genes were directly activated by Myc and were characterized by a strong binding of Myc at their promoters. In this view, Myc has the capacity to activate selective transcriptional programs.

We therefore decided to verify the presence of this specific Myc signature (102 most downregulated genes from Muhar et al., 2018) in BT168FO cells and to investigate Omomyc effect on gene expression. We found that 91 of 102 genes were expressed (FPKM≥1) in uninduced BT168FO cells.

Thereafter, to unravel whether they were bound by Myc at their respective promoters, we defined as Myc promoter-targets all genes with RPKM≥0.5 and subdivided them in two groups: targets highly bound by Myc (RPKM≥1) and targets weakly bound by Myc (0,5<RPKM<1). We found that 75 of 91 genes resulted highly bound by Myc, while 11 genes overlapped with weakly Myc bound targets set, and only 5 of 91 genes were not bound by Myc in BT168FO (Fig. 12 A). Further, we asked whether the set of 91 genes was differentially expressed, in the presence or absence of Omomyc. To this aim, we performed GSEA using all our RNA-seq data. We assessed that 82 of these 91 genes were significantly repressed in the presence of Omomyc (Fig. 12 B, top). We also evaluated how many genes were able to

respond to short times of Omomyc induction (4-8h). We found that 77% of these 82 genes were significantly repressed by Omomyc after 4h of doxycycline treatment and the repression persisted along the whole-time course (up to 48h) (Fig. 12 B, bottom).

Therefore, we concluded that 89% (91 of 102) of Myc Muhar signature is expressed in GSC cells. 95% (86 of 91) of these genes are bound by Myc and Myc could primarily act as a selective transcriptional activator, controlling protein and nucleotide biosynthesis, ribosome biogenesis factors, key regulators in AMP metabolism (MsigDB GO analysis, Fig. 12 C; Muhar et al., 2018). This supports the hypothesis that Myc may directly activate specific transcriptional programs, which, in turn, may induce the expression of other downstream genes, increasing transcripts level as secondary effect.

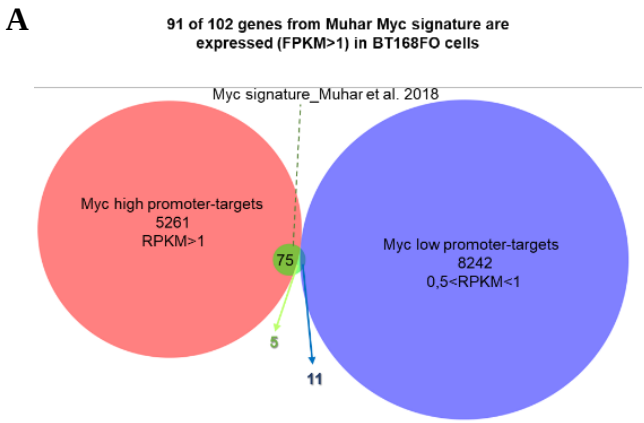

B

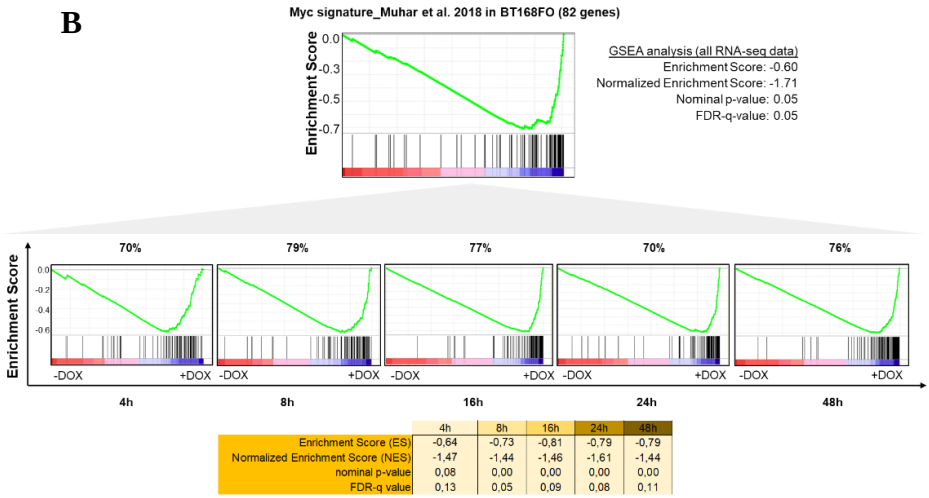

	4h	8h	16h	24h	48h
Enrichment Score (ES)	-0,64	-0,73	-0,81	-0,79	-0,79
Normalized Enrichment Score (NES)	-1,47	-1,44	-1,46	-1,61	-1,44
nominal p-value	0,08	0,00	0,00	0,00	0,00
FDR-q value	0,13	0,05	0,09	0,08	0,11

C

MsigDB Gene Ontology analysis

Gene set name	FDR q-value
GO_RIBOSOME_BIOGENESIS	1.37E-20
GO_POLY_A_RNA_BINDING	1.37E-20
GO_RIBONUCLEOPROTEIN_COMPLEX_BIOGENESIS	5.98E-20
GO_RNA_BINDING	4.27E-19
GO_NCRNA_METABOLIC_PROCESS	4.68E-17
GO_RRNA_METABOLIC_PROCESS	3.64E-15
GO_NCRNA_PROCESSING	1.67E-14
GO_RNA_PROCESSING	5.22E-14
GO_SNORNA_BINDING	9.06E-13
GO_RIBOSOMAL_LARGE_SUBUNIT_BIOGENESIS	1.99E-6
GO_SMALL_MOLECULE_METABOLIC_PROCESS	7.05E-6
GO_POSITIVE_REGULATION_OF_GENE_EXPRESSION_EPIGENETIC	1.79E-5
GO_ORGANONITROGEN_COMPOUND_METABOLIC_PROCESS	6.1E-5
GO_MATURATION_OF_SSU_RRNA	7.57E-5
GO_NUCLEOBASE_CONTAINING_SMALL_MOLECULE_METABOLIC_PROCESS	8.58E-5
GO_NUCLEOTIDYLTRANSFERASE_ACTIVITY	1.8E-4
GO_RIBOSOMAL_SMALL_SUBUNIT_BIOGENESIS	2.5E-4
GO_ORGANOPHOSPHATE_METABOLIC_PROCESS	2.98E-4
GO_NUCLEOSIDE_PHOSPHATE_BIOSYNTHETIC_PROCESS	8.85E-4
GO_ORGANONITROGEN_COMPOUND_BIOSYNTHETIC_PROCESS	8.85E-4

Fig. 12 - Omomyc decreases the expression of specific Myc signature. (**A**) Venn diagrams between Myc promoter-targets and Myc Muhar signature (Muhar et al. 2018) gene sets. (**B**) GSEA enrichment profiles of Myc Muhar signature gene set using all RNA-seq (0-48h of Omomyc induction) data from BT168FO cells (**top**), and GSEA profiles for each time point of DOX treatment

(4-48h) (**bottom**). The Myc Muhar gene set is significantly decreased by Omomyc (see also orange table). Abbreviations: NES, normalized enrichment score; FDR, false discovery rate. **(C**) MsigDB Gene Ontology analysis on each Myc Muhar gene set of **A.**

5.7 Myc promotes the symmetrical di-methylation of Arginine 1810 (R1810) residue of RNAPII. Myc regulates many aspects of transcription by RNAPII (Rahl et al., 2010) but its role in transcript termination is unknown. Recently, it has been reported that termination of transcription is regulated by the symmetrical di-methylation of RNAPII carboxy-terminal domain (CTD) mediated by PRMT5. This modification allows the recruitment of proteins like SMN necessary for resolving R-loops in transcription termination regions, thus allowing proper termination and splicing of transcripts (Zhao et al., 2016). Myc and Omomyc functionally interact with PRMT5 (Mongiardi et al., 2015). Therefore, we asked whether Myc may regulate transcription termination and if Omomyc may interfere with this process. To investigate the potential role of Myc in the symmetrical di-methylation of R1810-CTD-RNAPII we overexpressed Myc transfecting CbS-Flag-Myc construct in HEK-293T cells. In parallel, we transfected also Flag-Omomyc (CbS-Flag-Omomyc) either alone or in combination with Flag-Myc. We also performed the same experiment in the presence of a short-hairpin RNA for Myc (shMyc). Cell extracts from transfected cells underwent several immunoprecipitation analyses, to pull down RNAPII using the 8WG16 antibody. We found that Myc overexpression induced a significant (p-value 0,001) symmetrical di-methylation of R1810, whereas Myc inhibition by shMyc decreased the di-methylation level (p-value 0,05) (Fig. 13 A). Omomyc seems to counteract the capacity of Myc to promote R1810me2s in co-transfection experiments. Surprisingly, Omomyc alone appeared to increase the RNAPII-R1810me2s level (Fig. 13 A and see also B). We did not observe

a coherent increase or decrease of SMN proteins associated with RNAPII in parallel to the symmetrical di-methylation of R1810 (Fig. 13 A). We have also found that Myc and Omomyc co-immunoprecipitated with RNAPII (Fig. 13 B).

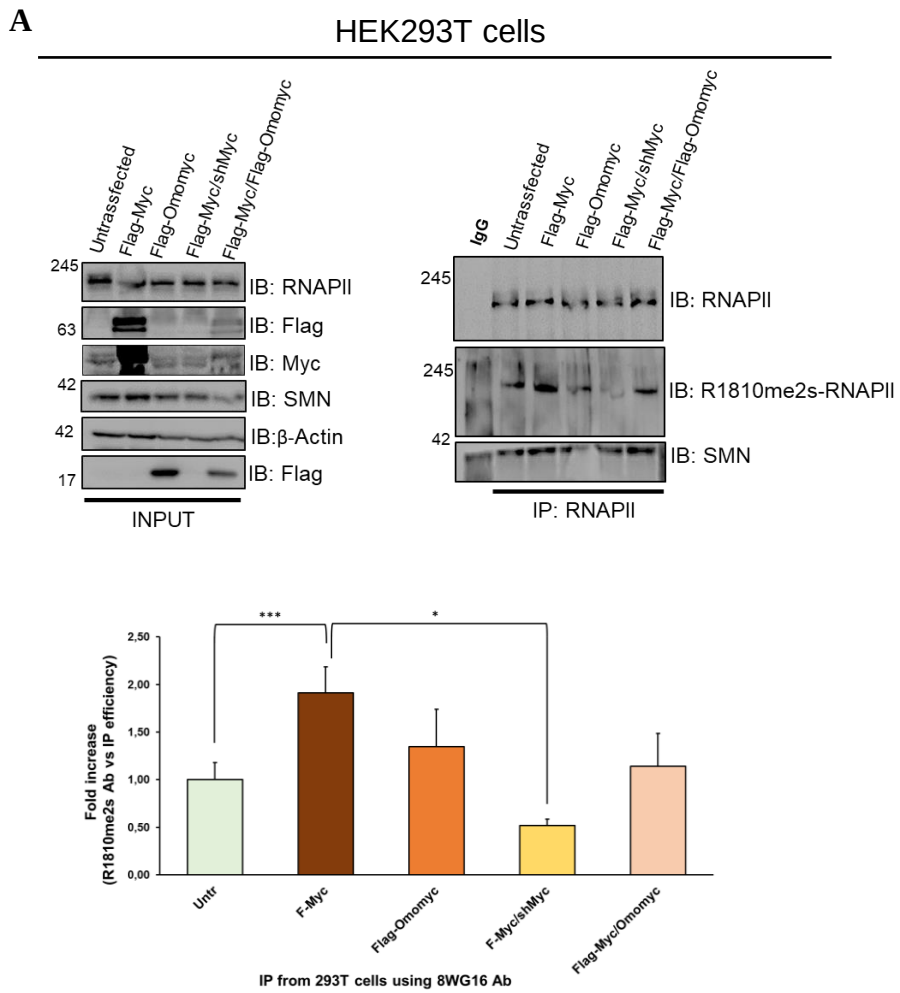

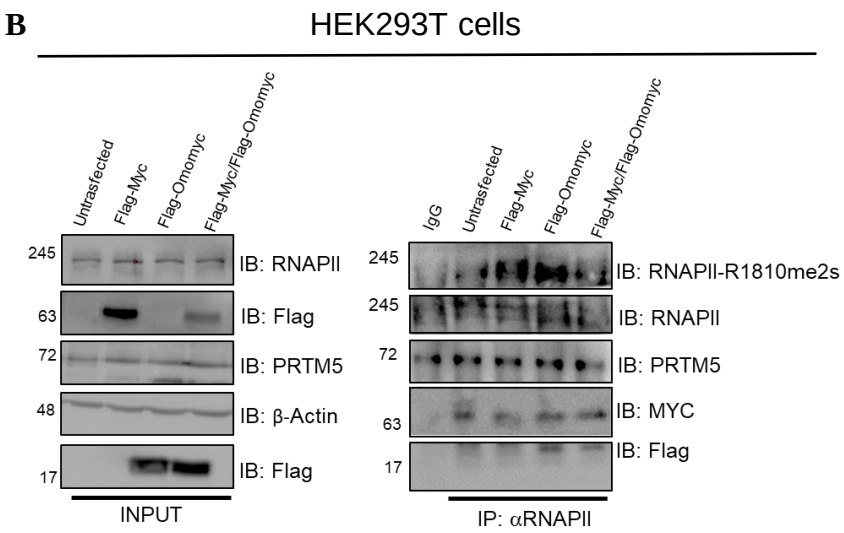

Fig. 13 - Myc modulates the symmetrical di-methylation of R1810 on the RNAPII CTD. (**A**) HEK293T cells were transfected with CbS-Flag-Myc, CbS-Flag-Omomyc vectors, either alone or in combination, and with CbS-Flag-Myc/pSLIK-shMyc plasmids. RNAPII was immunoprecipitated using the 8WG16 antibody and the symmetrical di-methylation level of R1810 on RNAPII CTD was mesaured by immunoblot, using a R1810me2s antibody, courtesy of J. F. Greenblatt's lab, Donnelly Center – University of Toronto, Canada. **Bottom.** The graph shows densitometry of western blots. Each bar represents mean±SEM. ***p-value 0,001, *p-value 0,05 repeated measures one-way ANOVA. (**B**) Representative immunoblot of immunoprecipitation (IP) experiments from HEK293T cells showing Myc and Omomyc immunoprecipitated with RNAPII.

To gain more insights into Myc capacity to promote the symmetrical di-methylation of R1810-CTD-RNAPII, we induced Omomyc for 24h both in BT168FO and RamosFO cells. By co-immunoprecipitation experiments, we found that Omomyc significantly inhibited R1810me2s in both cell lines (Fig. 14 A and B) and Myc and Omomyc co-purify with RNAPII (Fig. 14 B). The same result was obtained in BT168 cells stably transduced with a doxycycline-inducible lentivirus encoding for a shRNA for Myc (pSLIK-shMyc, Fig. 14 C). Myc inhibition

through the shMyc decreased the symmetrical di-methylation of R1810, and the association of either PRMT5 or SMN with RNAPII (Fig. 14 C).

A

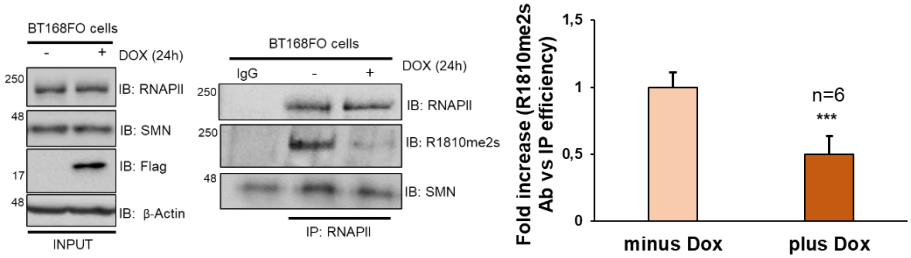

B

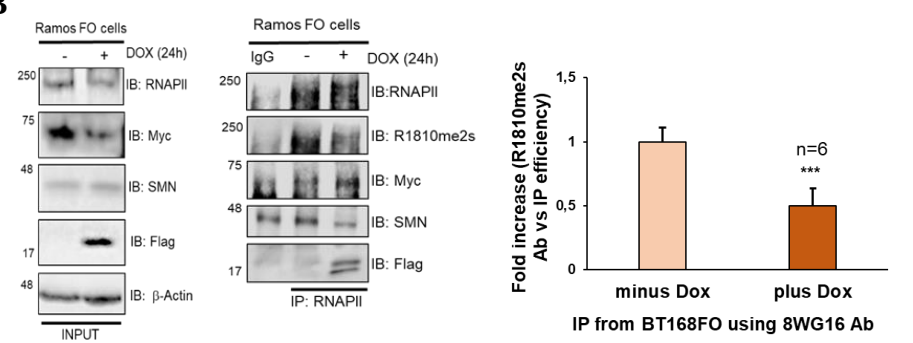

C

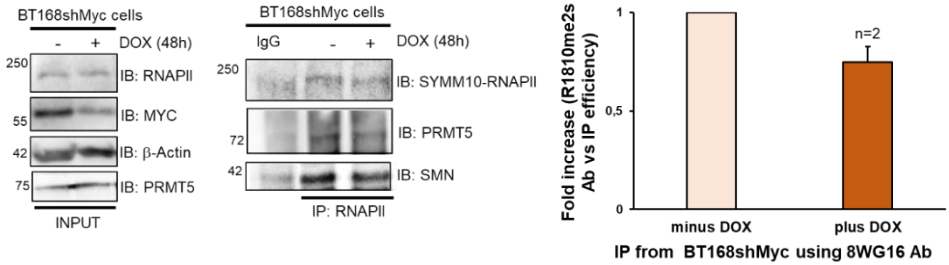

Fig. 14 - Omomyc or shMyc inhibits the symmetrical di-methylation of R1810 residue on the CTD of RNAPII. Left panel show representative immunoblots of IPs from BT168FO (**A**), RamosFO (**B**) and BT168shMyc (**C**) cells induced for 24h or 48h, performed using the 8WG16 antibody against RNAPII. R1810me2s antibody was used to reveal the symmetrical methylation signal of RNAPII on R1810 residue. Each bar represents mean±SEM. ***p-value 0,001*p-value 0,05 paired t-tests.

5.8 Myc-dependent R1810 symmetrical di-methylation requires PRMT5 catalytic activity. PRMT5 associates with Myc mediating H4R3me2s) (Mongiardi et al., 2014). Further, Myc induces the transcription of *prmt5* gene (Koh et al., 2015) and R1810me2s modification requires PRMT5 (Zhao et al., 2016). To verify whether Myc-induced R1810 symmetrical di-methylation of RNAPII was PRMT5-dependent, we transfected HEK293T cells with CbS-Flag-Myc. The day after, transfected cells were treated with EPZ015666, a selective inhibitor of PRMT5 function, or control vehicle for 24h. Thereafter, immunoprecipitation experiments were performed. PRMT5 catalytic inhibition strongly restrains Myc-dependent R1810 symmetrical di-methylation of RNAPII (Fig. 15).

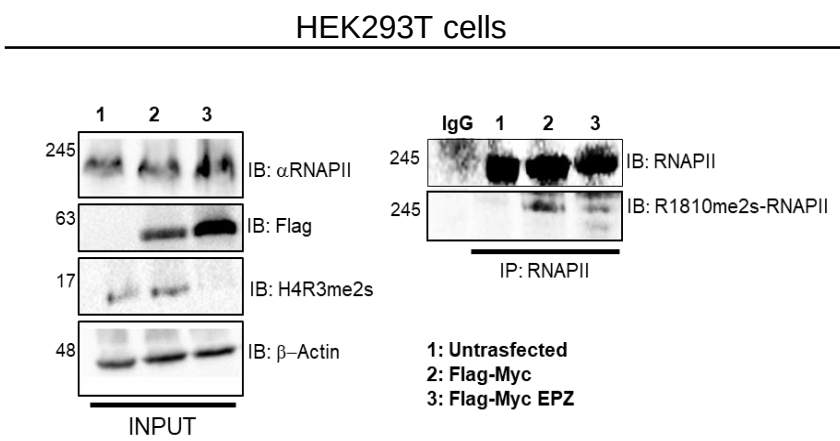

Fig. 15 – PRMT5 catalytic inhibition restrains Myc-dependent R1810 symmetrical di-methylation. Immunoblots of immunoprecipitation or input

from HEK293T cells transfected with CbS-Flag-Myc and treated or untreated with EPZ. H4R3me2s signal (INPUT) confirms the inhibition of PRMT5 function upon EPZ treatment. EPZ=EPZ015666

5.9 Myc and Omomyc modulate RNAPII carbossi-terminal domain (CTD) phosphorylation on Serine 2 (Ser2). Human RNAPII CTD contains 52 tandem heptad repeats of the consensus sequence Tyr1-Ser2-Pro3-Thr4-Ser5-Pro6-Ser7. The CTD has been demonstrated to play an important role in the transcription cycle from initiation to elongation and termination. The transition between initiation and productive elongation is elicited by Ser5-(Ser5P), followed by the Ser2-CTD-phosphorylation. CTD post-translational modifications occur during distinct steps of the transcription cycle and influence the transcription rate and hence mRNAs expression (Phatnani et al., 2006; Buratowski, 2009; Rahl al et al., 2010; Koga et al., 2015; Harlen et al., 2016). Therefore, we asked whether Omomyc may act on the transcription rate, modulating RNAPII phosphorylation on Ser2 (Ser2P), thus affecting mRNAs expression. First, HEK293T cells were transfected with the CbS-Flag-Myc and CbS-Flag-Omomyc plasmids, either alone or in combination. The same experiment was performed by using the CbS-Flag-Myc construct and the pSLIK-shMyc. Immunoblot analyses, using a specific antibody against Ser2P-CTD-RNAPII, showed that Myc overexpression induces the phosphorylation on Ser2 of RNAPII (Rahl et al., 2010) (Fig. 16 A). The same result was obtained upon Omomyc expression, whereas, in co-tranfection experiments, a reduction of Ser2P phosphorylation level was found (Fig. 16 A). In parallel, we observed also an increase of CDK9 protein expression either when Myc was overexpressed or co-transfected with Omomyc (Rahl et al., 2010; Huang et al., 2014). In co-tranfection experiments with CbS-Flag-Myc, pSLIK-shMyc strongly inhibited Ser2 phosphorylation on RNAPII (Fig. 16A). In BT168FO, the Ser2-CTD-RNAPII phosphorylation significantly

decreased in the presence of Omomyc (Fig. 16 B). In conclusion, consistent with our previous observations, Omomyc expression can act on gene expression inducing changes in RNAPII post-translational modifications and, probably, influencing the transcription rate.

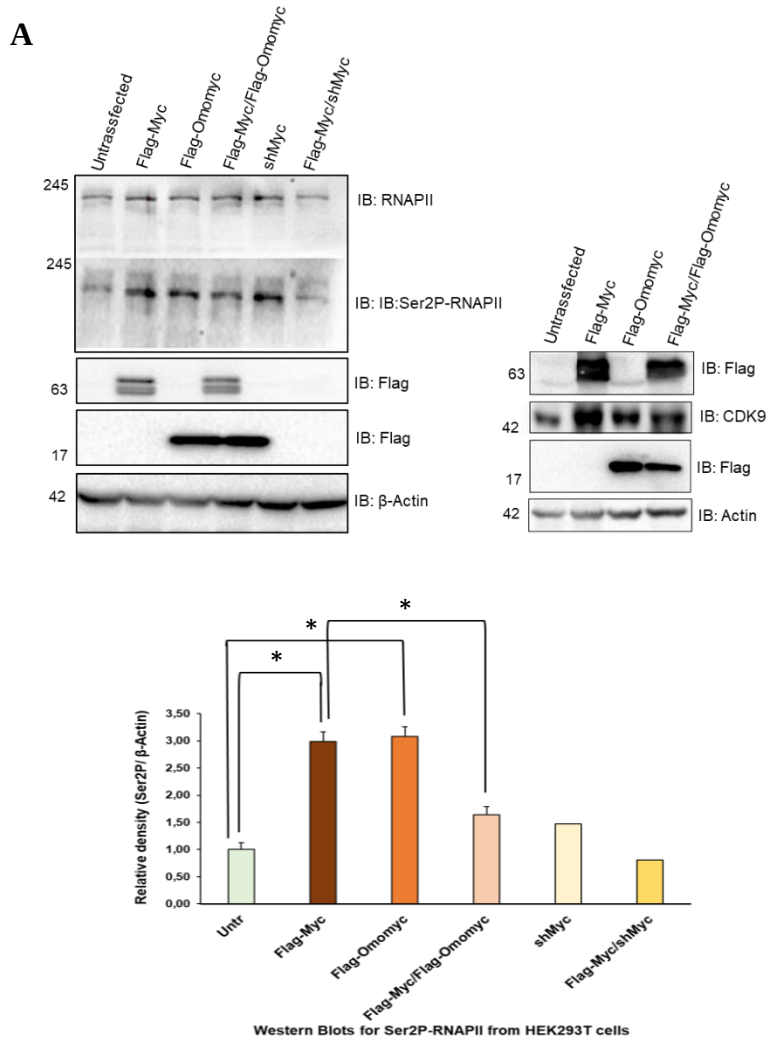

B

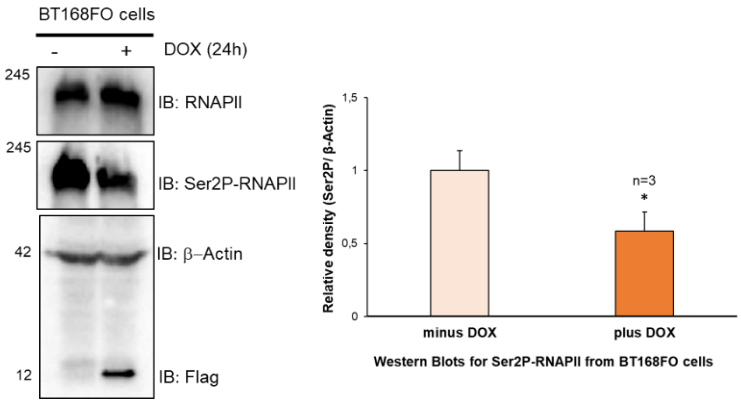

Fig. 16 - Myc and Omomyc play a role in Ser2 phosphorylation of RNAPII CTD. (**A**) **Top**. Immunoblots from HEK293T cells transfected with CbS-Flag-Myc, CbS-Flag-Omomyc and with pSLIK-shMyc vectors, alone or in combination showing Ser2P or CDK9 expression levels. **Bottom**. The graph shows the densitometry of the western blot. Each bar represents mean±SEM. *p-value 0,05 was determined by repeated measures one-way ANOVA. (**B**) **Left.** Western blot from BT168FO induced for 24h and depicting Ser2P level. **Right.** Densitometry of the western blot. Each bar represents mean±SEM, *p-value 0,05 was determined by paired t-test).

5.10 Relationship between Omomyc expression, changes in RNA Polymerase II distribution at transcriptional start and termination sites (TSS and TTS), and changes in gene expression. Myc has a relevant role in the symmetrical di-methylation of R1810 residue (Fig. 13,14,15). Therefore, we asked whether Omomyc was able to alter RNAPII amount at Transcription Termination Sites (TTSs) *versus* Transcription Start Sites (TSSs). We analyzed ChIP-seq data from BT168FO cells. In particular, the RNAPII ratio, calculated as RPKM at TTS/ RPKM at TSS, was evaluated (see methods). RPKM values from untreated and treated BT168FO cells were normalized by their inputs. We analyzed all genes which had a cut-off threshold value of FPKM ≥10 in untreated cells.

For Myc targets, we found that RNAPII ratios in -DOX cells *versus* +DOX cells are anti-correlated: genes showing a higher RNAPII ratio in untreated cells decrease this ratio in Omomyc expressing cells, while those characterized by a lower RNAPII ratio in uninduced cells showed an increase upon DOX treatment (Fig. 17 A). The same analysis was performed on non-Myc target genes (Fig. 17 B), confirming the finding observed for Myc targets (Fig. 17 A).

A

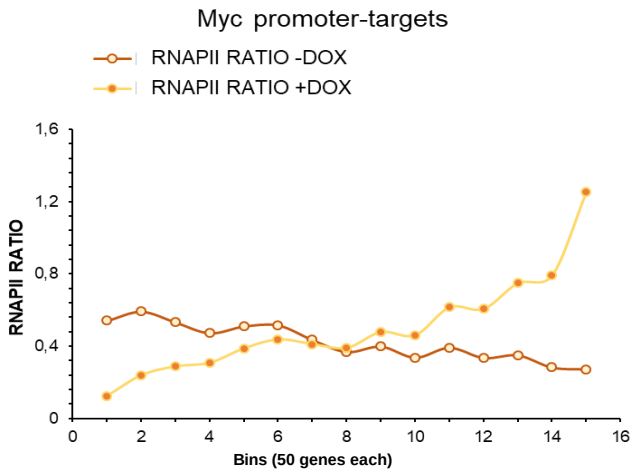

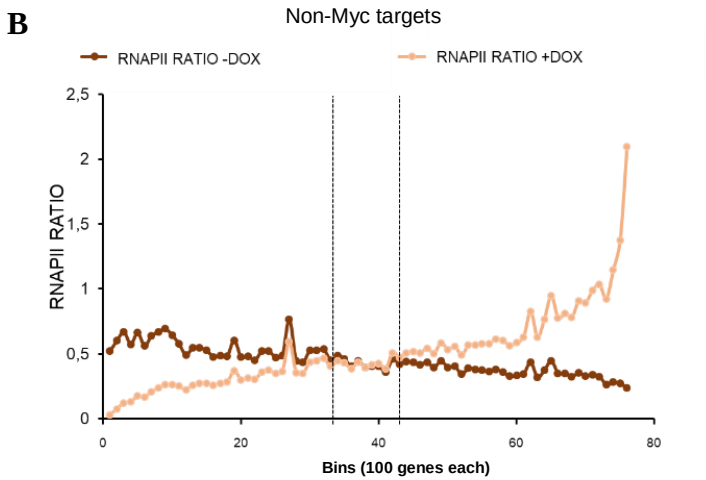

Fig. 17 – Omomyc changes RNAPII occupancy. (**A-B**) Binned scatter plot of genes ranked in ascending order of RNAPII occupancy fold change (FC) calculated as RNAPII Occupancy FC = [(TTS /TSS) $_{n°reads\ (+DOX\ cells)}$ / (TTS /TSS) $_{n°reads\ (-DOX\ cells)}$, with FPKM≥10 for comparing relative RNAPII ratio from untreated and treated of each bin.

Since Myc promotes symmetrical di-methylation of R1810 on the RNAPII CTD and Omomyc counteracts this capacity, we wanted to verify whether changes in RNAPII ratio are correlated with gene expression. To this end, we calculated the log_2RNAPII ratio FC and plotted this data against the respective log_2FC expression (24h) of each gene. We did not find a significant correlation between changes in RNAPII ratio and the Omomyc-dependent downregulation or upregulation of gene transcription (Fig. 18 A). Nevertheless, we decided to investigate whether the modulation in gene expression of Muhar Myc target gene set signature and GSC regulatory genes by Omomyc was correlated with the RNAPII ratio changes observed in the +DOX condition. As previously shown, Muhar gene set (Muhar et al. 2018) is a

specific Myc signature also in BT168FO cells. Genes belonging to the Muhar gene set are bound at promoters by Myc (Fig. 12) and are characterized by an early response to Omomyc induction (Fig. 12 B). GSC gene set, instead, includes all those genes related to cancer stem cell behavior according to literature data and which are significantly modulated by Omomyc in BT168FO cells (Fig. 11). Most of the genes of Muhar Myc target genes show a higher RNAPII amount at TSSs *versus* TTSs also in the presence of Omomyc (Fig. 18 B and C), and increased RNAPII ratio in treated *versus* untreated cells, compared to GSC gene set. Analyzing the RNAPII changes at TTS *versus* TSS regions, we found a strong correlation between RNAPII ratio FC changes and the downregulation of Muhar Myc target genes, in the presence of Omomyc, compared to GSC regulatory genes (Fig. 18 D and E). Altogether, these data may suggest that Omomyc, inhibiting the RNAPII R1810me2s, may reset the expression of specific Myc gene networks through changes in RNAPII distribution on TTS *versus* TSS regions.

A

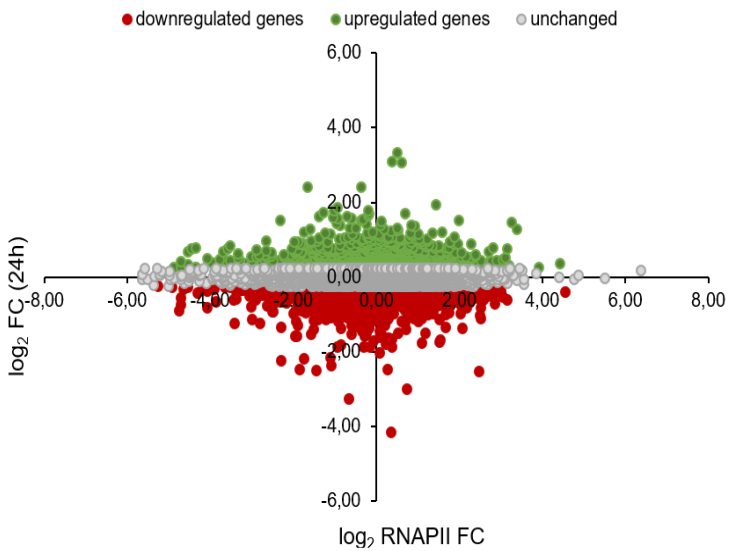

B

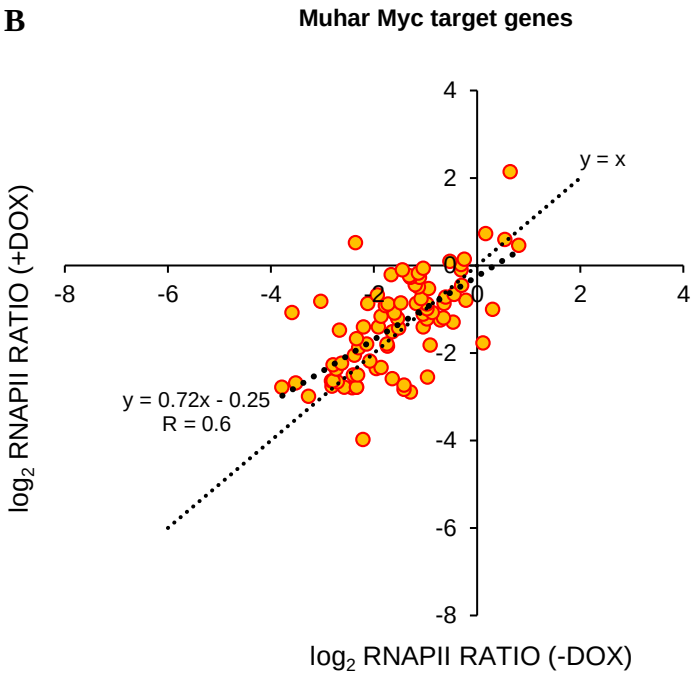
Muhar Myc target genes
y = x
y = 0.72x - 0.25
R = 0.6
log2 RNAPII RATIO (+DOX)
log2 RNAPII RATIO (-DOX)

C

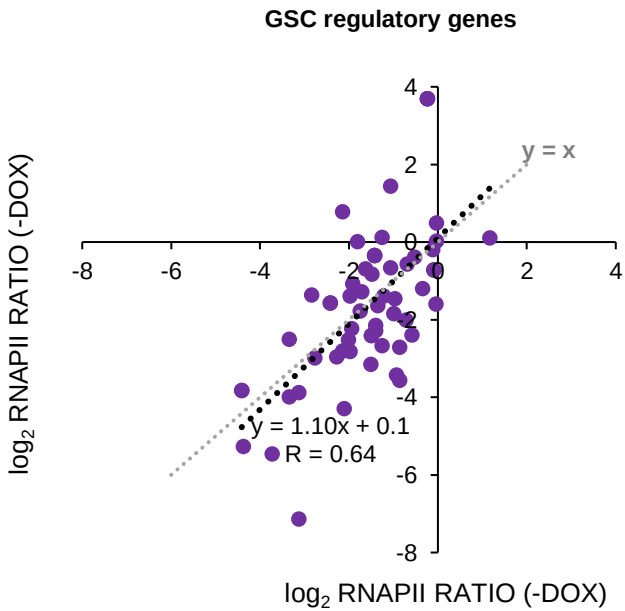
GSC regulatory genes
y = x
y = 1.10x + 0.1
R = 0.64
log2 RNAPII RATIO (-DOX)
log2 RNAPII RATIO (-DOX)

D

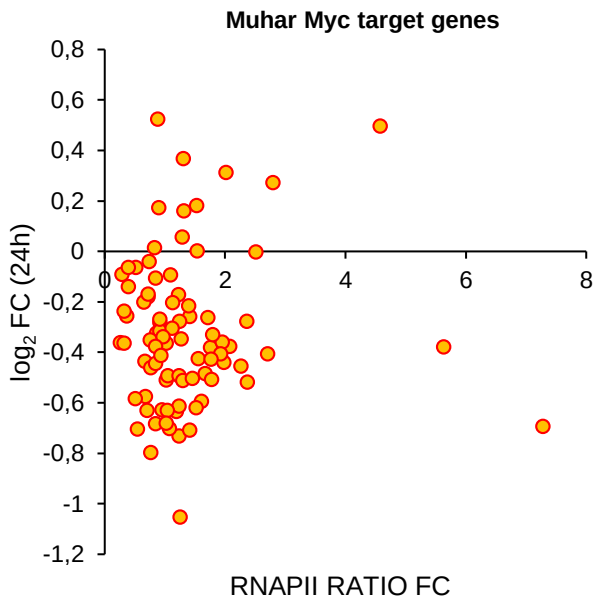
Muhar Myc target genes
0,8
0,6
0,4
0,2
0
-0,2
-0,4
-0,6
-0,8
-1
-1,2
0
2
4
6
8
log2 FC (24h)
RNAPII RATIO FC

E

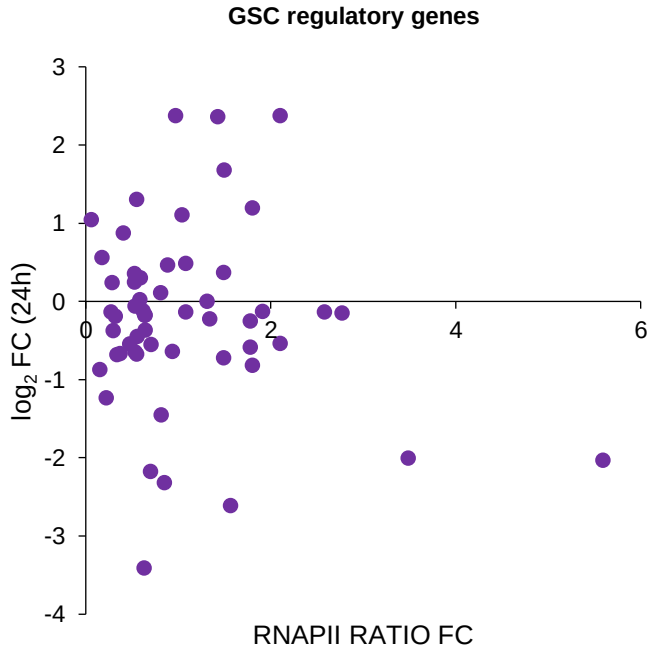
GSC regulatory genes
3
2
1
0
-1
-2
-3
-4
0
2
4
6
log2 FC (24h)
RNAPII RATIO FC

Fig. 18 – Relation between the gene expression and changes in RNAPII ratio upon Omomyc induction. (**A**) Dispersion graph displaying the correlation between RNAPII FC, calculated as RNAPII $RATIO_{+DOX}$/RNAPII $RATIO_{-DOX}$, and $log_2FC_{expression\ 24h}$ from RNA-seq data (3 experiments) of Myc Muhar signature and GSC regulatory genes. (**B-C**) Scatter plots showing the relation between log_2 RNAPII RATIO (-DOX) and log_2 RNAPII RATIO (+DOX) of Muhar Myc targets and GSC genes sets. (**D-E**) Scatter plots describing the relation between gene expression ($log_2FC_{expression\ 24h}$) and RNAPII FC of Muhar Myc and GSC gene sets.

5.11 Discussion. The molecular details of the outstanding action of Omomyc in cancer are still largely unknown. In the present study, we attempted to shed light on the significant impact of Omomyc expression in glioblastoma cancer stem cells (GSCs) and Burkitt's lymphoma cells. We found that Omomyc replaces Myc on E-box regions around transcription start sites (TSSs) (Fig. 4). This phenomenon influences also genomic loci bound by Myc and other transcription factors (Table 1), suggesting that Myc may cooperate with other proteins to regulate subsets of genes involved in different aspects of GSCs behavior. We also found that Omomyc binds to Myc genomic loci as homodimers (Fig. 5 C), which are more stable and with higher DNA affinity than Myc/Max heterodimers (Savino et al., 2011; Jung et al., 2017). Accordingly, we observed a 40-50% reduction of Myc binding at promoters upon Omomyc induction. Further, Omomyc recruitment seems to be *proportional* to the amount of bound Myc (Fig. 4 and 6 A, B). Consequently, Omomyc occupancy of genomic loci, usually bound by Myc/Max heterodimers, may influence many processes, such as cancer cells differentiation and metabolism (Carroll et al., 2015). The sustained and persistent Myc expression contributes to the formation of high number of Myc/Max dimers which invade the transcriptional active sites of chromatin containing E-box or non-E-box sequences. This makes tumor cells addicted to Myc-dependent transcriptional amplification (Nie et al., 2012; Lin et al., 2012; Guo et al., 2014; Sabò et al., 2014; Wolf et al., 2015). Max can form stable

homodimers even in the presence of Myc and bind DNA with comparable affinity to the Myc/Max heterodimer (Wolf et al., 2015; Maltais et al., 2017). In addition, it has been demonstrated that the alternative spliced form of Max provokes an increase in overall chromatin-bound Myc, compromising the ability of *wild-type* Max/Max complex to attenuate the binding of Myc to specific (E-boxes) and non-specific (non-E-boxes) DNA regions (Gu et al., 1993; Lindeman et al., 1995; Maltais et al., 2017). Moreover, increased Mad/Max and Max/Max dimers formation slows down proliferation, committing the cells towards apoptosis or differentiation (Eisenman, 1997; Grandori et al., 2000). Therefore, by either inducing Max or reducing Myc proteins expression, Omomyc may facilitate Max/Mad or Max/Max formation, affecting the stoichiometry of Max and Myc molecules (Fig 5 B and C). It is known that Myc occupancy is related to the expression level of transcripts (Lin et al., 2012; Walz et al., 2014; Conacci-Sorrell et al., 2014; Wolf et al., 2015; De Pretis et al., 2017). Consistently, in GSCs, we observed that highly expressed Myc-target genes, which are significantly downregulated by Omomyc, show a higher amount of Myc bound at promoters than Omomyc upregulated genes (Fig. 6 C). This is in agreement with the finding that highly expressed genes - both Myc and non-Myc targets - are preferentially downregulated by Omomyc. Less expressed genes, instead, may either be similarly upregulated or downregulated, while the expression of the vast majority of transcripts do not substantially change (Fig. 7 and 8). This is in line with the minimal effect on RNAPII loading at TSSs and with the decreased transcript amounts only of a subset of targets upon loss of Myc binding at promoters (Fig. 10).

Indeed, Omomyc affects specific gene groups, both Myc and non-Myc target, in GSCs (Fig. 11 and 12), and regulates multiple gene signatures, whose expression is altered by Myc overexpression in different types of tumors (Fig. 11 B, C and 12). Taken into consideration all these data, we propose the following mechanism to explain Omomyc ability to specifically hit cancer features (Fig. 2 and 3): Omomyc recognizes Myc “invaded”, low affinity

promoters and reshapes the Myc interactome, competing with Myc/Max heterodimers. This is consistent with the model describing Omomyc capacity to sense oncogenic Myc levels at weakly or unbound promoters in normal conditions (low affinity promoters, Jung et al., 2017). In this way, Omomyc may redistribute Myc occupancy on the genome, resetting the Myc-dependent GSC oncogenic gene expression pattern. Indeed, the decrease in Myc binding is not uniform for all promoters (Fig. 4). Omomyc homodimers may compete with Myc/Max heterodimers more easily at low-affinity sites than at high affinity sites, where Myc-Max complexes are stabilized also by protein-protein interactions through Myc N-terminal domain, which lacks in Omomyc (Guo et al., 2014; Thomas et al., 2015; Lorenzin et al., 2016; Jung et al., 2017). This may lead to the inhibition of Myc transcriptional programs in GSCs (Fig. 11).

In summary, GSC Myc targets, whose level of expression changes upon Omomyc induction, may represent genes under the control of low affinity promoters, more sensitive to Myc inhibition. On the contrary, genes insensitive to Omomyc induction may be controlled by the so-called high affinity promoters. In this scenario, it is still debated whether Myc globally enhances transcription (amplifier model) or it is a gene specific regulator (specifier model) or the transcription amplification by Myc is a secondary effect of Myc overexpression, due to the occupancy of previously empty chromatin loci (Sabò et al., 2014; Lorenzin et al., 2016). At strictly controlled normal levels, Myc acts on specific gene sets, regulating distinct biological processes. Conversely, when Myc is expressed at supraphysiological levels, may boost global gene expression, invading promoter and enhancer regions (Wolf et al., 2015; Nie et al., 2012; Lin et al., 2012; Sabò et al., 2014), with different binding affinities (Lorenzin et al., 2016), or chromatin sites where the transcription machinery is already active (Guo et al., 2014). In this regard, our findings may clarify how Myc enhances transcription in cancer cells. High and persistent Myc levels tend to saturate weak binding sites, which are normally not

bound by Myc, while high-affinity sites are already occupied (Lorenzin et al., 2016). The increase of Myc binding to the low affinity promoters may induce the amplification of the relative genes and in turn downstream targets, promoting an increase in total cellular RNA content, as a secondary effect (*domino* effect) (Kress et al., 2015, Muhar et al., 2018). Thus, Omomyc acting on key Myc promoter-targets, responsible of GSC behavior (Fig. 11 and 12), indirectly affects the expression of other downstream genes, as a sort of *domino* effect. In this view, Myc could not act as universal amplifier (Lin et al., 2014; Nie et al 2014; Walz et al., 2015), but rather as a specifier, that is, it may act on specific gene sets, indirectly inducing global changes in RNA and mRNA levels (Fig. 7,8,9 and 11 Sabò and Amati, 2014; Kress et al., 2015, 2016). In support to this hypothesis, in a very recent study, a rapid Myc protein degradation was induced and direct changes on newly mRNA outputs were measured, to identify Myc direct transcriptional targets. A set of genes, conserved in many tumor cell lines, was found. These genes were directly activated and bound at promoters by Myc, they are, instead, negatively modulated by Omomyc (Muhar et al., 2018). We also found that the genes belonging to this Myc signature are expressed and the corresponding promoters are bound by Myc in GSCs (Fig. 12). Therefore, Omomyc may help to unmask Myc function – i.e. the transcriptional control of specific gene subgroups – undetectable in cancer cells, where Myc overexpression appears to drive a genome-wide transcriptional amplification, which may be, instead**,** considered a secondary effect of a gene expression cascade. Hence, Omomyc expression may lead to the detachment of the excess of Myc from certain key gene promoters, probably from low-affinity sites.

The relative levels of Myc-modulated transcripts appear to be rebalanced in the presence of Omomyc: those commonly enhanced by Myc are repressed, and vice versa (Fig. 7 and 11). This suggests that Myc can act not only as an activator but also as a repressor (Sabò et al., 2014; Walz et al., 2014). Although the molecular mechanism of Myc transcriptional repression is not

totally clear (Loven et al., 2012), many studies report that Myc may repress genes through the interaction with Miz-1 (Seoane et al. 2001; Staller et al., 2001). Therefore, we may hypothesize that Omomyc, interacting with Miz-1 (Savino et al., 2011), may weaken Myc-dependent repression. Consequently, several genes may result induced by Omomyc (Fig. 7 and 8).

Based on these considerations, Omomyc appears to be a sensitive controller of deregulated Myc levels, both when Myc is bound at DNA and when Myc associates to coregulatory proteins, such as RNAPI,II and III complexes and their co-factors (Gomez-Roman et al., 2003; Arabi et al., 2005; Rahl et al., 2010; Kaur, Cole et al., 2013; Campbell, White et al., 2014; WB et al., 2015; De Pretis et al., 2017).

Indeed, Myc is involved in many aspects of RNAP II-dependent transcription: activation, pause release, elongation (Rahl et al., 2010). It also affects mRNA splicing, regulating the transcription of the core of pre-mRNA splicing machinery, including PRMT5 (Koh et al., 2015). In this regard, we previously observed that PRMT5 functionally interacts with both Myc and Omomyc (Mongiardi et al., 2015). PRMT5, in turn, symmetrically di-methylates RNAPII at R1810, thus allowing proper termination and splicing of transcripts (Zhao et al., 2016). Here, for the first time, we demonstrate that Myc is also involved in transcription termination, both in GSCs and BL cells.

We found that Myc induces symmetrical di-methylation of R1810 residue, while Omomyc counteracts this capacity (Fig. 13 and 14). Both Myc and Omomyc co-purified with RNAPII (Fig. 13 B and 14 B). Further, Myc inhibition by RNA interference led to a decrease of R1810me2s modification (Fig. 14 C), while PRMT5 catalytic activity was necessary for Myc-dependent symmetrical di-methylation of RNAPII-R1810 (Fig. 15). These data address a specific role to Myc in regulating the transcriptional termination through the R1810me2s-RNAPII. Furthermore, we observed that Omomyc modulates RNAPII amount at TTSs *versus* TSSs in several genes (Fig. 17). In particular, the RNAPII ratio for the Muhar Myc signature (Fig. 12, Muhar et al., 2018) is increased in

Omomyc expressing cells (Fig. 18 B) compared to GSC regulatory genes (Fig.11, Galardi et al., 2016), in which this ratio does not significantly change (Fig. 18 C). The correlation between RNAPII increase at TTSs and the Omomyc-dependent downregulation of Muhar Myc target genes, suggests that the PRMT5/Myc/RNAPII-R1810me2s pathway could represent a novel molecular axis perturbed by Omomyc, in cell systems characterized by Myc overexpression. However, to better clarify the specific role of Myc in transcription termination, it would be useful to investigate the formation of DNA:RNA hybrid structures, called R-loops, which are elongated at pause sites downstream of poly(A) signals. R-loops have great physiological roles in transcription and chromatin structure and their resolution is important for correct termination of transcripts. An accumulation of R-loops may lead to genomic instability, splicing defects and chromatin alterations, all phenomena frequently associated to cancer (Santos-Pereira & Aguilera 2015; Lionel et al., 2016). Therefore, Myc-dependent increase of R1810me2s in FlagMyc-overexpressing HEK293T cells and in BT168FO cells (Fig. 13 and 14) may cause an overload of RNAPII at termination sites with the consequent accumulation of R-loops and the expression of aberrant transcripts. Omomyc expression, inducing a reduction of R1810me2s-RNAPII level, may promote R-loops resolution.

Moreover, Omomyc is able to modulate Ser2 phosphorylation on RNAPII CTD (Fig. 16). However, Omomyc seems to counteract Myc functions only when Myc is overexpressed (Fig. 14 and 16; Soucek et al., 2002), while at low Myc levels (e.g in HEK293T cells), Omomyc may not negatively influence Myc activity, but may have additional effects (Fig. 13, 16 A). This may be due to relevant differences in Myc protein amount expressed in different cell systems. Indeed, Myc is very low in HEK293T cells (Fig. 13 A), while in BT168FO cells is highly expressed (De Bacco et al., 2012; Fig. 5 C). Since Myc regulates transcription from initiation (Rahl et al. 2010) to termination (Fig. 13), we think that these data may suggest another mechanism by which Omomyc expression

may influence Myc-driven transcription. Specifically, Omomyc may remove the "excess" of Myc from protein complexes involved in the transcription process, such as the RNAPII transcriptional machinery.

The involvement of Myc in many steps of RNAPII-mediated transcription confirms, at least in part, our hypothesis regarding the capacity of Omomyc to recognize deregulated Myc levels in cancer cells. Indeed, the gain in Myc binding is correlated with the RNAPII recruitment. This leads to an overload of the transcriptional machinery at active loci, with a reduction of RNAPII elongation and increase of RNAPII amount at gene-bodies, leading to an accumulation of unprocessed mRNAs (De Pretis et al., 2017). Omomyc may revert this condition inhibiting RNAPII R1810me2s and Ser2P modifications, normalizing the transcript expression levels altered by Myc.

In this view, Omomyc seems to reset the gene expression of Myc target and non-target genes associated with GSCs phenotype affecting Myc binding at DNA (Omomyc action model I, see below) and maybe disrupting Myc protein-protein interactions (Omomyc action model II, see below). In summary, we conclude that Myc directly binds and controls specific gene sets, whose amplification promotes an increase of transcripts level of downstream genes, as a secondary effect (domino effect). This consequent transcriptional amplification may depend, at least in part, by Myc ability to accelerate the transcription cycle, by acting on RNAPII post-transcriptional modifications. Omomyc function as a sensitive controller of oncogenic Myc levels in cancer cells may also explain how the small peptide expressed *in vivo* does not elicit significant side effects (Soucek et al., 2008). In these terms, Omomyc represents both a good tool to elucidate how cells lose the control of Myc and a very promising therapeutic strategy for inhibiting Myc oncogenic functions (Wang et al., 2018).

Omomyc action model (I)

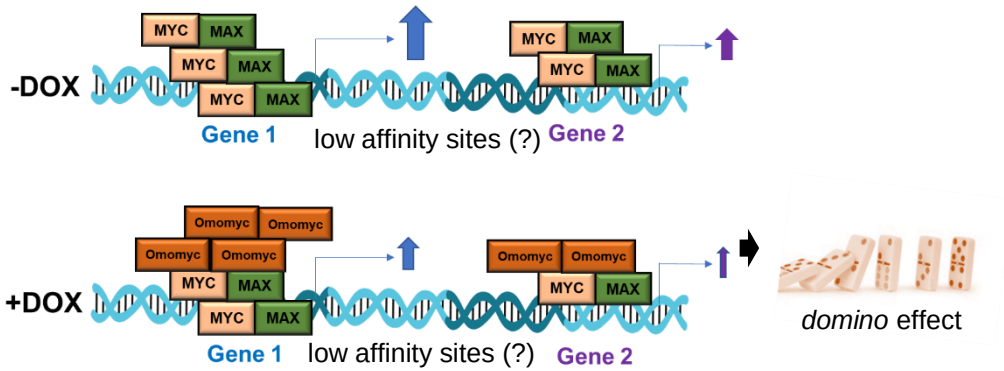

Omomyc action model (II)

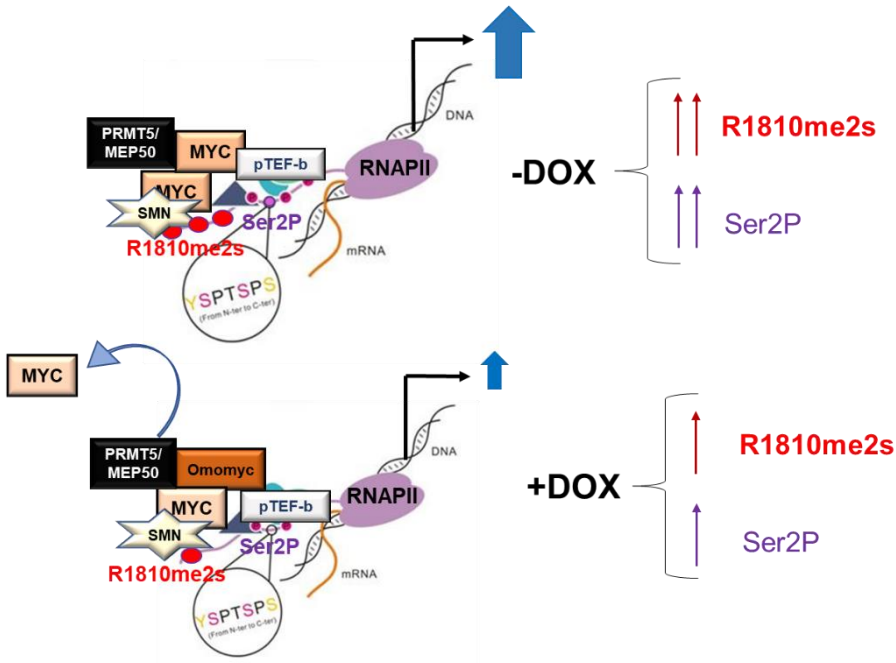

In brief:

- Omomyc normalizes Myc levels bound at DNA and in Myc protein complexes, resetting the gene expression altered by Myc overexpression in cancer.

Figure modified by Stefan et al., 2015

Materials and Methods

Cell culture, proliferation, self-renewal, cell-migration assays, and treatments. BT168 Glioblastoma stem cells (GSCs) were previously described in De Bacco et al. 2012. Cells were grown as neurospheres in serum-free medium, DMEM/F-12 (SIGMA, St.Louis, Mo, USA) supplemented with B-27™ Supplement (50X), 1% penicillin/streptomycin, 2mM Glutammine (Thermo Fisher Scientific, Waltham, USA), 10 ng/mL EGF and bFGF (Life Technologies, Carlsband, CA, USA). Cell proliferation was estimated by seeding GSCs in six-well plates (2×10^4 cells/well) and counting cells daily: the cell suspension was thoroughly homogenized with micropipette and aliquots of 10 µl were used for counting on a haemocytometer (Bright-Line; Hausser Scientific, Horsham, PA, USA) in combination with trypan blue dye. Team of two individuals counted triplicate samples from three identical sample sets. For self-renewal, GSCs were seeded in 96-well plates at 100 cells/well. The neurospheres number was counted after 7 days and plotted against the number of cells seeded; team of two individuals counted triplicate samples from three identical sample sets. *In vitro* migration was assayed by Transwell-96 system (BD Bioscience, San Jose, CA). After 24 h, migrated cells were stained with crystal violet solubilized with 10% acetic acid and 10 fields were counted per assay. Burkitt's lymphoma Ramos cells were characterized by Dalla Favera et al. 1982. Cells were cultured in RPMI-1640 medium supplemented with 10% FBS (Thermo Fisher Scientific), 1% penicillin/streptomycin, 2mM Glutammine. HEK293T cells were cultured in Dulbecco's Modified Eagle Medium (DMEM, SIGMA), supplemented with 10% FBS, 2 mM Glutamine and penicillin/streptomycin.

Cells harbouring a doxycycline inducible Flag-Omomyc (FO) were obtained by lentiviral infection. BT168FO and Ramos FO cells were treated respectively with 0.25 µg/mL and 0.1 µg/mL doxycycline (SIGMA) to induce Omomyc expression. To obtain BT168shMyc cells, BT168 cells were transduced with an

inducible lentivirus expressing a short hairpin RNA for Myc and treated with 0.25 μg/mL doxycycline to induce shMyc. HEK293T cells were treated with 5uM EPZ-015666 (1:1000). Cells were harvested 48h after treatment and the inhibition of PRMT5 activity was tested with Immunoblots for H4R3me2s.

Lentiviral infection. The lentiviral plasmid pSLIK-FO was constructed by Gateway cloning (Life Technologies). A Flag-Omomyc insert was amplified by PCR with primers introducing 5'KpnI and 3'XhoI restriction sites. The KpnI-XhoI fragment was purified and cloned in entry vector pEN_TTmcs (courtesy of Debbie Burkhart) downstream of TRE-tight promoter. The TRE-tight promoter/FlagOmomyc construct was subcloned into pSLIK-Hygro (Addgene #25737) co-expressing a hygromycin resistance gene and Tet-transactivator rtTA3. The lentiviral plasmid pSLIK-shMyc (shMyc sequence: TGCTGTTGACAGTGAGCGAAAGATGAGGAAGAAATCG ATGTAGTGAAGCCACAGATGTACATCGATTTCTCCTCA TCTTCTGCCTACTGCCTCGGA) was engineered cutting pSLIK-FO using PacI and SnaBI to cut away Gateway platform. The fragment PacI-SnaBI was purified. PCR from GEPIR (all-in-one shRNA-vector; Fellmann et al., 2013) for TRE3G-EGFP-mir30E band inserting the SnaBI and PacI sites. The fragment TRE3G-EGFP-mir30E was purified and cloned in pSLIK-PacI-SnaBI vector. pSLIK-SnaBI-mir30E-PacI was cutted with SnaBI for re-inserting RRE and Flag sequence. The final vector pSLIK-shMyc co-express hygromycin resistance gene and Tet-transactivator rtTA3. Lentiviruses were prepared by co-transfecting (Lipofectamine 2000 reagent, Thermo Fisher Scientific) HEK293T cells with pSLIK-FlagOmomyc and packaging plasmids PLP1, PLP2 and pMD VSV-G diluted in Opti-MEM (Thermo Fisher Scientific). The medium was removed after 12-24h and replaced with 4mL fresh culture medium. Supernatants were collected every 24h between 48 to

72h after transfection, pulled together and concentrated by ultracentrifugation in a Beckman SW-28 rotor for 2h at 25000 rpm, 4°C. For infection, 2-5 × 10^5 cells were seeded in 35mm dishes and infected the following day in the presence of 4 μg/mL polybrene. BT168FO cells were selected with 50–200 μg/mL hygromycin B (SIGMA), and Ramos FO cells with 400-800 μg/mL. After selection, Flag-Omomyc and shMyc expression were assessed by western blots.

RNA isolation and Real Time-PCR. Total RNA was isolated by TRIzol (Invitrogen). RNA was reverse-transcribed by M-MLV Reverse Transcriptase and random hexamer primers (Invitrogen). Real Time-PCR was performed using the SYBR Green select master mix (Life Technologies).

Primers:

CCND1: FW gaagatcgtcgccacctg
REV gacctcctcctcgcacttct
SOX2: FW atgggttcggtggtcaagt
REV ggaggaagaggtaaccacagg
PTEN: FW cagccgttcggaggattat
REV ttctcctcagcagccagag
NESTIN: FW gaggtggccacgtacaggacc
REV ctgaaagctga gggaagtcttgga
NOTCH1: FW gctccttccggctgatttat
REV cttaaccaggcttggcaca.
c-MYC: FW agctgcttagacgctggatt
REV aagttctcctcctcgtcgc

Flow cytometry evaluation. **Cell cycle analysis.** 5 × 10^5 Ramos cells were centrifuged at 2500 r.p.m for 5 min and washed in 1 mL PBS. Then, cells were pelleted and fixed by the dropwise addition of 500 μL of cold 70% methanol and gently mixing. Following 2h fixation at 4°C, the cells were pelleted (2500 rpm for 5 min) and washed twice with PBS. Cells were resuspended in 1mL PBS-RNAase A 50μg/mL for 30min at 37°C. After that,

the cells were pelleted and resuspended in staining buffer – 500 µl PBS-0,01% Tryton, 10 µl propidium iodide PI (stock solution 1 mg/mL, SIGMA) - and incubated in the dark at 4°C for 20 min. Cells were pelleted, washed twice in PBS (1000 rpm for 5 min), and resuspended in 500 µL PBS. For each sample, 10,000 events were analyzed using a FACSCalibur cytometer (Becton Dickinson, Franklin Lakes, New Jersey, Stati Uniti). Data were analyzed with ModFit software (Verity Software House, Inc.) **Annexin V staining**. 5×10^5 Ramos cells were collected, washed with PBS and resuspended in 500 µL of 1X binding buffer. Annexin V-FITC/PI were added to a final concentration of 1 mg/mL and the cells were incubated at room temperature in the dark for 15 min. A total of 10,000 events were collected per sample.

Transfection. Flag-Omomyc (pCbsFlag-Omomyc), Flag-Myc (pCbsFlag-Myc), pSLIK-shMyc plasmids were transfected using Lipofectamine 2000 (Thermo Fisher Scientific) according to the manufacturer's instructions. Cells were harvested 48h after transfection.

Immunoprecipitation. IP was performed with RIPA buffer (140mM NaCl, 10mM Tris pH 7.6-8.0, 1% Triton, 0.1% sodium deoxycoholate, 1mM EDTA, Zhao et al., 2016) containing protease inhibitors (Roche, Basilea, Svizzera) and benzonase (SIGMA). 10 to 20×10^6 cells were lysed on ice for 25 minutes by vortexing and forcing them through a 27-gauge needle, at least 10 times, and centrifuged at 13000 rpm for 15 min at 4°C. The supernatant was incubated with 10µL-25µL of protein A/G beads (Thermo Fisher) and 1-2µg of antibodies for 4h to overnight. The samples were washed 3 times with RIPA buffer and boiled in SDS gel sample buffer. To detect R1810me2s modification on RNA polymerase II (RNAPII), alkaline phosphatase (Roche) treatment (5µL) at 37°C for 30 min was performed for RNAPII immunoprecipitated samples before boiling.

Immunoblotting. Proteins were resolved in 6-8-10 or 12% polyacrilammide gels and transferred to PVDF (Bio-Rad, Hercules, CA,USA) or nitrocellulose membranes (GE Heath Care, Little Chafont, Buckinghamshire, UK) for 2h at 250 mA on ice or over-night at 30V. Filters were blocked in phosphate buffered saline plus 0.1% Tween-20 (PBST, SIGMA) added with 10% non-fat dry milk, for 1 hour and half at room temperature (RT). Primary antibodies were incubated over-night (O/N) at 4 °C, according to the concentration recommended by the manufacturer, in PBST plus 2.5%-5% non-fat dry milk. After three 10 minutes washes, filters were incubated for 1 hour at RT with either goat-anti rabbit (1:5000) or goat-anti mouse (1:2000) horseradish peroxidase (HRP)-conjugated secondary antibodies (Merck Millipore, Darmstadt, Germany). Blots were developed using SuperSignal West Pico Chemiluminescent Substrate or *Femto* Maximum Sensitivity (Thermo Fisher Scientific). Images were captured with a Chemidoc XRS+ (Bio-Rad, Hercules, CA, USA) and quantified using ImageJ software. Anti-Myc (9E10 and N-262), anti-CDK9, anti-RNAPII (8WG16) antibodies were from Santa Cruz Biotechnologies, anti-H4R3me2s, anti-PRMT5 antibodies were from Abcam; anti-Flag antibody was from SIGMA. Anti-R1810me2s was courtesy of J. F. Greenblatt's lab – University of Toronto, Canada (Zhao et al., 2016, Nature). Anti-dimethyl-Arginine Antibody, symmetric (SYM10) was from Merck. Anti-RNA polymerase II CTD repeat YSPTSPS (phospho S2) was from Abcam. Anti-β-Actin-peroxidase was from SIGMA.

Chromatin Immunoprecipitation (ChIP), ChIP-seq and RNA-seq. Samples for ChIP and ChIP-seq assays were prepared and analyzed according to Myers Lab ChIP-seq Protocol v041610 (http://myers.hudsonalpha.org/documents/) and MAGnify Chromatin Immunoprecipitation System protocol (Invitrogen). Antibodies used: Myc (sc-764Z, Santa Cruz Biotechnologies), Max (c-197X, Santa Cruz), RNAPII (sc-899X, Santa Cruz), RNAPII phosphor Ser5 (ab5131, Abcam). RNA Pol II phospho

Ser2 (ab24758, Abcam and 3E19, Active Motif), Flag (F1804, Sigma). Primers:

NCL	FW	gctcagtgactctgtctttcc
	REV	aagtctcgcgcgattagtg
miR17-92	FW	gaccacagcagttggagaaa
	REV	aaagcagcccacagactatt
HDAC1	FW	ccgactgacggtaggga
	REV	ccgtcgtagtagtaacagactttc
DUSP10	FW	aagtgtcacaggcggaatc
	REV	ccaaaggtgggtgagagaaa

For RNA-seq, 2µg total RNA purified by PureLinkRNA Mini Kit (Life Technologies) was used. ChIP-seq and RNA-seq libraries were prepared at Istituto di Genomica Applicata (IGA; www.appliedgenomics.org/) according to Illumina TruSeq DNA and TruSeq RNA Sample Preparation Guides. Samples were sequenced through Illumina HiSeq 2000 e 2500.

Bioinformatic analysis. ChIP-seq 50-bp reads were mapped to hg19 human reference genome (UCSC Genome Browser) using Bowtie (Langmead et al., 2009) version 0.12.7 allowing three mismatches; reads with multiple best matches were discarded. Peak calling was through MACS (Zhang et al. 2008) 1.4.2 with 10^{-4} P-value cut-off. The RefSeq transcript annotation of hg19 was used for computing intersections between peaks and promoters. Binding enrichment to promoters was calculated by the normalized number of ChIP-seq reads as Reads Per Million (RPM). In case of multiple TSSs, those with the highest enrichment were chosen. Motif enrichment analysis was through Pscan-ChIP (analysis performed by Giulio Pavesi, University of Milan, Zambelli et al., 2013). To calculate the distribution around TSSs (heat maps) Seqminer v.1.3.3 was used. The RAP (Zambelli et al., 2013) RNA-Seq pipeline Tophat v13 (https://bioinformatics.cineca.it/rap/) - including quality controls,

adaptor trimming and masking of low-quality sequences, tophat2, bowtie, and CuffLinks 2.2 - was used to reconstruct the transcriptome (hg19 reference) and calculate expression values as FPKM (Fragment per Kilobase Million per genes). Methods were published in Galardi et al. 2016. Comparisons between Myc, Omomyc occupancy with the gene expression (FPKM), were performed calculating the average values for groups of 100 genes (bins) and correlated by a scatter diagram. The linear regression model was used to assess the correlation between transcript levels in -DOX versus +DOX cells. RNAPII distribution, at TTS versus TSS regions, was evaluated using ChIP-seq data. Density reads, counted as RPKM, for each gene, at promoter (1500 nt) and termination (4200 nt) regions was calculated dividing the number of reads by the total number of reads obtained from each sequencing per condition (-DOX and +DOX), and by the length of the features. Data were normalized by their INPUT. Gene Set Enrichment Analysis (GSEA, http://www.broad.mit.edu/gsea/index.html) was used to determine whether an *a priori* defined set of genes shows statistical significance, according to the differences between -DOX and +DOX experimental conditions (phenotypes). In details, RNA-Seq dataset file – consisting of experiments performed in triplicate for each time point of DOX treatment – containing two labeled phenotypes (-DOX and +DOX) were prepared in TXT format: -DOX included all 0h time points (1° phenotype), while +DOX included from 4h to 48h of DOX treatment (2° phenotype). The expression dataset was compared with several gene sets either exported from GSEA-MsigDB database or homemade. The gene sets contained the gene set name and the list of included genes. A gene set file was in GMX or GMT format. GSEA software calculated an Enrichment Score (ES) describing the degree to which a gene set was overrepresented at the extremes (top or bottom) of the entire ranked list of data set – where genes are ranked according to the expression difference between -DOX and +DOX conditions. The Enrichment Score ES was calculated by walking down the list.

The value statistically increased when it found genes present in the gene set and decreased when genes were not present. The magnitude of ES was dependent on the correlation of each gene with the phenotype. The proportion of false positives was evaluated by calculating False Discovery Rate FDR-q value.

Statistical analysis. Statistical analyses were performed by using the GraphPad Prism version 5.0d (GraphPad, La Jolla, CA, USA) and Excel (Microsoft Excel, version 2018). All histograms represent the mean ±SEM of data obtained in 3 or more independent experiments. Statistical significance was determined by one-way repeated-measures ANOVA or paired t-test. The box plot p-values were calculated by paired Wilcoxon signed-rank tests. Regression lines were estimated using linear regression models. For genomic data, differential expression was assessed by CuffDiff2, as well as by Fold-Change thresholds, and Gene Set Enrichment Analysis (GSEA: www.broadinstitute.org/gsea/) subdividing Myc targets and non-Myc targets in groups of 500 genes.

REFERENCES

Abbas T & Dutta A. p21 in cancer: intricate networks and multiple activities. *Nat Rev Cancer* **9**, 400 – 14 (2009).

Adhikary S & Eilers M. Transcriptional regulation and transformation by Myc proteins. *Nat Rev Mol Cell Biol* **6**, 635-45 (2005).

Alitalo K *et al*. Homogeneously staining chromosomal regions contain amplified copies of an abundantly expressed cellular oncogene (c-myc) in malignant neuroendocrine cells from a human colon carcinoma. *Proc natl Acad Sci U.S.A.* **80**, 1707-11 (1983).

Allevato M *et al*. Sequence-specific DNA binding by MYC/MAX to low-affinity non-E-box motifs. *PLoS One* **12**, e0180147 (2017).

Annibali D. *et al*. Myc inhibition is effective against glioma and reveals a role for Myc in proficient mitosis. *Nature Communications* **5**, 4632 (2014).

Aprea J *et al*. Transcriptome sequencing during mouse brain development identifies long non-coding RNAs functionally involved in neurogenic commitment. *EMBO J* **32**, 3145 – 3160 (2013).

Arabi A *et al*. c-Myc associates with ribosomal DNA and activates RNA polymerase I transcription. *Nat Cell Biol* **7**, 303-10 (2005).

Bao S *et al*. Glioma stem cells promote radioresistance by preferential activation of the DNA damage response. *Nature* **444**, 756-60 (2006).

Bellail AC *et al.* SUMO1 modification stabilizes CDK6 protein and drives the cell cycle and glioblastoma progression. *Nat Commun* **5**, 4234 (2014).

Ben-Porath I *et al*. An embryonic stem cell-like gene expression signature in poorly differentiated aggressive human tumors. *Nat Genet* **40**, 499 – 507 (2008).

Billin AN *et al*. Mlx, a novel Max-like BHLHZip protein that interacts with the Max network of transcription factors. *J Biol Chem* **274**, 36344–36350 (1999).

Buratowski S Progression through the RNA polymerase II CTD cycle. *Mol Cell* **36**, 541-546 (2009).

Campaner S *et al*. Cdk2 suppresses cellular senescence induced by the c-myc oncogene. *Nat Cell Biol* **12**, 54-9 (2010).

Campbell KJ & White RJ. MYC regulation of cell growth through control of transcription by RNA polymerases I and III. *Cold Spring Harb Perspect Med*.**4**, pii: a018408 (2014).

Carroll PA *et al.* Deregulated MYC requires MondoA/Mlx for metabolic reprogramming and tumorigenesis. *Cancer Cell* **27**, 271 – 285 (2015).

Cesarman E *et al*. Mutations in the first exon are associated with altered transcription of c-myc in Burkitt's lymphoma. *Science* **238**, 1272-5 (1987).

Chang DW *et al*. The c-Myc transactivation domain is a direct modulator of apoptotic versus proliferative signals. *Mol Cell Biol* **20**, 4309-19 (2000).

Chen J *et al*. A restricted cell population propagates glioblastoma growth after chemotherapy. *Nature* **488**, 522 – 526 (2012).

Chou TY *et al*. c-Myc is glycosylated at threonine 58, a known phosphorylation site and a mutational hot spot in lymphomas. *J Biol Chem* **270**, 18961-5 (1995).

Cloughesy TF *et al*. Glioblastoma: From Molecular Pathology to Targeted Treatment. *Annual Rev Path* **9**, 1-25 (2013).

Cole MD & Nikiforov MA. Transcriptional activation by the Myc oncoprotein. *Curr Top Microbiol Immunol* **302**, 33-50 (2006).

Conacci-Sorell M *et al*. Myc-nick: a cytoplasmic cleavage product of Myc that promotes alpha-tubulin acetylation and cell differentiation. *Cell* **142**, 480-93 (2010).

Conacci-Sorrell M *et al.* An overview of MYC and its interactome. *Cold Spring Harb Perspect* **4**, a014357 (2014).

Cowling VH & Cole MD. An N-Myc truncation analogous to c-Myc-S induces cell proliferation independently of transactivation but dependent on Myc homology box II. *Oncogene* **27**, 1327 – 1332 (2008).

Cowling VH *et al*. Burkitt's lymphoma-associated c-Myc mutations converge on a dramatically altered target gene response and implicate Nol5a/Nop56 in oncogenesis. *Oncogene* **33**, 3519-27 (2014).

Cultraro CM *et al.* Function of the c-Myc antagonist Mad1 during a molecular switch from proliferation to differentiation. *Mol Cell Biol* **17**, 2353-9 (1997).

Dalla Favera R *et al*. Human c-myc oncogene is located on the region of chromosome 8 that is translocated in Burkitt lymphoma cells. *Proc Natl Acad USA* **79**, 7824 - 7827 (1982).

Dang CV. c-Myc target genes involved in cell growth, apoptosis, and metabolism. *Mol Cell Biol* **19**, 1-11 (1999).

Dang CV. MYC on the path to cancer. *Cell* 149, 22-35 (2012).

Daniel P *et al.* Selective CREB-dependent cyclin expression mediated by the PI3K and MAPK pathways supports glioma cell proliferation. *Oncogenesis* **3**, e108 (2014).

De Bacco F *et al*. The MET oncogene is a functional marker of a glioblastoma stem cell subtype. *Cancer Res* **72**, 4537 – 4550 (2012).

De Falco G *et al*. Burkitt lymphoma beyond MYC translocation: N-MYC and DNA methyltransferases dysregulation. *BMC Cancer* **15**, 668 (2015).

De Pretis S *et al.* Integrative analysis of RNA polymerase II and transcriptional dynamics upon MYC activation. *Genome Res* **27**, 1658-1664 (2017).

Dominguez-Sola D *et al*. Non-transcriptional control of DNA replication by c-Myc. *Nature* **448**, 445-51 (2007).

Eilers M & Eisenman RN. Myc's broad reach. *Genes Dev* **22**, 2755-66 (2008).

Eischen CM *et al*. Apoptosis triggered by Myc-induced suppression of Bcl-X(L) or Bcl-2 is bypassed during lymphomagenesis. *Mol Cell Biol* **21**, 5063-70 (2001).

Eisenman RN, The Myc/Max/Mad Transcription Factor Network, Springer (1997).

Farhana L *et al.* Down regulation of miR-202 modulates Mxd1 and Sin3A repressor complexes to induce apoptosis of pancreatic cancer cells. *Cancer Biol Ther* **16**, 115-24

Farina H *et al*. Glioblastoma Multiforme: A Review of its Epidemiology and Pathogenesis through Clinical Presentation and Treatment. *Asian Pac J Cancer Prev* **18**, 3-9 (2017).

Fellmann C *et al*. An optimized microRNA backbone for effective single-copy RNAi. *Cell Rep* **5**, 1704-13 (2013).

Ferré-D'Amaré AR *et al*. Recognition by Max of its cognate DNA through a dimeric b/HLH/Z domain. *Nature* **363**, 38-45 (1993).

Fiorentino FP *et al*. Growth suppression by MYC inhibition in small cell lung cancer cells with TP53 and RB1 inactivation. *Oncotarget* **7**, 31014-28 (2016).

Galardi S *et al*. Resetting cancer stem cell regulatory nodes upon MYC inhibition. *EMBO Rep* **17**, 1872-1889 (2016).

Gallant P & Steiger D. Myc's secret life without Max. *Cell cycle* **8**, 3848-53 (2009).

Gangemi RM *et al*. SOX2 silencing in glioblastoma tumor-initiating cells causes stop of proliferation and loss of tumorigenicity. *Stem Cells* **27**, 40 – 48 (2009).

Goldshmit Y *et al.* Interfering with the interaction between ErbB1, nucleolin and Ras as a potential treatment for glioblastoma. *Oncotarge*t **5**, 8602 – 8613 (2014).

Gomez-Roman N *et al.* Direct activation of RNA polymerase III transcription by c-Myc. *Nature* **421**, 290-4 (2003).

Grandori C *et al*. c-Myc binds to human ribosomal DNA and stimulates transcription. *Nat Cell Biol* **7**, 311-8 (2005).

Grandori C *et al.* The Myc/Max/Mad network and the transcriptional control of cell behavior. *Annu Rev Cell Dev Biol***16**, 653-99 (2000).

Grayson AR *et al*. MYC, a downstream target of BRD-NUT, is necessary and sufficient for the blockade of differentiation in NUT midline carcinoma. *Oncogene* **33**, 1736-42 (2014).

Gregory MA & Hann SR. c-Myc proteolysis by the ubiquitin-proteasome pathway: stabilization of c-Myc in Burkitt's lymphoma cells. *Mol Cell Biol* **20**, 2423-35 (2000).

Gu W *et al.* Opposite regulation of gene transcription and cell proliferation by c-Myc and Max. *Proc Natl Acad USA* **90**, 2935-9 (1993).

Guccione E *et al*. Myc-binding-site recognition in the human genome is determined by chromatin context. *Nat Cell Biol* **8**, 764-70 (2006).

Guo J *et al.* Sequence specificity incompletely defines the genome-wide occupancy of Myc. *Genome Biol* **15**, 482 (2014).

Harlen KM *et al.* Comprehensive RNA Polymerase II Interactomes Reveal Distinct and Varied Roles for Each Phospho-CTD Residue. *Cell Rep* **15**, 2147-2158 (2016).

Herms J *et al*. c-Myc oncogene family expression in glioblastoma and survival. *Surg Neurol* **51**, 536-42 (1999).

Hoang AT *et al.* A link between increased transforming activity of lymphoma-derived MYC mutant alleles, their defective

regulation by p107, and altered phosphorylation of the c-myc transactivation domain. *Mol Cell Biol* **15**, 4031-42 (1995).

Hopewell R & Ziff EB. The nerve growth factorresponsive PC12 cell line does not express the Myc dimerization partner Max. *Mol Cell Biol* **15**, 3470-8 (1995).

Huang CH *et al*. CDK9-mediated transcription elongation is required for MYC addiction in hepatocellular carcinoma. *Genes Dev* **28**, 1800-1814 (2014).

Jansen T *et al*. FasL gene knock-down therapy enhances the antiglioma immune response. *Neuro Oncol* **12**, 482-9 (2010).

Johansen LM *et al*. c-Myc is a critical target for c/EBPalpha in granulopoiesis. *Mol Cell Biol* **21**, 3789-809 (2001).

Jung LA *et al.* OmoMYC blunts promoter invasion by oncogenic MYC to inhibit gene expression characteristic of MYC-dependent tumors. *Oncogene* **36**, 1911-1924 (2017).

Kaadige MR *et al*. Coordination of glucose and glutamine utilization by an expanded Myc network. *Transcription* **1**, 36-40 (2010).

Kaur M & Cole MD 2013. MYC acts via the PTEN tumor suppressor to elicit autoregulation and genome-wide gene repression by activation of the Ezh2 methyltransferase. *Cancer Res* **73**, 695-705 (2013).

Kim J *et al*. A MYC network accounts for similarities between embryonic stem and cancer cell transcription programs. *Cell* **143**, 313 – 324 (2010).

Knoepfler PS *et al*. Myc influences global chromatin structure. *EMBO J* **25**, 2723-34 (2006).

Knoepfler PS *et al*. N-*myc* is essential during neurogenesis for the rapid expansion of progenitor cell populations and the inhibition of neuronal differentiation. *Genes Dev* **16**, 2699–2712 (2002).

Koga M *et al*. Splicing inhibition decreases phosphorylation level of Ser2 in Pol II CTD. *Nucleic Acids Res* **43**, 8258-8267 (2015).

Koh CM *et al*. MYC regulates the core pre-mRNA splicing machinery as an essential step in lymphomagenesis. *Nature* **523**, 96-100 (2015).

Kohl NE *et al*. Transposition and amplification of oncogene-related sequences in human neuroblastomas. *Cell* **35**, 359-67 (1983).

Kress TR *et al.* Identification of MYC Dependent Transcriptional Programs in Oncogene-Addicted Liver Tumors. *Cancer Res* **76**, 3462-72 (2016).

Kress TR *et al*. MYC: connecting selective transcriptional control to global RNA production. *Nat Rev Cancer* **15**, 593-607 (2015).

Langmead B *et al*. Ultrafast and memory-efficient alignment of short DNA sequences to the human genome. *Genome Biol* 10, **R25** (2009).

Larsson LG & Henriksson MA. The Yin and Yang functions of the Myc oncoprotein in cancer development and as targets for therapy. *Exp Cell Res* **316**, 1429-37 (2010).

Lathia JD *et al*. Cancer stem cells in glioblastoma. *Genes Dev* **29**, 1203-17 (2015).

Laurenti E *et al*. Myc's other life: Stem cells and beyond. *Curr Opin Cell Biol* **21**, 844–854 (2009).

Lee J *et al*. Tumor stem cells derived from glioblastomas cultured in bFGF and EGF more closely mirror the phenotype and genotype of primary tumors than do serum-cultured cell lines. *Cancer Cell* **9**, 391-403 (2006).

Li Y *et al.* MYC through miR-17-92 suppresses specific target genes to maintain survival, autonomous proliferation, and a neoplastic state. *Cancer Cell* **26**, 262 – 272 (2014).

Lin CH *et al*. Gene regulation and epigenetic remodeling in murine embryonic stem cells by c-Myc. *PLoS ONE* **4**, e7839 (2009).

Lin CY *et al*. Transcriptional amplification in tumor cells with elevated c-MYC. *Cell* **51**, 56 – 67 (2012).

Lindeman GJ *et al.* Overexpressed max is not oncogenic and attenuates myc-induced lymphoproliferation and lymphomagenesis in transgenic mice. *Oncogene* **10**, 1013–7 (1995).

Link JM *et al*. A critical role for Mnt in Myc-driven T-cell proliferation and oncogenesis. *Proc Natl Acad Sci* **109**, 19685–19690 (2012).

Lionel A *et al*. Prevalent, dynamic and conserved R-loops structures associate with specific epigenomic signatures in mammals. *Mol Cell* **63**, 167-178 (2016).

Lorenzin F *et al*. Different promoter affinities account for specificity in MYC-dependent gene regulation. *Elife* **5**, pii: e15161 (2016).

Loven J *et al*. Revisiting global gene expression analysis. *Cell* **151**, 476–482 (2012).

Lowe SW *et al*. Intrinsic tumor suppression. *Nature* **432**, 307-15 (2004).

Maltais L *et al*. Biophysical characterization of the b-HLH-LZ of ΔMax, an alternatively spliced isoform of Max found in tumor cells: Towards the validation of a tumor suppressor role for the Max homodimers. *PLoS One* **12**, e0174413 (2017).

Matsuda Y *et al*. Inhibition of nestin suppresses stem cell phenotype of glioblastomas through the alteration of post-translational modification of heat shock protein HSPA8/HSC71. *Cancer Lett* **357**, 602 – 611 (2015).

Matsumoto M *et al*. Control of the MYC-eIF4E axis plus mTOR inhibitor treatment in smal cell lung cancer. *BMC C*ancer **15**, 241 (2015).

McMahon SB. MYC and the control of apoptosis. *Cold Spring Harb Perspect Med* **4** a014407 (2014).

Meyer N & Penn LZ. Reflecting on 25 years with MYC. *Nat Rev Cancer* **8**, 976-90 (2008).

Molyneux EM *et al*. Burkitt's lymphoma. *Lancet* **2**, 1234-44 (2012).

Mongiardi MP *et al*. Myc and Omomyc functionally associate with the Protein Arginine Methyltransferase 5 (PRMT5) in glioblastoma cells. *Sci Rep* **5**, 15494 (2015).

Morris SL & Huang S. Crosstalk of the Wnt/β-catenin pathway with other pathways in cancer cells. *Genesis Dis* **3**, 41-7 (2016).

Morrow MA *et al*. Interleukin-7 induces N-myc and c-myc expression in normal precursor B lymphocytes. *Genes Dev* **6**, 61–70 (1992).

Muhar M *et al.* SLAM-seq defines direct gene-regulatory functions of the BRD4-MYC axis. *Science* **360**, 800-805 (2018).

Nair SK & Burley SK. Structural aspects of interactions within the Myc/Max/Mad network. *Curr Top Microbiol Immuno*l. **302**, 123-43 (2006).

Nie Z *et al.* c-Myc is a universal amplifier of expressed genes in lymphocytes and embryonic stem cells. *Cell* **151**, 68 – 79 (2012).

Oster H *et al*. Disruption of *mCry2* restores circadian rhythmicity in *mPer2* mutant mice. *Genes & Dev* **16**, 2633-38 (2002).

Oster SK *et al*. The myc oncogene: MarvelouslY Complex. *Adv Cancer Res* **84**, 81-154 (2002).

Perna D *et al*. Genome-wide mapping of Myc binding and gene regulation in serum-stimulated fibroblasts. *Oncogene* **31**, 1695-709 (2012).

Phatnani HP & Greenleaf AL. Phosphorylation and functions of the RNA polymerase II CTD. *Genes Dev* **20**, 2922-36 (2006).

Philippe J *et al*. c-Myc-induced sensitization to apoptosis is mediated through cytochrome c release. *Genes Dev* **13**, 1367-81 (1999).

Piccin D *et al.* Notch signaling imparts and preserves neural stem characteristics in the adult brain. *Stem Cells Dev* **22**, 1541 – 1550 (2013).

Poole CJ & van Riggelen J. MYC-Master Regulator of the Cancer Epigenome and Transcriptome. *Genes (Basel)* **8**, E142 (2017).

Popov N *et al*. The ubiquitin-specific protease USP28 is required for MYC stability. *Nat Cell Biol* **9**, 765-74 (2007).

Prabhakar S *et al*. Targeting DUSPs in glioblastomas - wielding a double-edged sword? *Cell Biol Int* 38, **145** – 153 (2014).

Rahl PB & Young RA. MYC and transcription elongation. *Cold Spring Harb Perspect Med* **4**, a020990 (2014).

Rahl PB *et al.* c-Myc regulates transcriptional pause release. *Cell* **141**, 432-45 (2010).

Sabò A & Amati B. BRD4 and MYC-clarifying regulatory specificity. *Science* **360**, 713-4 (2018).

Sabò A *et al*. Selective transcriptional regulation by Myc in cellular growth control and lymphomagenesis. *Nature* **511**, 488 – 492 (2014).

Sabò A and Amati B. Genome Recognition by MYC. *Cold Spring Harb Perspect Med* **4**, a014191 (2014).

Salghetti *et al*. Destruction of Myc by ubiquitin-mediated proteolysis: Cancer associated and transforming mutations stabilize Myc. *EMBO J* **18**, 717-26 (1999).

Santos-Pereira *et al.* R-loops: new modulators of genome dynamics and function. *Nat Rev Genet* **16**, 583-97 (2015).

Savino M *et al.* The action mechanism of the MYC inhibitor termed Omomyc may give clues on how to target MYC for cancer therapy. *PLoS One* **6**, e22284 (2011).

Schlosser I *et al.* Dissection of transcriptional programmes in response to serum and c-Myc in a human B-cell line. *Oncogene* **24**, 520 – 524 (2005).

Schmidt EV. The role of c-myc in regulation of translation initiation. *Oncogene* **19**, 3217-21 (2004).

Schuhmacher M *et al*. The transcriptional program of a human B cell line in response to Myc. *Nucleic Acids Res* **29**, 397 – 406 (2001).

Sears R *et al*. Multiple Ras-dependent phosphorylation pathways regulate Myc protein stability. *Genes Dev* **14**, 2501-14 (2000).

Sears R *et al*. Ras enhances Myc protein stability. *Mol Cell* **3**, 169-179 (1999).

Seoane J *et al*. TGFbeta influences Myc, Miz-1 and Smad to control the CDK inhibitor p15INK4b. *Nature cell biol* **3**, 400–408 (2001).

Seymour T *et al*. targeting Aggressive Cancer Stem Cells in Glioblastoma. *Front Oncol* **5**, 159 (2015).

Singh AM *et al*. The cell cycle and Myc intersect with mechanisms that regulate pluripotency and reprogramming. *Cell Stem Cell* **5**, 141-9 (2009).

Song JL *et al*. microRNA regulation of Wnt signaling pathways in development and disease. *Cell Signal* **27**, 1380-91 (2015).

Soucek L & Evan GI. The ups and downs of Myc biology. *Curr Opin Genet Dev* **20**, 91-5 (2010).

Soucek L *et al.* Design and properties of a Myc derivative that efficiently homodimerizes. *Oncogene* **17**, 2463-72 (1998).

Soucek L *et al*. Inhibition of Myc family proteins eradicates KRas-driven lung cancer in mice. *Genes Dev* **27**, 504-13 (2013).

Soucek L *et al*. Omomyc expression in skin prevents Myc-induced papillomatosis. *Cell Death Differ* **11**, 1038-45 (2004).

Soucek L *et al*. Modelling Myc inhibition as a cancer therapy. *Nature* **455**, 679-83 (2008).

Soucek L *et al*. Omomyc, a potential Myc dominant negative, enhances Myc-induced apoptosis. *Cancer Res*. **62**, 3507-10 (2002).

Soucie EL *et al*. Myc potentiates apoptosis by stimulating Bax activity at the mitochondria. *Mol Cell Biol* **21**, 4725-36 (2001).

Spencer CA *et al*. Control of c-myc regulation in normal and neoplastic cells. *Adv Cancer Res* **56**, 1-48 (1991).

Staller P *et al.* Repression of p15INK4b expression by Myc through association with Miz-1. *Nature cell biol* **2**, 392–399 (2001).

Suvà ML *et al.* Reconstructing and reprogramming the tumor-propagating potential of glioblastoma stemlike cells. *Cell* **157**, 580 – 594 (2014).

Takahashi K *et al*. Induction of pluripotent stem cells from adult human fibroblasts by defined factors. *Cell* **131**, 861-72 (2007).

Tansey WP. Mammalian MYC proteins and cancer. *New Journal of Science* **2014**, 1-27 (2014).

Taub R *et al*. Translocation of the c-myc gene into the immunoglobulin heavy chain locus in human Burkitt's lymphoma

and murine plasmacytoma cells. *Proc Natl Acad Sci U.S.A*. **79**, 7837-41 (1982).

Thomas LR *et al*. Interaction with WDR5 promotes target gene recognition and tumorigenesis by MYC. *Mol Cell* **58**, 440-52 (2015).

Ullius A. The interaction of MYC with the trithorax protein ASH2L promotes gene transcription by regulating H3K27. *Nucleic Acids Res* **42**, 6901-20 (2014).

van Riggelen J *et al*. MYC ad a regulator of ribosome biogenesis and protein synthesis. *Nat Rev Cancer* **10**, 301-9 (2010).

Verhaak RG *et al*. Integrated genomic analysis identifies clinically relevant subtypes of glioblastoma characterized by abnormalities in PDGFRA, IDH1, EGFR, and NF1. *Cancer Cell* **17**, 98 – 110 (2010).

Vervoorts J *et al*. Stimulation of c-MYC transcriptional activity and acetylation by recruitment of the cofactor CBP. *Embo r* **4**, 484-490 (2003).

Vervoorts J *et al.* The ins and outs of MYC regulation by posttranslational mechanisms. *J Biol Chem* **281**, 34725-9 (2006).

Vita M & Henriksson M. The Myc oncoprotein as a therapeutic target for human cancer. *Semin Cancer Biol* **16**, 318-30 (2006).

Walz S *et al*. Activation and repression by oncogenic MYC shape tumour-specific gene expression profiles. *Nature* **51**, 483 – 487 (2014).

Wang E *et al*. Tumor penetrating peptides inhibiting MYC as a potent targeted therapeutic strategy for triple-negative breast cancers. *Oncogene* **10**.1038/s41388-018-0421-y (2018).

Wang J *et al*. CD133 negative glioma cells form tumors in nude rats and give rise to CD133 positive cells. *Int J Cancer* **122**, 761-8 (2008).

WB T *et al*. Myc and its interactors take shape. *Biochim Biophys Acta* **1849**, 469-83 (2015).

Wiese KE *et al*. The role of MIZ-1 in MYC-dependent tumorigenesis. *Cold Spring Harb Perspect Med* **3**, a014290 (2013).
Wilson A *et al*. c-Myc controls the balance between hematopoietic stem cell self-renewal and differentiation. *Genes Dev* **18**, 2747-63 (2004).

Wolf E *et al*. Taming of the beast: shaping MYC-dependent amplification. *Trends Cell Biol* **25**, 241 – 248 (2015).

Yada M *et al*. Phosphorylation-dependent degradation of c-Myc is mediated by the F-box protein Fbw7. *EMBO J* **23**, 2116-25 (2004).

Yang G & Hurlin PJ. MNT and Emerging Concepts of MNT-MYC Antagonism. *Genes (Basel)* **8**, E83 (2017).

Yang P *et al*. RCOR2 is a subunit of the LSD1 complex that regulates ESC property and substitutes for SOX2 in reprogramming somatic cells to pluripotency. *Stem Cells* **29**, 791 – 801 (2011).

Zambelli F *et al*. Motif discovery and transcription factor binding sites before and after the next-generation sequencing era. *Brief Bioinform* **14**, 225-37 (2013).

Zeller KI *et al.* An integrated database of genes responsive to the Myc oncogenic transcription factor: identification of direct genomic targets. *Genome Biol* **4**, R69 (2003).

Zeller KI *et al*. Global mapping of c-Myc binding sites and target gene networks in human B cells. *Proc Natl Acad Sci U S A* **103**, 17834-9 (2006).

Zhang Y *et al*. Model-bases analysis of ChIP-Seq (MACS). *Genome Biol* **9**, R137 (2008).

Zhuang D *et al*. C-MYC overexpression is required for continuous suppression of oncogene-induced senescence in melanoma cells. *Oncogene* 27, 6623-34.

Zhao DY *et al*. SMN and symmetric arginine dimethylation of RNA polymerase II C-terminal domain control termination. *Nature* **529**, 48-53 (2016).

Zheng H *et al*. p53 and Pten control neural and glioma stem/progenitor cell renewal and differentiation. *Nature* **455**, 1129 – 1133 (2008).

Zheng Y & Levens D. Tuning the MYC response. *Elife* **5**, e18871 (2016).

Zindy F *et al*. Myc signaling via the ARF tumor suppressor regulates p53-dependent apoptosis and immortalization. *Genes Dev* **12**, 2424-33 (1998).

LIST OF PUBLICATIONS

1) Galardi S, Savino M, **Scagnoli F**, Pelegatta S, Pisati F, Zambelli F, Illi B, Annibali D, Beji S, Alberelli MA, Apicella C, Orecchini E, Michienzi A, Finocchiaro G, Farace MG, Pavesi G, Ciafrè SA., Nasi S.
Resetting cancer stem cell regulatory nodes upon MYC inhibition. (Embo Reports, 2016).

2) Mongiardi MP, Savino M, Bartoli L, Beji S, Nanni S, **Scagnoli F**, Falchetti ML, Favia A, Farsetti A, Levi A, Nasi S, Illi B.
Myc and Omomyc functionally associate with the Protein Arginine Methyltransferase 5 (PRMT5) in glioblastoma cells. (Sci Rep. Nov., 2015).

3) Montalban E, Mattugini N, Ciarapica R, Provenzano C, Savino M, **Scagnoli F**, Prosperini G, Carissimi C, Fulci V, Matrone C, Calissano P, Nasi S.
MiR-21 is an Ngf-modulated microRNA that supports Ngf signaling and regulates neuronal degeneration in PC12 cells. (Neuromolecular Medicine, 2014)